NASA CR-165,396

DOE/NASA/0083-1
NASA CR-165396

NASA-CR-165396
19820005637

# Development of a High-Temperature Durable Catalyst for Use in Catalytic Combustors for Advanced Automotive Gas Turbine Engines

H. Tong, G. C. Snow, E. K. Chu, R. L. S. Chang,
M. J. Angwin, and S. L. Pessagno
Energy & Environmental Division
Acurex Corporation

**September 1981**

Prepared for
NATIONAL AERONAUTICS AND SPACE ADMINISTRATION
Lewis Research Center
Under Contract DEN 3-83

for
**U.S. DEPARTMENT OF ENERGY**
**Conservation and Renewable Energy**
**Office of Vehicle and Engine R&D**

DOE/NASA/0083-1
NASA CR-165396

# Development of a High-Temperature Durable Catalyst for Use in Catalytic Combustors for Advanced Automotive Gas Turbine Engines

H. Tong, G. C. Snow, E. K. Chu, R. L. S. Chang,
M. J. Angwin, and S. L. Pessagno
Energy & Environmental Division
Acurex Corporation
Mountain View, California 94042

September 1981

Prepared for
National Aeronautics and Space Administration
Lewis Research Center
Cleveland, Ohio 44135
Under Contract DEN 3-83

for
U.S. DEPARTMENT OF ENERGY
Conservation and Renewable Energy
Office of Vehicle and Engine R&D
Washington, D.C. 20545
Under Interagency Agreement DE-AI01-77CS51040

#

N82-12510

TABLE OF CONTENTS

# SECTION 1

# INTRODUCTION

A compact, high-efficiency gas turbine is one candidate for fuel-efficient automobiles to be developed for the late 1980s and early 1990s. To meet the required goal of a 30 percent mileage advantage over the conventional Otto cycle, the gas turbine engine must operate at high turbine inlet temperatures and correspondingly high average combustor temperatures. In addition, efficiency increases will be obtained through the use of regenerative heat exchangers to thermally couple the exhaust gas to the combustor inlet gas. Thus, under contracts from the U.S. Department of Energy (DOE), the advanced automotive gas turbine is being designed to have both high combustor inlet and average combustion temperatures.

Simultaneous with the need for high combustion temperatures is the need for low $NO_x$ and low CO emissions. $NO_x$ levels are often characterized by the peak combustion temperature. For a conventional gas turbine diffusion flame, high peak temperatures result in unacceptably high $NO_x$ emissions. Therefore, alternative combustion techniques are being developed for gas turbines to yield simultaneously, high combustion efficiency, low $NO_x$ emissions, flame stability, and high turndown ratios.

Two favored methods for low-emission gas turbine combustors are the catalytic and lean premixed combustors (reference 1). Neither technique has been developed to where they can be considered suitable for widespread consumer acceptance in an automobile. Although both techniques use a premixed, and in the case of liquid fuels, prevaporized fuel-air mixture, they each have unique problems that must be overcome. Lean premixed, prevaporized combustors require extreme care in fuel preparation and are challenged to operate on the ragged edge of the flame stability limit. Catalytic combustion offers wider flame stability limits and lower $NO_x$ emissions but requires the development of catalysts and substrates which are durable at high combustion temperatures.

Both lean premixed and catalytic combustors are applicable to stationary as well as automobile gas turbines. Therefore, the development of these low $NO_x$ techniques is of great interest to the general gas turbine community. Success would result in improved fuel efficiency and ambient air quality. The program reported here was performed as part of a supporting research effort for DOE's Gas Turbine Highway Vehicles Systems Project. Technical monitoring was performed by the NASA Lewis Research Center.

The principle objective of this program was to develop catalytic reactors capable of operation in environments representative of those anticipated for advanced automotive gas turbine engines. Research activities prior to and during the course of this program (references 1 through 10) have demonstrated the benefits of catalytic combustion. Durability testing for up to 1,000 combustion hours was reported in references 3 and 4 for adiabatic flame temperatures up to approximately 1,530K with no. 2 diesel fuel on 0.025m diameter honeycomb catalysts. In this program, the combustion temperature was increased to 1,700K and the reactor diameter was increased to 0.063m.

Nominal design combustion conditions for catalytic reactor evaluation were:

| | |
|---|---|
| Pressure | $1 \times 10^5$ Pa |
| Reference velocity | 15 m/s |
| Reactor inlet temperature | 800K |
| Adiabatic flame temperature | 1,700K |
| Fuel | No. 2 diesel |

Specific subobjectives of the program were the:

- Evaluation of furnace aging as a cost-effective catalytic reactor screening test
- Measurement of reactor degradation characteristics (surface area and/or dispersion) as a function of furnace aging and combined aging/combustion time
- Development of a catalytic reactor to demonstrate 1,000 hours durability for the combustion of no. 2 diesel fuel with a reactor temperature of about 1,700K
- Definition of a catalytic reactor system with a high probability of successful integration into an automotive gas turbine engine

In this catalyst evaluation program, four different tests were conducted: catalyst characterization, furnace aging, combustion at 1,700K, and parametric combustion. The objectives of each test, facilities, and procedures are given in section 2. The technical approach used in this program is shown in figure 1-1. The three principle tasks of this experimental program were a preliminary furnace aging evaluation, a catalyst screening test series, and a combustion durability test.

In the preliminary furnace aging evaluation, 14 candidate catalytic

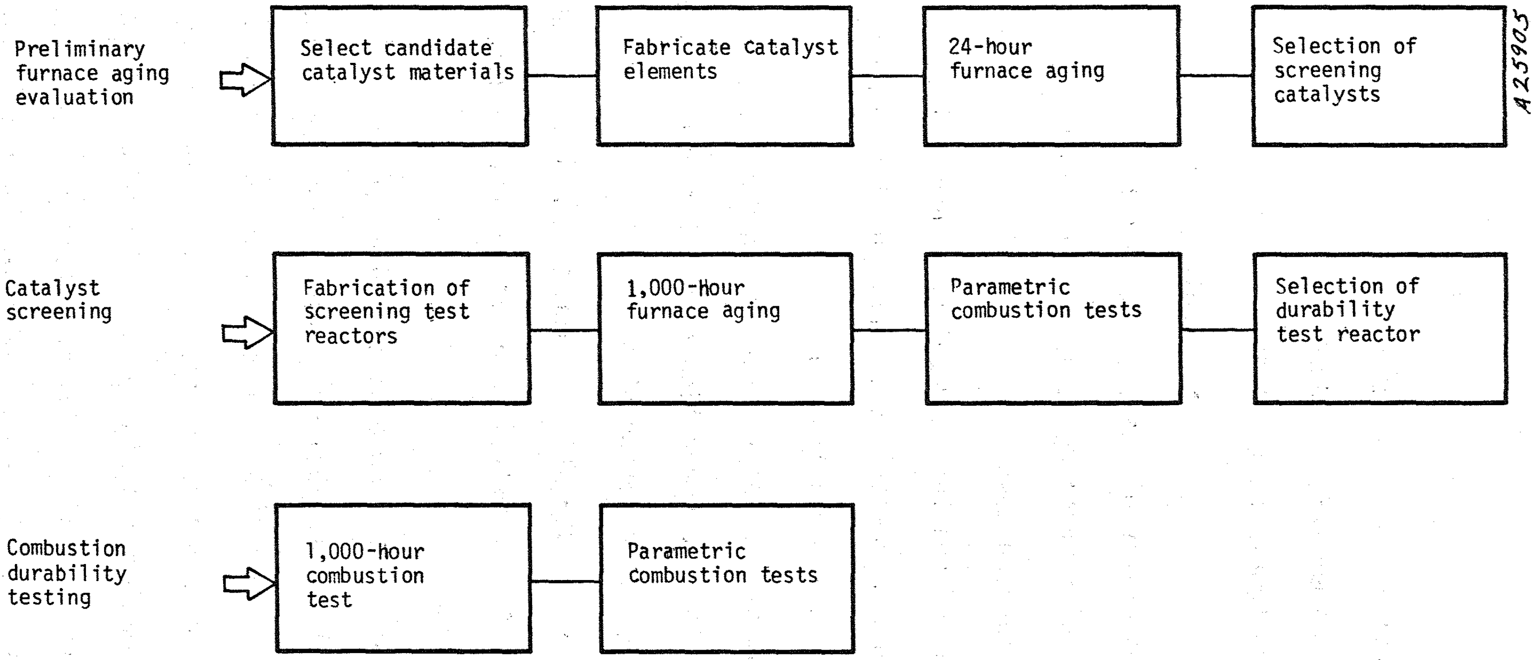

Figure 1-1. Program Technical Approach

reactor concepts, consisting of a catalyst and substrate combination, were selected from a larger number of recommendations from catalyst suppliers. These candidates were then fabricated and aged in a high-temperature (1,700K) furnace for 24 hours. Through pre- and posttest examinations, six catalytic reactor concepts were selected for further catalyst screening.

In the catalyst screening tests, sufficient catalytic reactors of each of the six selected concepts were prepared for long-term furnace aging and combustion evaluation. Furnace aging was conducted at 1,700K for 1,000 hours. At prescribed intervals, the furnace was cooled to ambient conditions and appropriate samples removed for examination. Also, after 24 hours and 1,000 hours of aging, combustion tests were conducted with each reactor concept at the nominal design combustion conditions. From an evaluation of the catalyst screening results, a single candidate was selected for durability testing under combustion conditions.

In the combustion durability testing, the selected catalytic reactor was to be tested for 1,000 hours at the nominal design conditions. In this program, the catalyst failed after about 280 hours and this test was terminated. Following a second catalyst selection effort, a candidate reactor concept was selected and combustion tested for 1,000 hours. However, due to some potential diesel fuel preparation problems, propane, a gaseous fuel, was used.

Most samples for this program were prepared by applying a catalyst to a honeycomb substrate. Honeycomb materials were selected for their anticipated high-temperature durability, possible interactions with washcoats and catalyst coatings, and availability. Exceptions to this approach were taken with ceramic-like materials which were expected to have some inherent catalytic activity. These materials were fabricated into configurations which would permit some evaluation of their degree of catalytic activity and possible thermostructural response.

In all cases, catalyst material selections were based on conversations with catalyst suppliers and their recommendations for specific formulations which they believed would meet program goals. Many of these formulations are proprietary and identified only with regards to the supplier and a general description. Other formulations are unrestricted and more specifically described. All materials used in this program are defined in section 3.

Sections 4, 5, and 6 describe the preliminary furnace aging tests, the combined furnace aging and combustion screening tests, and the durability tests, respectively. In the course of this research effort, the durability test program was modified after the original durability sample failed to complete the planned 1,000 hours of combustion time. A new and different sample was prepared and tested with propane (rather than diesel) at 1,700K for the planned 1,000 hours. A major part of the funding for this final test was provided by EPA under contract 68-02-3122. In addition, the results of this program would not have been possible without the cooperation of the persons and organizations shown in table 1-1.

The program and results described in the following sections show that materials are not yet available for high-temperature catalytic combustion applications such as the advanced automotive gas turbines. However, the 1,000 hours of combustion at 1,700K show that there is a high probability that materials and systems could be developed in the next 5 years to meet the durability requirements of advanced automotive as well as stationary powerplant gas turbines.

Table 1-1. Program Contributors

Dr. William C. Pfefferle
51 Woodland Drive
Middletown, NJ 07748

Mr. Miguel Hnatow
Catalysis Research Corporation
450 East Edsall Boulevard
Palisades Park, NJ 07650

Dr. James Wells
Houdry Air Products
Houdry Laboratory
Sun and Hewes Avenues
Lynwood, PA 19061

Dr. William B. Retallick*
OxyCatalyst
E. Biddle Street
West Chester, PA 19380

Mr. Howard A. Lowenstein
Corning Glass Works
Corning, NY 14830

Dr. George R. Lester
UOP Inc.
Ten UOP Plaza, Algonquin &
Mt. Prospect Roads
Des Plaines, IL 60016

Mr. Edmond R. Tucci
Matthey Bishop, Inc.
Malvern, PA 19355

Dr. James Masselli
W. R. Grace & Company
7379 Rt. 32
Columbia, MD 21044

Mr. Louis P. Domingues
Trans-Tech, Inc.
12 Meem Avenue
Gaithersburg, MD 20760

* Currently, Consulting Chemical Engineer, 1432 Johnny's Way, West Chester, Pennsylvania 19380.

# SECTION 2

# TESTS, FACILITIES, AND PROCEDURES

In this program, two types of noncombustion tests and two types of combustion tests were conducted. They are described in the following paragraphs.

## 2.1 CATALYST CHARACTERIZATION TESTS

The catalyst characterization tests included the measurement of surface area and noble metal dispersion (when applicable). The surface area and dispersion are usually measures of the potential catalytic activity of the catalyst. For low-temperature applications (less than 1,000K) these parameters degrade rather slowly; however, at high temperatures significant degradation can occur in a very short time (perhaps minutes). Qualitative assessments of the surface condition of the catalysts and elemental materials near the surface were also performed using scanning electron microscope (SEM) analyses (when permitted by the catalyst suppliers).

In this program, measurements were taken of all pretest samples and, in most cases, post-test samples. Pretest measurements of surface area and catalyst dispersion allow a comparison of similar catalyst materials and preparation techniques. From a given vendor, these measurements also represent a quality control check on processing reproducibility.

The gas adsorption apparatus used for the surface area and dispersion measurements is shown in figure 2-1. The major components are: (1) the pumping and vacuum control system, (2) the gas delivery, storage, and cleaning system, and (3) the working volume and sample cell. For nondestructive testing, sample cells large enough to accommodate the complete catalytic reactor are utilized.

Measurement of total surface area by physical adsorption of argon is carried out at liquid nitrogen temperature (77K). The surface area is determined by the calculation of an adsorption isotherm. Successive charges of adsorbate (argon) are admitted to the sample cell from the dosing volume. After each admission, readings of pressure are taken until there is no further detectable change. Equilibrium is assumed at this state. The amount adsorbed is calculated for each equilibrium pressure as the difference between the total quantity of gas admitted and the quantity remaining in the dead space.

The basis for the surface area measurement is the Langmuir gas adsorption theory where the surface of a solid is regarded as an array of active adsorption sites, each site with the capacity to adsorb one molecule. Brunauer, Emmett, and Teller (BET, reference 11) extended the Langmuir theory to apply to the second and higher layers of adsorbed molecules. Based on this work, the total BET surface area is given by:

$$SA = \frac{V_m A}{W} \ (m^2/g) \qquad (2\text{-}1)$$

where $W$ = catalyst weight in grams

$A$ = area occupied per molecule (for argon, $A = 14.6 \text{Å}^2$)

and $V_m$ is found from the BET equation

$$\frac{P}{(P_o - P)} = \frac{1}{V_m C} + \frac{C-1}{V_m C} \frac{P}{P_o} \qquad (2\text{-}2)$$

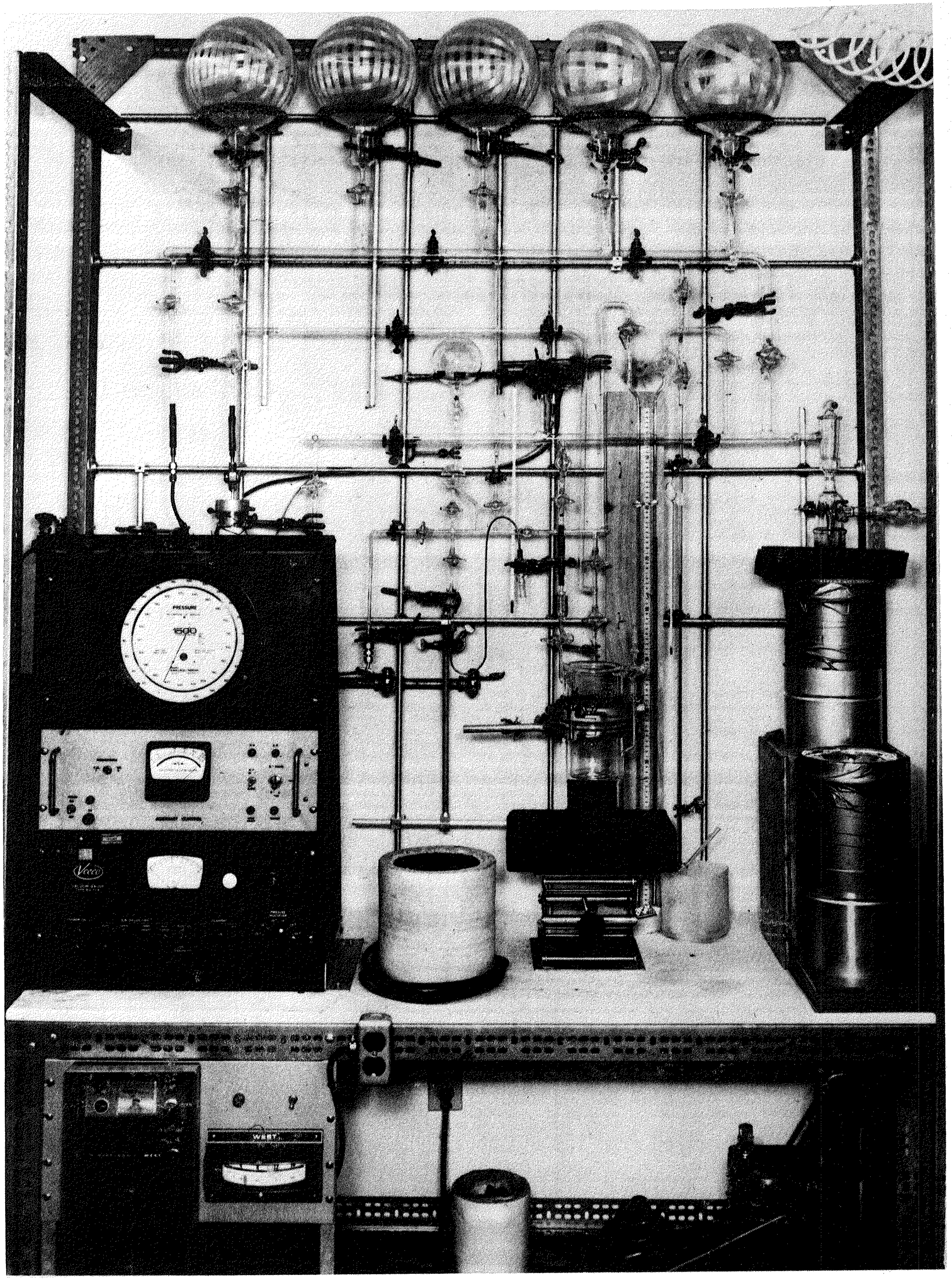

Figure 2-1. High Vacuum Gas Adsorption Apparatus

Experimentally, it is found that a plot of $P/V\ (P_0-P)$ versus $P/P_0$ is linear in the range of relative pressures from 0.05 to 0.35. The slope is $(C-1)/V_mC$ and the intercept is $1/V_mC$. Thus, $V_m$ can be found from the measured slope and intercept of this line. Total surface area can then be determined from equation 2-1.

For dispersion measurements the catalyst is first reduced with hydrogen at an elevated temperature. The system is then evacuated, subsequently exposed briefly to air to form a noble metal oxide layer on the catalyst, and reevacuated. A titration with hydrogen is then conducted at liquid nitrogen temperature. The titration procedure is virtually the same as the BET surface area measurement procedure except that hydrogen is used in place of argon. The hydrogen reacts with the noble metal oxide and essentially "adsorbs" hydrogen molecules. The amount of hydrogen "adsorbed" is then a measure of the density of active noble metal sites.

The stoichiometry of the reaction of hydrogen with PtO, or titration, is:

$$PtO(surface) + 3/2\ H_2 \rightarrow PtH(surface) + H_2O$$

In the case of platinum on an alumina washcoat, the water formed is adsorbed by the alumina. The consumption of 1.5 $H_2$ molecules for each atom of surface Pt results in an increased sensitivity in the surface area measurement compared with the alternate chemisorption technique.

When permitted by the supplier, catalysts were examined with SEM at various magnifications and X-ray diffraction analysis (Kevex) for before and after test comparisons of topography and surface composition. Both are qualitative but in several cases, revealed significant changes in surface characteristics due to high temperature exposure.

## 2.2 FURNACE AGING TEST

Furnace testing of catalyst material combinations is a relatively low cost technique for investigation of temperature effects on catalyst fixation to the substrate, catalyst chemical interactions with the substrate, and thermostructural properties of the support material. It does not provide a direct evaluation of combustion performance since catalyst surface reactions and fluid transport are not simulated. However, the low cost and ease of furnace testing make it a potentially valuable tool for initial screening of catalyst material durability for systems known to have significant catalytic activity.

The furnace aging facility, installed at Catalysis Research Corporation in Palisades Park, New Jersey, is a "Unique Kiln" gas-fired model, Model U.S.-A-6, rated to 2,700$^{\circ}$F, with a 6-ft$^3$ load space (constant temperature zone). The chamber size is 24 by 21 inches, with an overall size of 66 by 46 by 44 inches. The oven temperature is automatically regulated with a Baker Coleman Model 202C controller. Excellent temperature control was shown by a close temperature-time agreement between and within furnace runs.

For aging tests, the catalysts are placed in the center of the furnace, supported by a plate of silicon carbide raised off the floor of the furnace. The catalyst test area is surrounded by six plates of silicon carbide, which shield the catalysts from the radiation of the furnace walls. Figure 2-2 shows the furnace and figure 2-3 shows the "radiation shield" box of silicon carbide. Figure 2-4 shows a typical arrangement of catalysts in place within the box; however the catalysts are hidden from view by their protective cylindrical alumina sheath. Figure 2-5 shows a typical catalyst in its protective sheath. Each

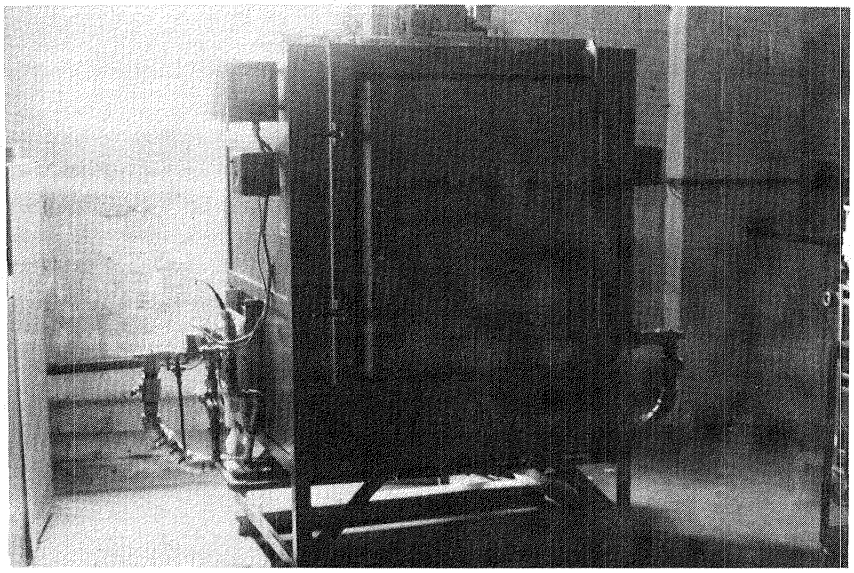

Figure 2-2. Furnace

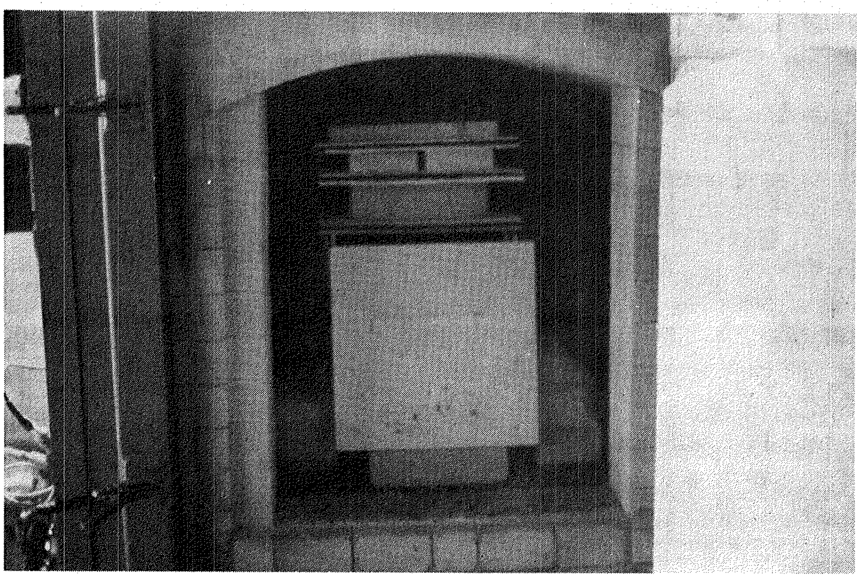

Figure 2.3. Radiation Shield in Furnace

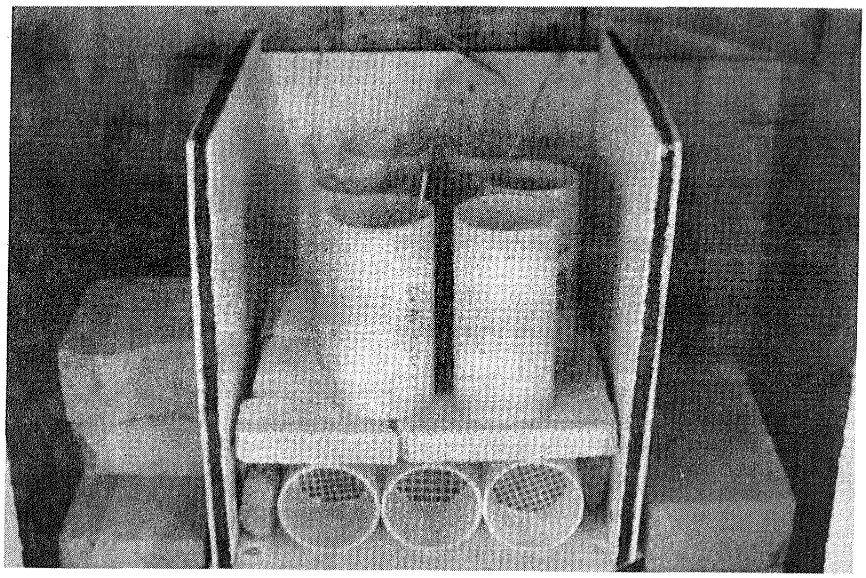

Figure 2-4. Catalysts in Place Within Furnace

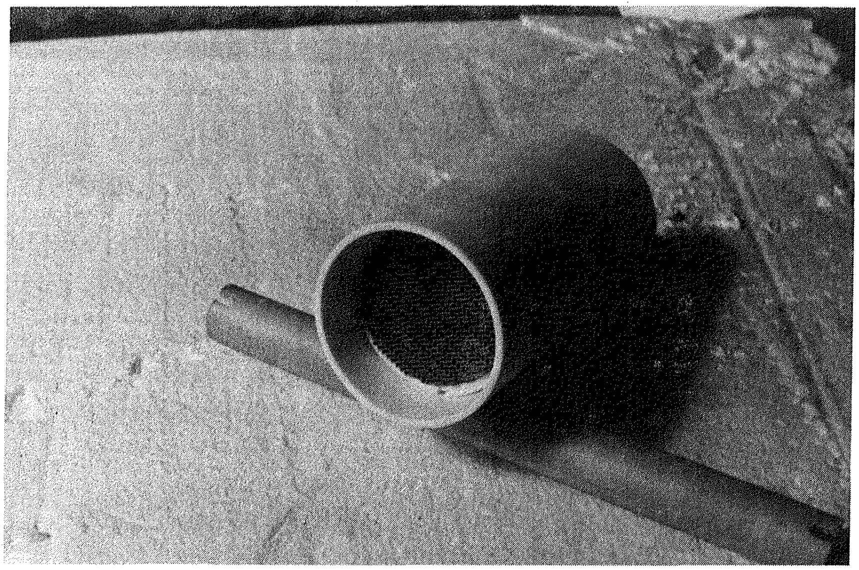

Figure 2-5. Catalyst in Sheath, Out in Furnace

catalyst is supported (within its sheath) by a small piece of alumina, so catalysts do not rest on the silicon carbide base plate.

The furnace temperature is monitored with six thermocouples, two that read absolute temperatures, and two pairs that read differential temperatures. One of the absolute temperature thermocouples was used with a stripchart recorder to obtain furnace temperature-time histories. Frequent reading of the remaining thermocouples provides a record that ensures that catalysts in different portions of the furnace experience the same temperature. During typical tests, measured furnace temperatures stayed within 10°C of the required temperature and the differential thermocouples read within 2°C of each other.

Due to the large refractory mass of the furnace, it was not possible to obtain any information on thermal shock effects on the substrates, only time-at-temperature effects could be deduced. Typical kiln heatup times were programmed to attain 1,700K in about 5 hours. Following a prescribed number of hours at 1,700K, the furnace gas and air flow was terminated and the furnace allowed to cool for about 24 hours or until the sample temperatures were less than 500K before the kiln was opened to the atmosphere.

## 2.3 COMBUSTION TESTS AT 1,700K

Selected catalyst samples were combustion tested at an adiabatic flame temperature of about 1,700K. These tests were conducted as screening tests and durability tests. With the exception of the final durability test, combustion tests were conducted with diesel fuel at the specified nominal conditions (section 1). A detailed analysis of the commercial no. 2 diesel fuel used in these tests is shown in table 2-1.

Table 2-1. Fuel Properties

| Analysis Type | Truesdail Analysis Technique | No. 2 Diesel Truesdail |
|---|---|---|
| Elemental Analysis, wt percent | | |
| Carbon | ASTM E191 | 86.62 |
| Hydrogen | ASTM E191 | 12.90 |
| Nitrogen | ASTM E258 | 0.035 |
| Sulfur | ASTM D129 | 0.13 |
| Ash | ASTM D482 | 0.003 |
| Oxygen | By difference | 0.31 |
| Heat of Combustion, Btu/lbm | ASTM D240 | |
| Net | | 18,230 |
| Gross | | 19,410 |
| Trace Metals, ppm wt | Wet chemical/ spectrographic | |
| Calcium | | 0.25/0.55 |
| Iron | | 0.70/1.90 |
| Manganese | | <0.05/0.05 |
| Magnesium | | 0.08/0.51 |
| Nickel | | <0.05/0.13 |
| Vanadium | | <1.0/--- |
| Sodium | | 0.14/0.02 |
| Zinc | | ---/2.0 |
| Copper | | ---/0.15 |
| Silicon | | ---/5.70 |
| Tin | | ---/0.26 |
| Aluminum | | ---/1.10 |
| Boron | | ---/0.03 |
| Lead | | ---/0.66 |
| Molybdenum | | ---/--- |
| Titanium | | ---/0.11 |
| Silver | | ---/0.35 |
| Cobalt | | ---/--- |
| Cadmium | | ---/0.35 |
| Potassium | | ---/--- |
| Phosphorus | | ---/0.26 |
| Chromium | | ---/--- |
| Physical Properties | | |
| Flash point, °F | 175 | |
| Pour point, °F | -10 | |
| Gravity, °API | 32.0 | |
| Boiling range, °F | 358-672 | |
| Kinematic viscosity, cs at 100°F | 2.61 | |

## Combustion Test Facility

All combustion testing was performed in the Acurex catalytic combustion test facility. This facility is shown schematically in figure 2-6 and physically in figure 2-7.

Combustion air passed through preheaters before entering the mixing chamber (fuel-air preparation spool). The preheaters consist of a series of six 6,000-watt exposed-element heaters (GTE Sylvania Model 138825, Style A). The preheat temperature is electronically controlled by the use of a proportional controller (Chromalox series C76, 0-800K) in conjunction with a silicon-controlled rectifier (Chromalox Thyristor Power Controller Model CSCR 005-1208-60) effectively pulsing the current to the heaters in 1/60-second increments every 1/3 second. The combustion air then enters the top of the mixing chamber through a four-way manifold to provide even distribution around the liquid fuel nozzle. Both the propane and liquid fuels bypass the heater to avoid preignition due to the exposed heater elements. Propane is introduced to the mixing chamber through two opposed ports immediately below the four-way manifold.

A pressurized air atomization fuel nozzle is used to deliver the liquid fuels, and is located at the top of the mixing chamber. The nozzle was modified from a Spraying Systems Company design (Model 1/4 JALL) by replacing viton seals with Teflon and constructing a cooling air jacket to surround the liquid passages. This cooling was necessary to prevent fuel coking in the passages since the nozzle senses heating both from the preheat temperature and radiation from the catalyst bed. Also, it was found that maximizing the atomizing airflow enhanced cooling and prevented clogging of the spray orifice.

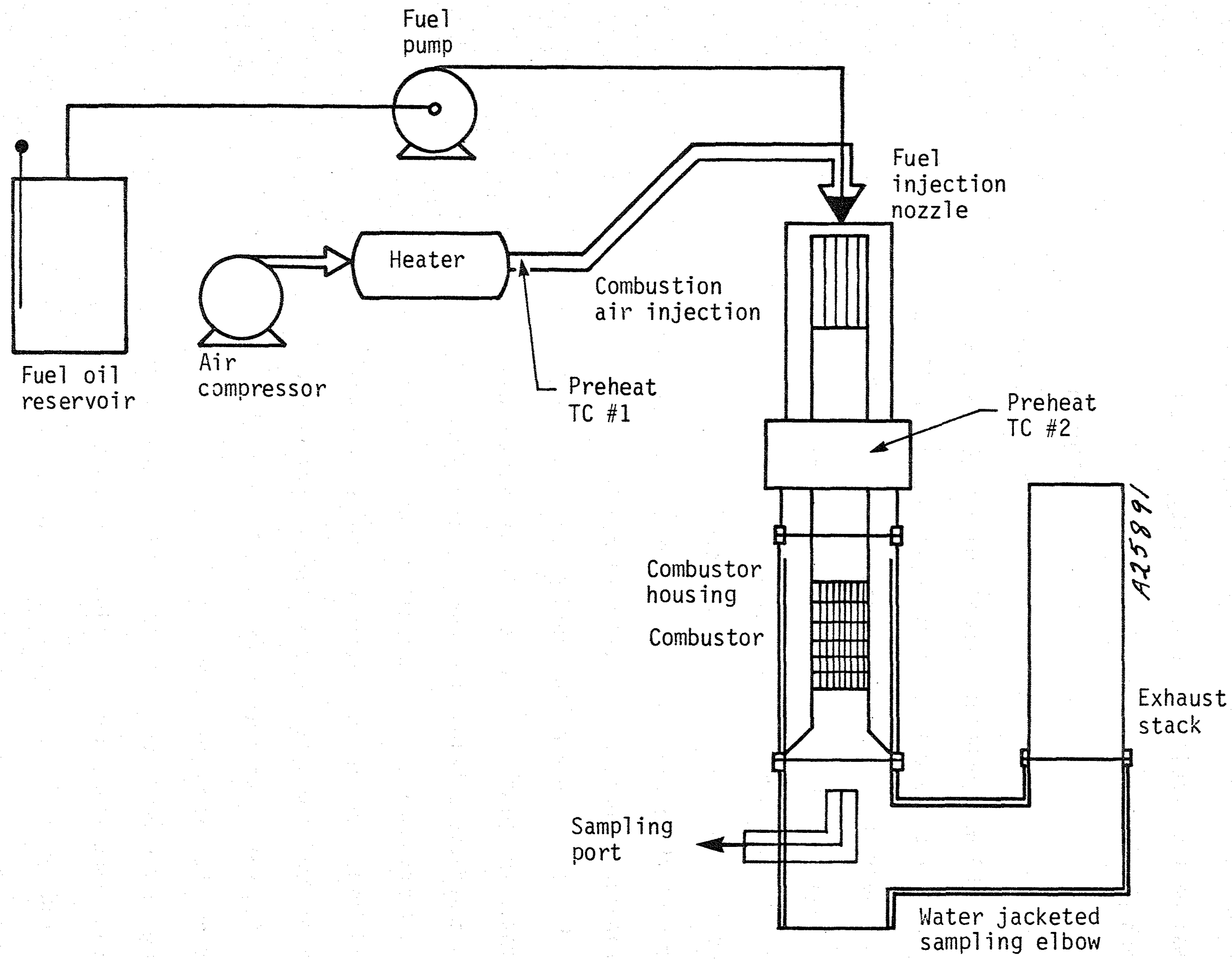

Figure 2-6. Test Facility Schematic

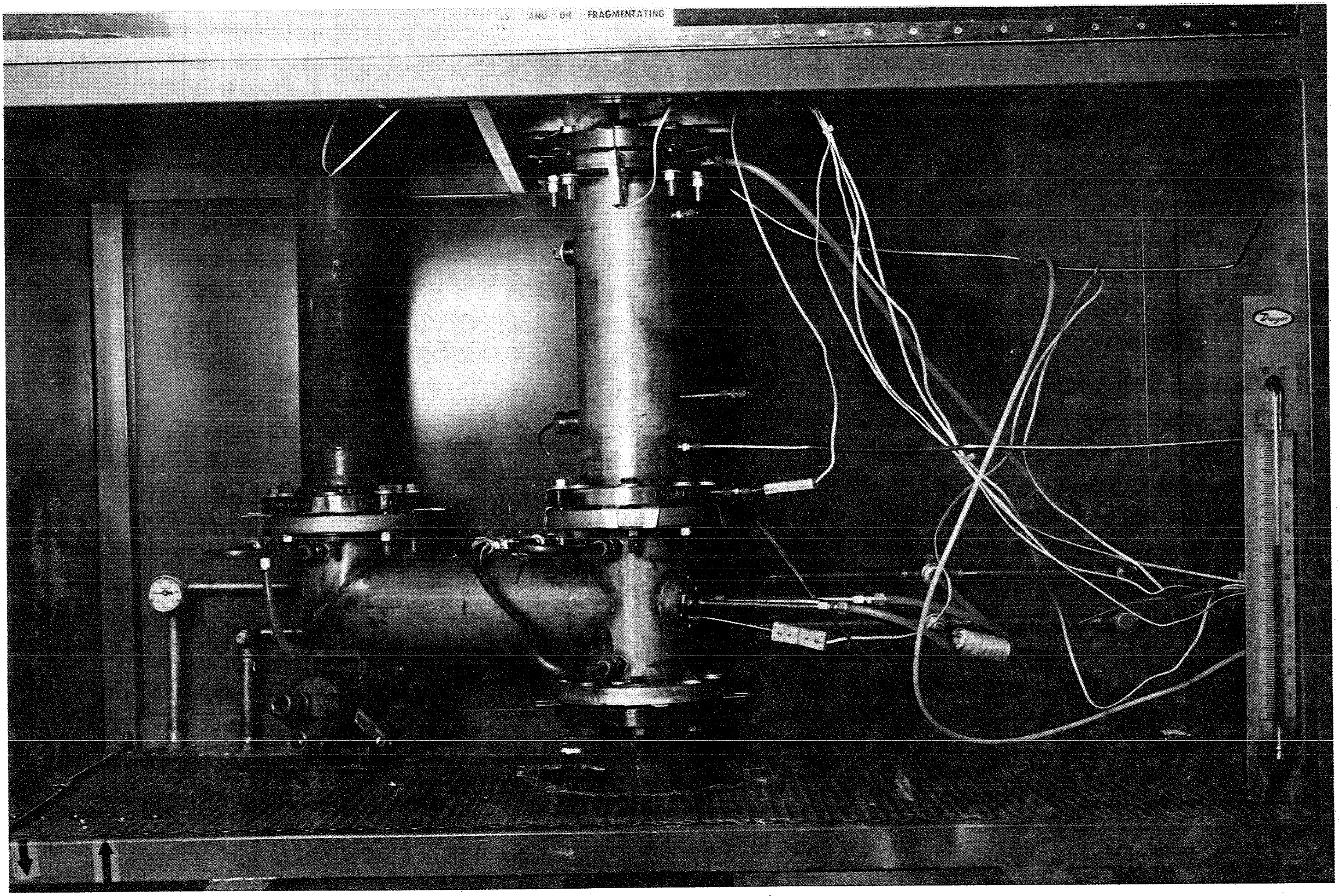

Figure 2-7. Acurex Catalytic Combustion Test Facility

Since no direct measurements were made on the extent of the fuel-air mixing, the combustion mixture uniformity can only be defined qualitatively. In previous tests with this fuel preparation system (reference 6) the degree of vaporization at 640K preheat was assessed by traversing an impaction probe across the reactor duct immediately ahead of the catalyst bed. The impaction probe was constructed from 0.25-inch diameter ceramic tubing, chosen for its low thermal conductivity. To reduce condensation of vaporized fuel on a cool surface and biasing the results, the ceramic was heated to the preheat temperature. The probe was inserted transverse to the flow stream for a period of time, then withdrawn and immediately inspected for unvaporized fuel droplets. Under all fuel-lean conditions, the fuel appeared to be fully vaporized and no droplets could be seen.

The impaction probe technique was also useful for getting an indication of mixing uniformity in the reactor duct. After each vaporization test, the probe was inspected to determine if the fuel loading varied with position; no differences were detected.

As a further check on the mixing uniformity, a simple gas sample probe was constructed to traverse across the reactor duct. The probe was connected to the emission bench so that a sample could be drawn in and analyzed for hydrocarbon and oxygen content. Mixing nonuniformities would be manifested in varying levels of these species as the probe was moved across the duct. Again, no differences were detected.

Subsequent combustion tests (with preheated air) with noble metal catalyst showed that the catalyst face was uniformly bright, again indicating a reasonably uniform fuel-air mixture. No further assessments of the fuel-air uniformity were conducted.

Since the main control panel of the catalytic combustion facility is capable of providing only gaseous fuel control, a separate system was used to control and measure liquid fuel flows. Figure 2-8 is a schematic diagram of the liquid fuel delivery system. The system uses a return loop after the fuel pump back to the 55-gallon storage drum. Thus only a small portion of the total pump output is diverted to the combustor. This arrangement damps out pressure variations in the liquid system, gives smooth startup capabilities from zero flow, allows rapid response to control changes, and yields a high turndown ratio.

In operation propane was used as a light-off and preheating fuel except in the final durability test in which it was the test fuel. The flowrates of the propane and air were measured by glass tube rotameters at their respective inlet temperatures and pressures.

The catalytic reactor assembly is held within the water-jacketed combustor housing spool, as shown in figure 2-6, such that the catalyst front face is positioned about 90 cm downstream of the liquid fuel nozzle.

The combustor housing assembly is completed by the water-jacketed sampling elbow, viewing window, and exhaust stack. The elbow serves as a mount for the gas sampling probe, exhaust thermocouple, and viewing window. The viewing window allows physical observation of the reactor exit face to supplement temperature and combustion product measurements. During testing, the operator is able to note changes in reactor activity as evidenced by visual nonuniformities and downstream reactions. The physical integrity of the monolith support can also be assessed in this manner.

The preheat temperature of the air flowing to the reactor was measured at two locations as shown in figure 2-6. One thermocouple

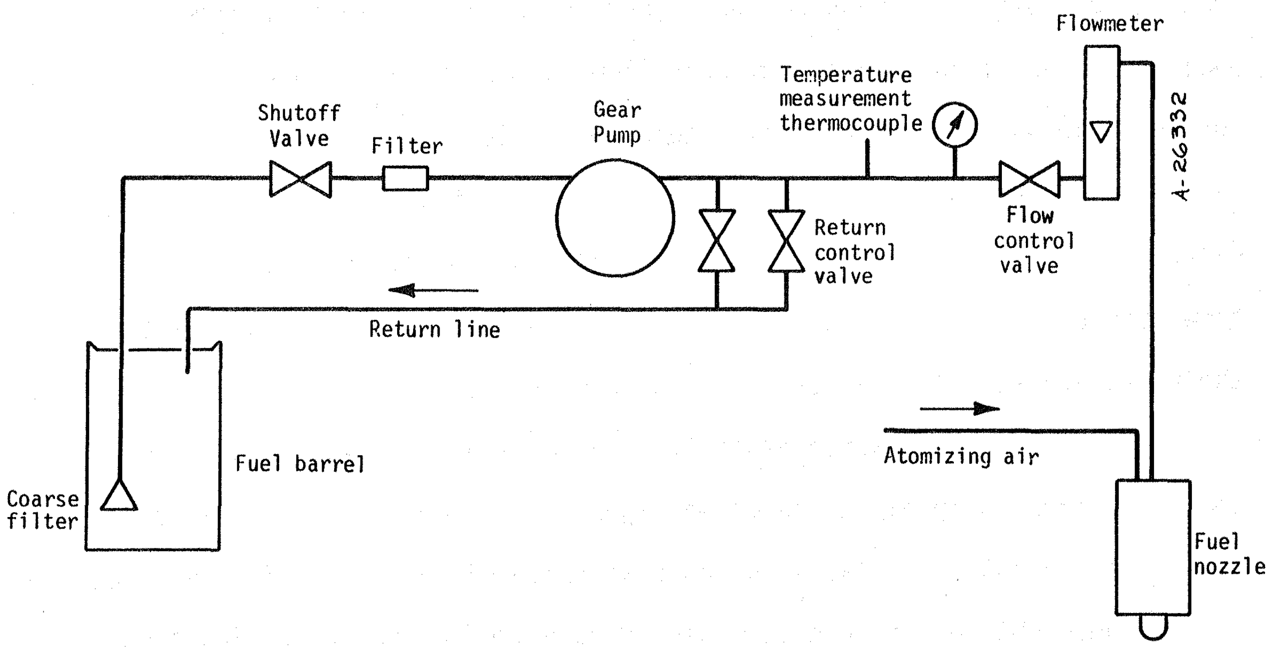

Figure 2-8. Liquid Fuel Delivery System

(preheat TC #1) was located in the main supply pipe downstream of the heaters and immediately upstream of the air injection manifold. The second thermocouple (preheat TC #2) was located midway between the fuel nozzle and the reactor bed in the fuel-air preparation spool.

The test air preheat conditions were established by first flowing air alone through the system with the heaters operating. After steady state was attained, the temperature readings of the two thermocouples were recorded along with the heater control setting required to maintain 800K in the reactor bed. These levels were often checked before combustion testing to note possible differences due to varying operating conditions. During combustion testing, the heater was adjusted to maintain the reading of TC #1 which gave a temperature of 800K in the reactor bed when fuel was not flowing.

## Catalytic Reactors

Most of the catalytic reactors were assembled from 5.0- to 6.35-cm diameter honeycomb segments cemented together to form an integral 7.6-cm long catalytic reactor. (Some developmental materials were not available in honeycomb form. To evaluate these materials, drilled cylinders and bundles of tubes were used to simulate a reactor.) The reactors are wrapped with ceramic fiber insulation felt and fitted inside a cylinder made of castable refractory. The refractory cylinder is, in turn, wrapped in insulation felt and inserted within the combustor spool. The felt is packed snugly around the monolith and cylinders to provide a firm but nonrigid mounting. This mounting system provides insulation to thermally isolate the reactor bed and gas flows from the water-cooled combustor housing walls.

Temperature measurements were taken upstream and downstream of the reactor bed as well as within the bed itself. Chromel versus alumel (K-type) thermocouples were used upstream to measure the preheat temperature entering the reactor. Exit gas temperature was monitored by a K-type thermocouple located near the entrance to the sample probe. This location puts the measurement junction about 20 cm behind the reactor bed. Bed temperature measurements were taken with up to six in-depth thermocouples, platinum versus platinum with 13 percent rhodium (R-type). Figure 2-9 illustrates a representative thermocouple placement diagram for the reactor bed and a typical reactor installation method in the test section.

### Probe and Sample Transfer System

A water-cooled stainless steel sample probe was used in this experiment. This probe was designed for durability in hostile environments. The probe was located about 20 cm downstream of the catalytic combustor with the inlet nozzle facing upstream and aligned with the duct axis. With the exception of CO from inefficient combustion conditions, the combustion reactions will have essentially reached equilibrium before the gases enter the probe nozzle, extremely rapid quenching as achieved by aerodynamic expansion then is not required to freeze rapidly progressing reactions. Therefore, the convection cooling rate of this probe of approximately $10^5$ $^{o}$F/s, was sufficient for major species sampling.

From the sample probe, the gas passes through a filter and is transferred in a 0.375-inch OD heated Teflon line to the emission bench. Thermodynamic calculations predict a maximum dew point temperature of about 320K for the products of stoichiometric combustion at 1 atmosphere

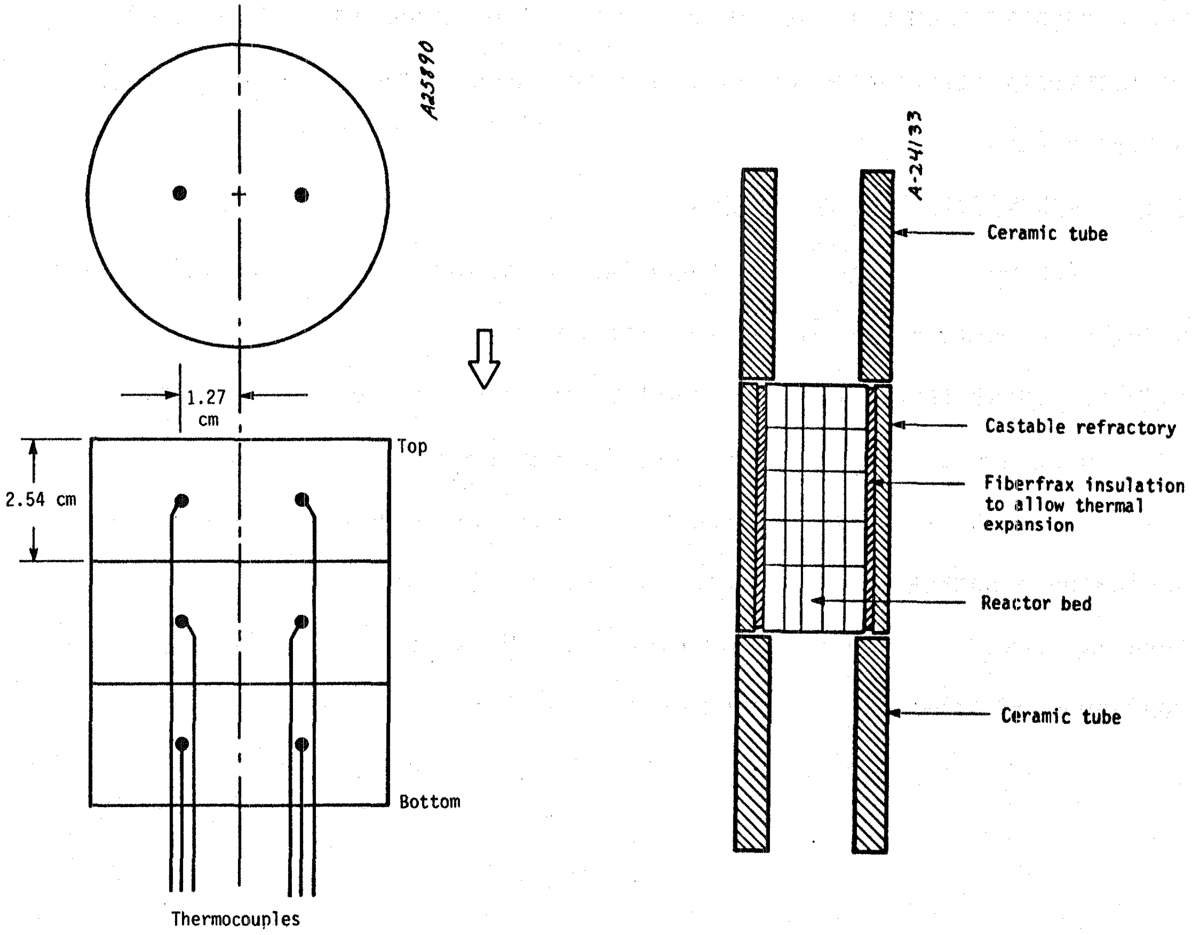

Figure 2-9. Catalytic Reactor Instrumentation and Installation

pressure. Therefore, the temperature of the sample line was maintained at approximately 360K at all times to prevent water condensation within the transfer system.

### Analytical Equipment

Table 2-2 summarizes the analytical equipment used and the corresponding chemical species measured. The compounds of NO and $NO_2$, collectively referred to as $NO_x$, were measured by the chemiluminescent analyzer (CLA).

## 2.4 PARAMETRIC COMBUSTION TESTS

Parametric tests were conducted on catalytic reactors to determine changes in performance as the temperature was gradually reduced below 1,700K. These tests were performed along with the combustion tests described in section 3.3. The catalyst bed temperature was decreased in 50K increments by decreasing the fuel flow until emissions measurements indicated a noticeable change in combustion efficiency. The fuel rate was then increased to attain the original 1,700K condition and the test either continued or terminated, depending on the planned sequence.

Table 2-2. Analytical Equipment (Emissions Bench No. 2)

| Instrument | Principle of Operation | Manufacturer | Model | Instrument Range |
|---|---|---|---|---|
| $NO_x$ analyzer | Chemiluminescence | Thermo Electron | 10A | 0 to 2.5 ppm<br>0 to 10<br>0 to 25<br>0 to 100<br>0 to 250<br>0 to 1000<br>0 to 2500<br>0 to 10000 |
| UHC analyzer | Flame ionization | Beckman | 400 | 0 to 100 ppm<br>0 to 1000<br>0 to 10000<br>0 to 100000 |
| $O_2$ analyzer | Micro fuel measuring cell | Teledyne | 326A | 0 to 5 percent<br>0 to 10<br>0 to 25 |
| CO analyzer | Infrared | Beckman | 315B | 0 to 300 ppm<br>0 to 900<br>0 to 1200 |
| $CO_2$ analyzer | Infrared | Beckman | 215A | 0 to 15 percent |
| Sample gas conditioner | Refrigerant dryer-condenser | Thermo Electron | 600 | 25 scfh |

# SECTION 3

# MATERIALS DESCRIPTIONS

A large number of catalyst formulations were tested in Phase I of this program. These catalysts were divided into three categories: noble metals, metal oxides with moderate vaporization potential, and metal oxides with low vaporization potential. A list of catalytic reactors, their suppliers, and general descriptions is shown in table 3-1.

Table 3-1. Catalyst Descriptions

| Designation | Supplier | Substrate | Catalyst/Washcoat | Element No. |
|---|---|---|---|---|
| UOP-A | UOP, Inc. | DuPont Torvex alumina, 100 cells/in$^2$, hexagonal | Proprietary washcoat, Noble metal "A" | All |
| UOP-B | UOP, Inc. | Corning MCB-12 100 cells/in$^2$, "Flexcell" | Proprietary washcoat, Noble metal "B" | All |
| UOP-C | UOP, Inc. | DuPont Torvex alumina, 100 cells/in$^2$, hexagonal | Proprietary washcoat, Noble metal"C" | All |
| MBI-B | Matthey Bishop, Inc. | DuPont Torvex alumina, 100 cells/in$^2$, hexagonal | Proprietary washcoat, stabilizer and catalyst | All |
| OC-B | Oxy-Catalyst | Corning MCB-12, 100 Cells/in$^2$, "Flexcell" | Metal oxide coating | All |
| WRG-A | W. R. Grace, Inc. | Corning MCB-12, 100 cells/in$^2$, "Flexcell" | Slip coat of base and noble metals stabilized with metal oxide anchoring | All |
| HAP-A | Houdry Air Products | Corning MCB-12 100 cells/in$^2$, "Flexcell" | Proprietary alumina washcoat, noble metal | All |
| HAP-C | Houdry Air Products | Corning MCB-12, 100 cells/in$^2$, "Flexcell" | Chromium "activated" substrate | All |
| ATT-A | Acurex | Corning MCB-12, 100 cells/in$^2$, "Flexcell" | 5-10% wt NiO, 1.5% wt Pt<br>5-10% wt NiO | 1<br>2, 3 |

Table 3-1. Concluded

| Designation | Supplier | Substrate | Catalyst/Washcoat | Element No. |
|---|---|---|---|---|
| ATT-B | Trans-Tech | $NiAl_2O_4$ (25% mole)<br>$MgAl_2O_4$ (75% mole)<br>approximately 60 cells/in$^2$, circular | NA | NA |
| ATT-C | Trans-Tech | $LaCrO_3$ (25% mole)<br>$LaAlO_3$ (75% mole)<br>approximately 60 cells/in$^2$, circular | NA | NA |
| ATT-D | Acurex | Corning Proprietary Honeycomb<br>100 cells/in$^2$, "Flexcell" | None | All |
| ATT-E | Acurex | DuPont Torvex alumina, 100 cells/in$^2$, hexagonal | $La_2O_3$-$Cr_2O_3$ (5-10% wt), Pt (1.5% wt)<br>$La_2O_3$-$Cr_2O_3$ (5-10% wt) | 1<br>2, 3 |
| ATT-F | Trans-Tech | $MgAl_2O_4$: $Fe_3O_4$<br>(9/1 mole ratio)<br>approximately 60 cells/in$^2$, circular | NA | NA |

# SECTION 4

# PRELIMINARY FURNACE AGING EVALUATION

The objective of this task was to select five catalytic reactor concepts for long-term aging and combustion testing. This selection was based on an initial evaluation of catalyst candidates in the aging furnace. The 14 catalytic reactor concepts listed in table 3-1 were selected from an initially larger list of candidates for this preliminary furnace aging. Each reactor was characterized by measuring the BET surface area and noble metal dispersion (when applicable) before and after a 24-hour exposure to the hot 1,700K aging environment. These results are summarized in table 4-1.

From both cost and time considerations, it was not practical to furnace age each reactor element separately so reactors were grouped into catalyst types for testing in three separate furnace runs. The groupings shown in table 4-2 were: (1) noble metals, (2) metal oxides with moderate volatility, and (3) low volatility metal oxides. In some cases, as shown in table 3-1, some of the base metal reactors also contained some noble metal(s). These reactors were included in group 2. To minimize the possible effects of cross contamination between different catalysts, each reactor was isolated in a cylindrical alumina tube. A narrative discussion is given below and includes some applicable experience with each reactor type on other test programs (references 2 and 6).

## Table 4-1. Preliminary Furnace Aging Results Summary

| Material | Pretest BET and Dispersion |  | Posttest BET and Dispersion |  | Previous Combustion Test Results | Posttest Condition |
|---|---|---|---|---|---|---|
|  | $m^2/g$ | $\mu$mole $H_2/g$ | $m^2/g$ | $\mu$mole $H_2/g$ |  |  |
| UOP-A | 5.66 | 45.5 | 0 | 14.66 | Not available | Blistered coating |
| UOP-B | 3.49 | 9.3 | 0 | 0.39 | Good with all fuels | No visual degradation |
| UOP-C | 4.84 | 40.0 | 0 | 11.14 | Not available | Flaking coating |
| MBI-B | 3.27 | 0.79 | 0 | 0.33 | Not available | Fractured |
| HAP-A | 0.25 | 0.95 | 0 | 0.16 | Poor | No visual degradation |
| HAP-C | 0.79 |  | 0 |  | Poor | No visual degradation |
| WRG-A | 1.06 | 1.42 | 0 | 0.16 | Moderate/poor | Material volatilized |
| OC-B | 1.83 |  | 0 |  | Good | Slightly darkened |
| ATT-A | 0.26 | 1.16 | 0 | 0.26 | Good | Some material depletion |
| ATT-D |  |  |  |  | Good with clean fuels,poor with others | Material volatilized |
| ATT-E | 0.09 | 1.36 | 0 | 0.31 | Good | No degradation |
| ATT-B |  |  |  |  | Not available | No degradation |
| ATT-C |  |  |  |  | Good with applied material | No visual degradation |
| ATT-F |  |  |  |  | Not available | No degradation |

Table 4-2. Aging Test Grouping

| Group No. | 1 | 2 | 3 |
|---|---|---|---|
| Reactors | UOP-A | HAP-C | OC-B |
|  | UOP-B | WRG-A | ATT-B |
|  | UOP-C | ATT-A | ATT-C |
|  | MBI-B | ATT-D | ATT-F |
|  | HAP-A | ATT-E |  |

## 4.1 TEST RESULTS, GROUP 1 -- NOBLE METALS

### UOP-A

UOP-A was a proprietary noble metal formulation on Torvex alumina. This type had not previously been combustion-tested at Acurex. Pretest BET was 5.66 $m^2/g$ catalyst, dispersion was 45.5 $\mu$moles $H_2/g$ catalyst. Posttest BET and dispersion were 0 $m^2/g$ and 14.66 $\mu$moles $H_2/g$ catalyst, respectively. Posttest visual examination showed the catalyst had survived the test in fair condition with some blistering of the washcoat from the Torvex substrate.

### UOP-B

UOP-B was a proprietary noble metal formulation on MCB-12. This formulation was combustion-tested on another Acurex test program (reference 6) with solvent refined coal as well as clean fuels, and had good life and combustion characteristics. For the preliminary furnace aging reactors the pretest BET was 3.49 $m^2/g$, posttest BET was 0. Pretest dispersion was 9.3 $\mu$moles $H_2/g$, posttest was 0.39 $\mu$moles

$H_2$/g. Visual examination of the catalyst showed no noticeable degradation posttest.

UOP-C

UOP-C was a proprietary noble metal on Torvex alumina. It is of a formulation that had not previously been combustion-tested at Acurex. Pretest BET and dispersion were 4.84 $m^2$/g and 40 $\mu$moles $H_2$/g; posttest were 0 $m^2$/g and 11.14 $\mu$moles $H_2$/g. Visual inspection showed that it survived the oven test poorly with some flaking of the washcoat from the substrate.

MBI-B

MBI-B is a stabilized noble metal on Torvex alumina. This formulation had also not been combustion-tested at Acurex previously. This monolith sample was received broken at Acurex and was cemented together for furnace testing. The pretest BET was 3.27 $m^2$/g, posttest was 0. Pretest dispersion was 0.79 $\mu$moles $H_2$/g catalyst -- posttest was 0.33. The sample broke again in the furnace and the surface showed some blistering.

HAP-A

HAP-A was a noble metal with an alumina washcoat on MCB-12. This catalyst had been combustion-tested on another program (reference 2) and showed poor combustion characteristics. The pretest BET on this catalyst was 0.25 $m^2$/g, the posttest BET was 0. The pretest dispersion was 0.95 $\mu$moles $H_2$/g catalyst, the posttest dispersion was 0.16. Visual inspection of the catalyst after testing showed no significant blistering or other problems.

## 4.2 TEST RESULTS, GROUP 2 -- METAL OXIDES

### HAP-C

HAP-C was a chromium catalyst on zirconia spinel. This catalyst was also combustion-tested in reference 2. From reference 2, the catalyst showed good early activity; however after 10 hours of combustion testing, the bed could not be relighted. Posttest examination of the catalyst revealed severe substrate cracking.

In this program, pre-oven test BET was 0.79 $m^2/g$, posttest BET was 0. Since this was a base metal catalyst, dispersion was not measured. Posttest visual examination showed that the catalyst was intact and not visibly degraded by the furnace test.

### WRG-A

WRG-A was a proprietary catalyst on zirconia spinel. This noble-base metal mixture has been combustion-tested as described in reference 2. In the reference 2 tests, this catalyst showed good combustion ability under fuel-lean conditions, though there were higher-than-expected CO emissions.

In this program, pretest BET was 1.06 $m^2/g$ and dispersion was 1.42 $\mu$moles $H_2/g$ catalyst. Posttest results were 0 $m^2/g$ and 0.16 $\mu$moles $H_2/g$, respectively.

Visual examination of the posttest reactor showed the structural integrity of the reactor to be good, but there was significant evidence of catalyst volatility from staining on the alumina sleeve (which was not in contact with the catalyst).

### ATT-A

ATT-A was a nickel oxide and platinum catalyst on MCB-12. This formulation has previously been combustion-tested at Acurex (reference 16). During combustion testing, the bed temperature showed a tendency to rise several hundred degrees spontaneously; fuel and air flow adjustments were then required to control the bed temperature. Temperatures ranged between 2,100°F and 2,800°F during these cycles. After cycling, the bed operated stably at 2,500°F under both lean and rich conditions. It was a good combustor, and survived 15 hours of testing with some minor fracturing. Although good catalyst life had been exhibited during combustion testing, posttest scanning electron microscope work showed that the surface was severely depleted of nickel.

Before oven aging on the NASA program, the BET of this material was 0.26 $m^2/g$ and dispersion was 1.16 $\mu$moles $H_2/g$. Posttest BET was 0, and dispersion was 0.26. Posttest SEM analysis showed a surface similar to the surface of bare MCB-12 with spheres of platinum. Elemental analysis showed nickel to still be present on the surface, though depleted.

### ATT-D

This material had been combustion-tested at Acurex in another program (reference 6), doing extremely well with clean fuels, and poorly with solvent-refined coal. Because of the nature of the material, BET and dispersion work were not relevant. Because of the proprietary nature of the material, SEM work could not be performed. Visual inspection after oven testing showed that the alumina sleeve surrounding the catalyst was heavily stained. This showed that there had been significant catalyst volatility.

### ATT-E

This catalyst was a mixture of lanthanum and chromium oxide and some platinum on Torvex alumina, prepared at Acurex. It was intended to form the compound $LaCrO_3$ in situ during the formulation. It is probable that $LaCrO_3$ actually was formed; however, to test whether $LaCrO_3$ was formed would require an X-ray diffraction study, which was not done. Therefore, the catalyst is described as a $La_2O_3$-$Cr_2O_3$ catalyst, rather than a $LaCrO_3$ catalyst. The same formulation was combustion-tested on another program (reference 16), where it performed well under fuel-lean conditions for over 17-1/2 hours at 2,200°F to 2,400°F. Postcombustion-test analysis of this material showed that the lanthanum and chromium were depleted in places.

In this program's furnace test, the pretest BET was 0.09 $m^2/g$, and the posttest BET was 0. The pretest dispersion was 1.36 $\mu$moles $H_2/g$ catalyst, and the posttest dispersion was 0.31. Visual inspection of the catalyst after furnace testing showed good integrity and no noticeable change in color. Posttest SEM analysis of the catalyst showed a surface very similar in appearance to pretest surfaces as shown in figure 4-1, with visible spheres of platinum. The Kevex analyses show lanthanum and chrome to be present in quantities similar to those before combustion testing, and greater than those after combustion testing.

## 4.3 TEST RESULTS, GROUP 3 -- METAL OXIDES

### OC-B

This catalyst consisted of a base metal oxide applied to MCB-12. A very similar catalyst was combustion-tested on another program (reference 16), where it showed excellent combustion efficiency and long life.

The BET of this catalyst before the oven test showed a surface area of 1.83 $m^2/g$; posttest BET was zero. Visual inspection showed the catalyst to be slightly darkened posttest, but the structural integrity of the catalyst was very good.

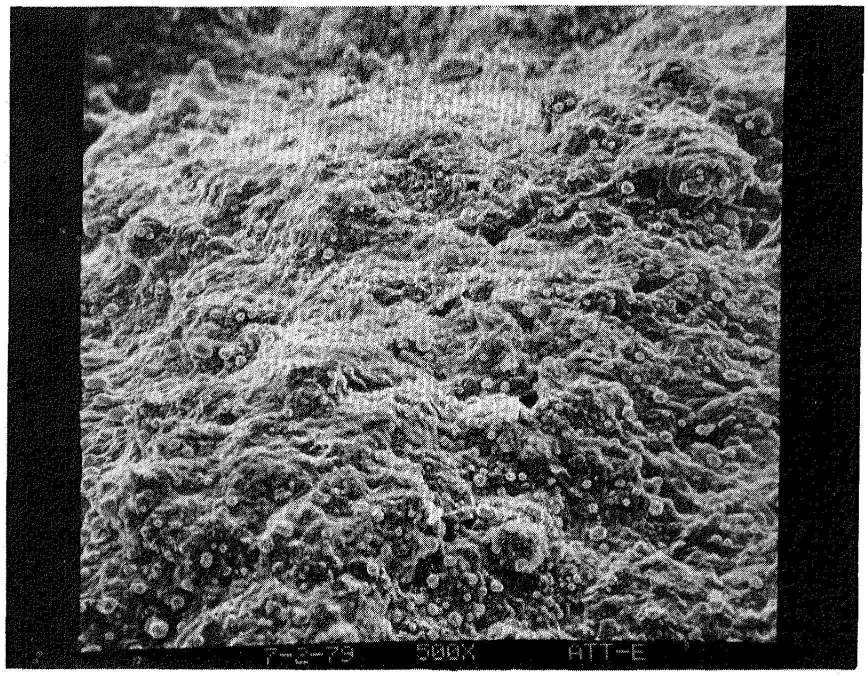

Figure 4-1. SEM photograph, 500X Magnification, Surface of ATT-E Before Aging

## ATT-B

This monolith (as all the remaining monoliths) was prepared as follows. Reactive powders of precursor oxides (nickel oxide, alumina and magnesium oxide) were mixed, pelletized and fired. The fired material was checked with X-ray diffraction to ensure that reaction of the precursor oxides was complete. The material was spray-dried, then pressed (6,000 psi) into monolithic form and fired to 670K. After cooling, holes were drilled and the material was fired again to 1,823K. This process produced a very dense monolith of low surface area and showed strains induced by the drilling. It is not an optimum process for producing combustion monoliths. Making active monoliths (mixed metal oxides) is a new technology, and the current monolith manufacturing process leaves much to be desired.

The ATT-B monolith looked the same, visually, before and after oven testing. This is not surprising, since the monolith was fired at a higher temperature than the oven test, and remained at that temperature for an extended time. SEM inspection shows posttest surfaces having larger sinter planes than pretest surfaces (figures 4-2 and 4-3). Posttest samples seemed to be slightly enriched in nickel compared to pretest samples, but the difference was insignificant.

## ATT-C

This monolith was manufactured in the same way as the previous monolith, pressed from the reacted powder, sintered, drilled, and resintered. An active monolith of this type had not previously been combustion-tested, but combustion tests of $LaCrO_3$ on alumina were very good (see description under ATT-E). Posttest visual inspection of this catalyst showed no change, as expected. Pretest and posttest SEM analysis

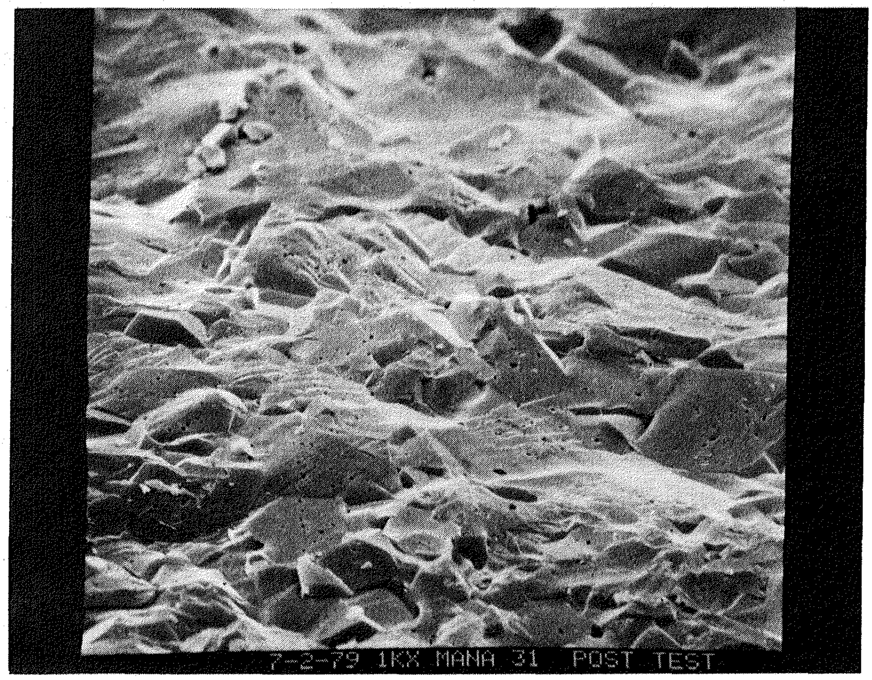

Figure 4-2. SEM Photograph, 1,000X Magnification, Surface of ATT-B Before Aging

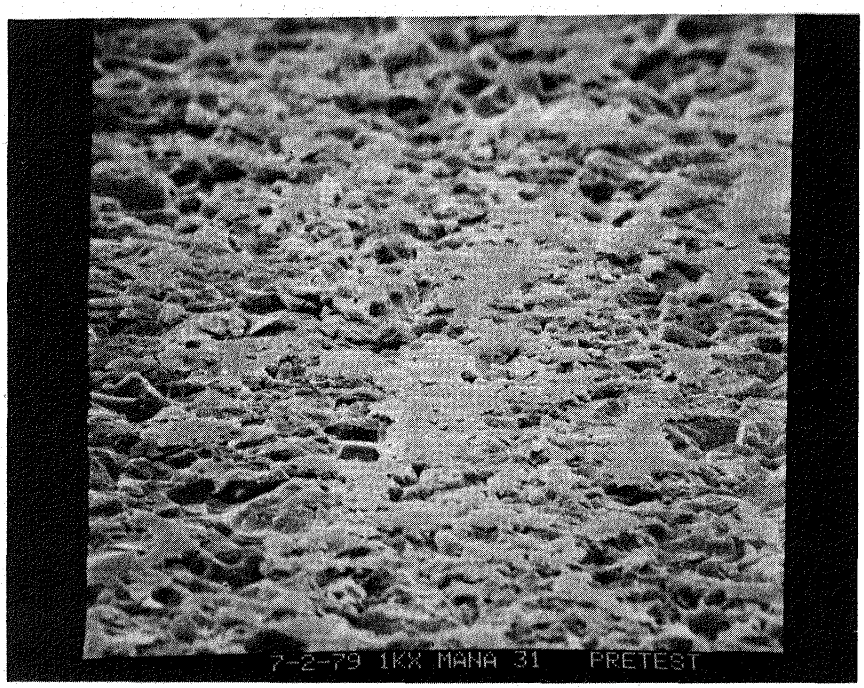

Figure 4-3. SEM Photograph, 1,000X Magnification, Surface of ATT-B After 24 Hours of Aging

showed a more granular surface posttest (figures 4-4 and 4-5). Pre- and posttest elemental analysis show the posttest sample to be depleted in chromium and alumina. In the light of this unexpected result, a fracture surface of the posttest sample was examined. In the fracture surface, lanthanum, chromium, and aluminum were present in quantities similar to the original amount.

It is difficult to explain these findings. A surface coating of lanthanum oxide seems to be present posttest. This would be understandable if the monolith were entirely $LaCrO_3$ -- it would mean that the more volatile chromium had evaporated. However, the absence of aluminum in the surface layer is much more difficult to understand, since aluminum oxide has no significant volatility. Any explanation would require a hypothesis involving migration. The forces driving such a migration are difficult to postulate.

## ATT-F

This monolith was manufactured the same way as the previous two monoliths: pressed from the reacted powders, sintered, drilled, and resintered.

This sample had "rusty" light-brown colored deposits on the surface, both pre- and posttest. It is hypothesized that these areas are $MgFe_2O_4$-type spinel (probably $MgAl_2O_4 \cdot MgFe_2O_4$ solid solution) in which all the iron is in the +3 oxidation state.

Pre and posttest SEM analysis showed a rough, crystalline surface for the bulk sample, and a more porous surface for the "rusty" sample (figures 4-6, 4-7, and 4-8). Pre- and posttest chemical analysis of rusty and nonrusty sections were the same within instrument reliability.

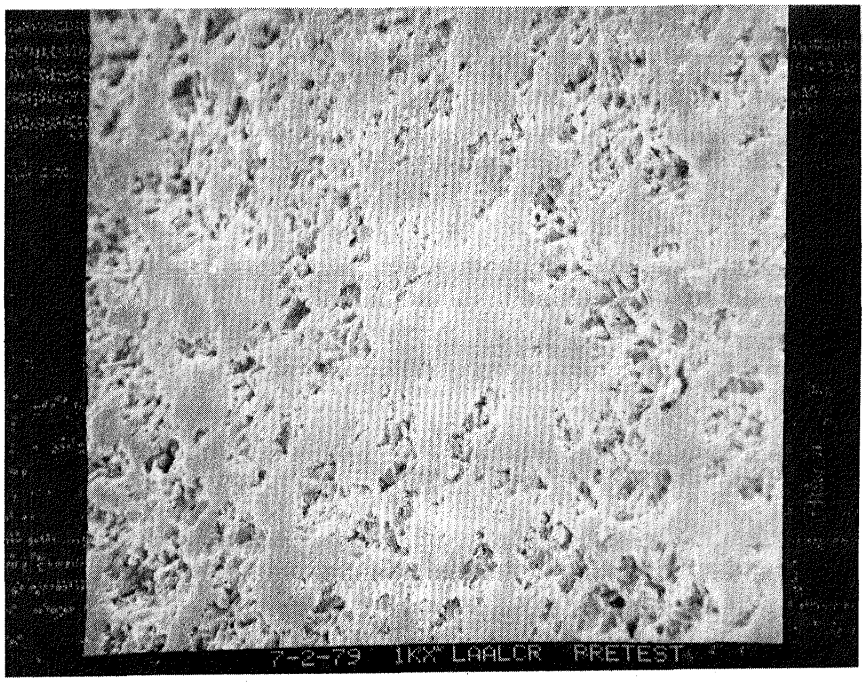

Figure 4-4. SEM Photograph, 1,000X Magnification, Surface of ATT-C Before Aging

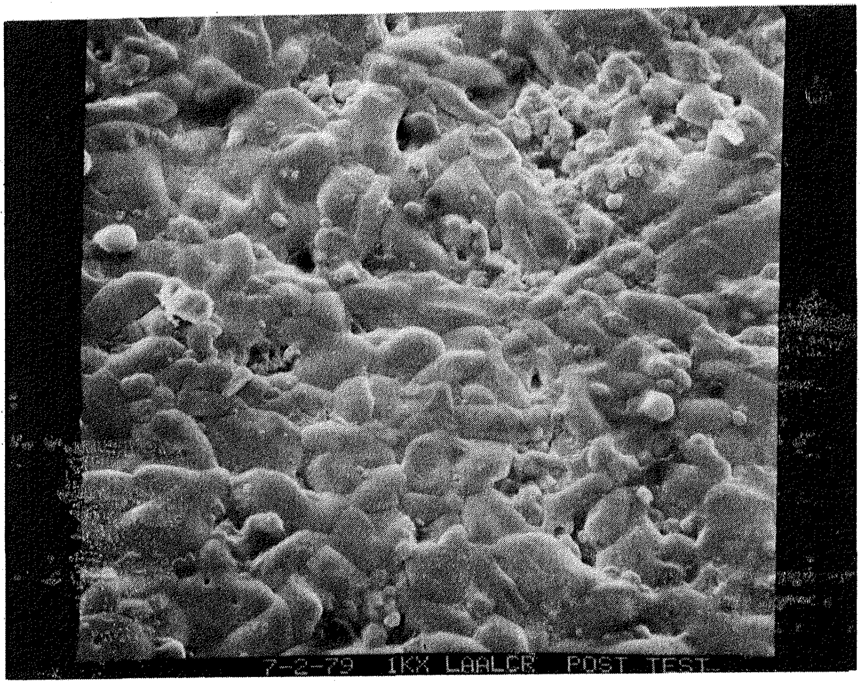

Figure 4-5. SEM Photograph, 1,000X Magnification, Surface of ATT-C After 24 Hours of Aging

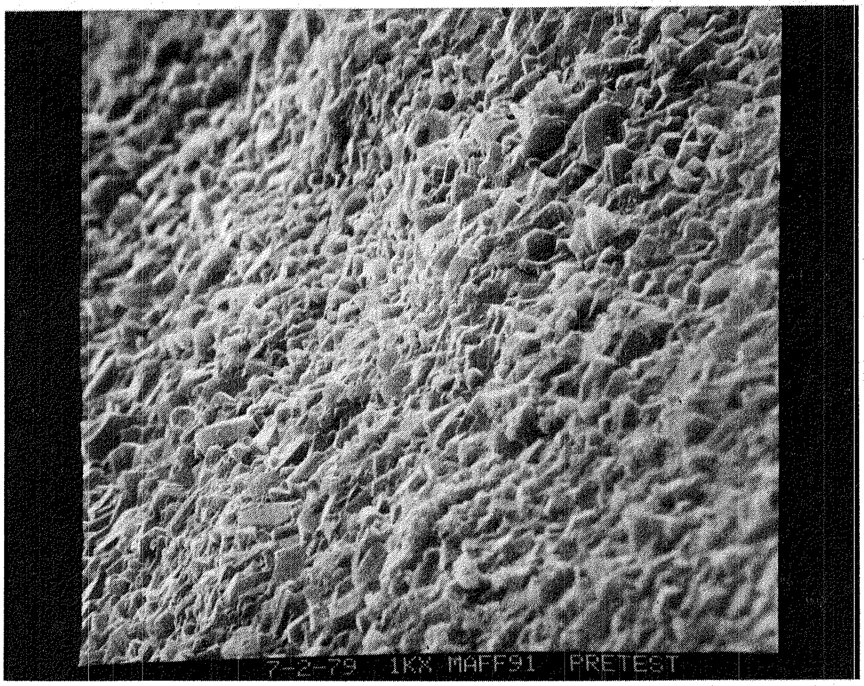

Figure 4-6. SEM Photograph, 1,000X Magnification, Surface of ATT-F Before Aging

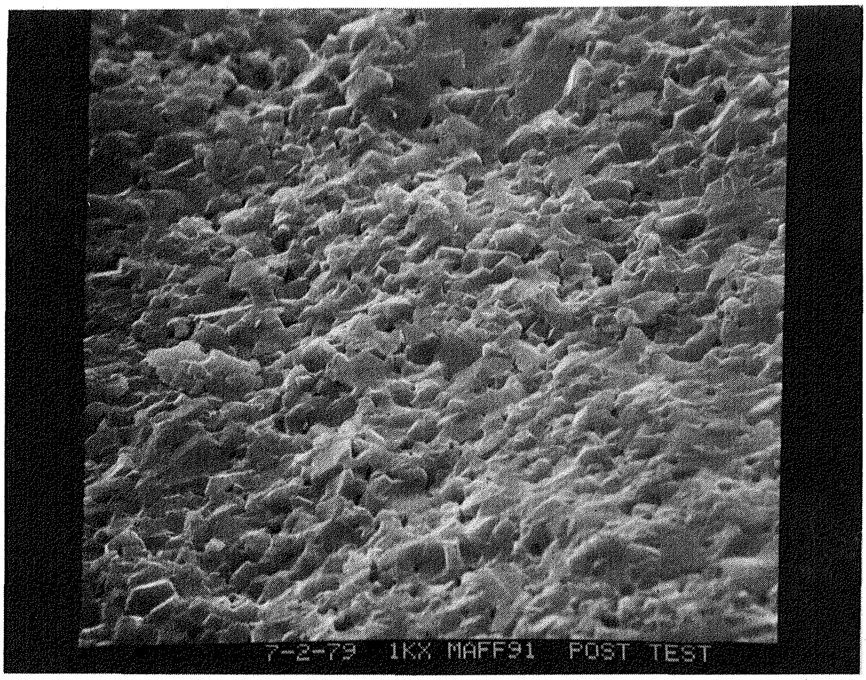

Figure 4-7. SEM Photograph, 1,000X Magnification, Surface of ATT-F After 24 Hours of Aging

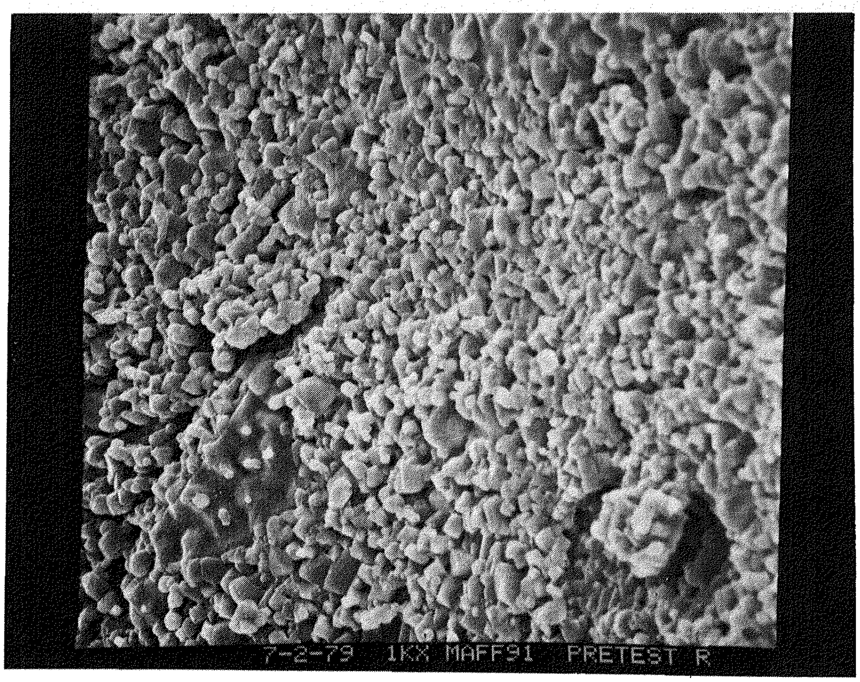

Figure 4-8. SEM Photograph, 1,000X Magnification, Surface of ATT-F After 24 Hours of Aging (Rusty Area)

## 4.4 SUMMARY OF PRELIMINARY FURNACE AGING RESULTS

The results of the preliminary furnace aging tests were not as conclusive as desired. In general, all of the materials survived the test with only minor observable damage. Since no combustion testing was performed conclusions about the combustion performance of each reactor could only be implied from the posttest characterization measurements and previous combustion experience with similar reactor concepts.

The posttest characterization measurements showed a significant decrease in BET surface area and catalyst dispersion (for noble metal reactors). Within the accuracy of the measuring apparatus, the BET surface area of all reactors was reduced to essentially zero due to the 24-hour exposure at 1,700K. Catalyst dispersion was reduced by about 96 percent compared to the pretest value for UOP-B whereas MBI-B was reduced only by about 60 percent. Except for UOP-A and UOP-C, which had exceptionally high pretest dispersions, the dispersions of all reactors with noble metals were reduced to about 0.2 to 0.4 $\mu$moles $H_2$/g.

For the noble metal group, UOP-A, UOP-B, UOP-C, MBI-B and HAP-A, the three that had Torvex substrates (UOP-A, UOP-C and MBI-B) appeared to have washcoat-to-substrate bonding problems. This was evidenced by blistering, flaking, or delamination of the washcoat and catalyst coating. The two reactors with MCB-12 substrates were visually good after the aging test.

For the second group of reactors (HAP-C, WRG-A, ATT-A, ATT-D, and ATT-E), two (WRG-A and ATT-D) volatilized significantly. The other three (HAP-C, ATT-A and ATT-E) showed little if any visual degradation from the aging test.

In the third group of reactors (OC-B, ATT-B, ATT-C and ATT-F), except for a slight darkening of OC-B, none showed any signs of degradation from the aging test.

The five nonproprietary reactors* were examined with an SEM and revealed a combination of physical and chemical changes to the surface of the reactors. The three active monoliths (ATT-B, ATT-C and ATT-F) showed little surface change from the aging test except for ATT-C which had a lanthanum oxide surface layer. The cause and significance of this layer is not clear. ATT-B appeared very good under pre- and posttest SEM examination; however there is very little knowledge of the catalytic activity of nickel aluminate at the design combustion conditions. The SEM appearance of ATT-F was very good except for the appearance of the rusty second phase which raises doubts on the stability of the parent substrate. ATT-A, which had a combination of platinum and nickel oxide for the catalyst, showed significant agglomeration of the platinum and some depletion of nickel due to the aging test. Likewise, posttest SEM examination of ATT-E showed a surface very similar to the pretest surface except for the presence of platinum agglomerates.

## 4.5 SELECTION OF MATERIALS FOR CATALYST SCREENING TESTS

Recommendations for materials to be included in the catalyst screening tests were based on the results of the preliminary furnace aging evaluation and available information on possible combustion activity of the reactors. Of the 14 reactors, 5 were selected for further evaluation. These 5 reactors and the rationale for their selection are shown in table 4-3. Based on the delamination problems of washcoats on

---

*The ATT series except for ATT-D

Table 4-3. Reactors Recommended for Catalyst Screening Tests

| Catalyst | Rationale |
|---|---|
| UOP-B | No visual degradation, significant previous combustion experience, modest post-aging dispersion |
| OC-B | Slight visual degradation, previous combustion experience, nonnoble metal coating |
| ATT-A | Slight catalyst depletion, previous combustion experience, modest post-aging dispersion |
| ATT-C | No visual degradation, previous combustion experience, developmental active monolith material |
| ATT-E | No visual degradation, previous combustion experience, nonwash-coated catalyst on Torvex alumina |
| MBI-D | MBI-B coating on MCB-12 instead of Torvex alumina |

Torvex alumina substrates, it was also recommended that the proprietary MBI coating be applied to an MCB-12 substrate for limited additional evaluation to determine if a better bond would be achieved on this material.

Shown in table 4-4 are the remaining nine reactors with rationale for why they were not recommended. The fact that a particular reactor was not recommended should not imply that the materials used are unacceptable. In fact, it is highly probable that slight changes in processing or formulation could result in significant improvements.

Table 4-4. Reactors Not Recommended for Catalyst Screening Tests

| Catalyst | Rationale |
|---|---|
| UOP-A | Poor bonding between coating and substrate |
| UOP-C | Poor bonding between coating and substrate |
| HAP-A | Poor combustion characteristics (reference 2) |
| HAP-C | Poor combustion characteristics (reference 2) |
| WRG-A | Coating volatilization |
| ATT-B | No previous combustion experience, not available in honeycombs |
| ATT-D | Material volatilization |
| ATT-F | No previous combustion experience, not available in honeycombs |
| MBI-B | Poor bonding between coating and substrate |

# SECTION 5

# CATALYST SCREENING TESTS

Additional samples of the reactors selected in section 4 were procured and evaluated in long-term aging and parametric combustion tests. Six 5-cm diameter by 7.6-cm long reactors of each material were to be furnace aged at 1,700K and combustion tested according to the test plan shown in figure 5-1. Five of these reactors were identified as samples "24," "250," "500," "750," and "1000." The sample "number" represented the number of hours that that sample was to be furnace aged. Where applicable, BET, catalyst dispersion, and SEM examinations were made on these furnace-aged samples. In order to permit furnace shutdown and sample removal to be done during the day shift, the actual aging times differ slightly from those planned. Thus, actual aging periods for the "24," "250," "500," "750," and "1000" samples were 24, 180, 430, 680, and 1,000 hours, respectively. The sixth sample was identified as sample "2000" to denote that this sample was to be aged for 1,000 hours and possibly combustion tested for an additional 1,000 hours. Parametric combustion tests were conducted on these "2000" samples following 24 and 1,000 hours of aging.

Based on the recommendations from the preliminary aging tests, complete sets of four reactor concepts (UOP-B, ATT-A, ATT-C, and OC-B) were prepared. Incomplete sets of material for an MBI-D and ATT-E were

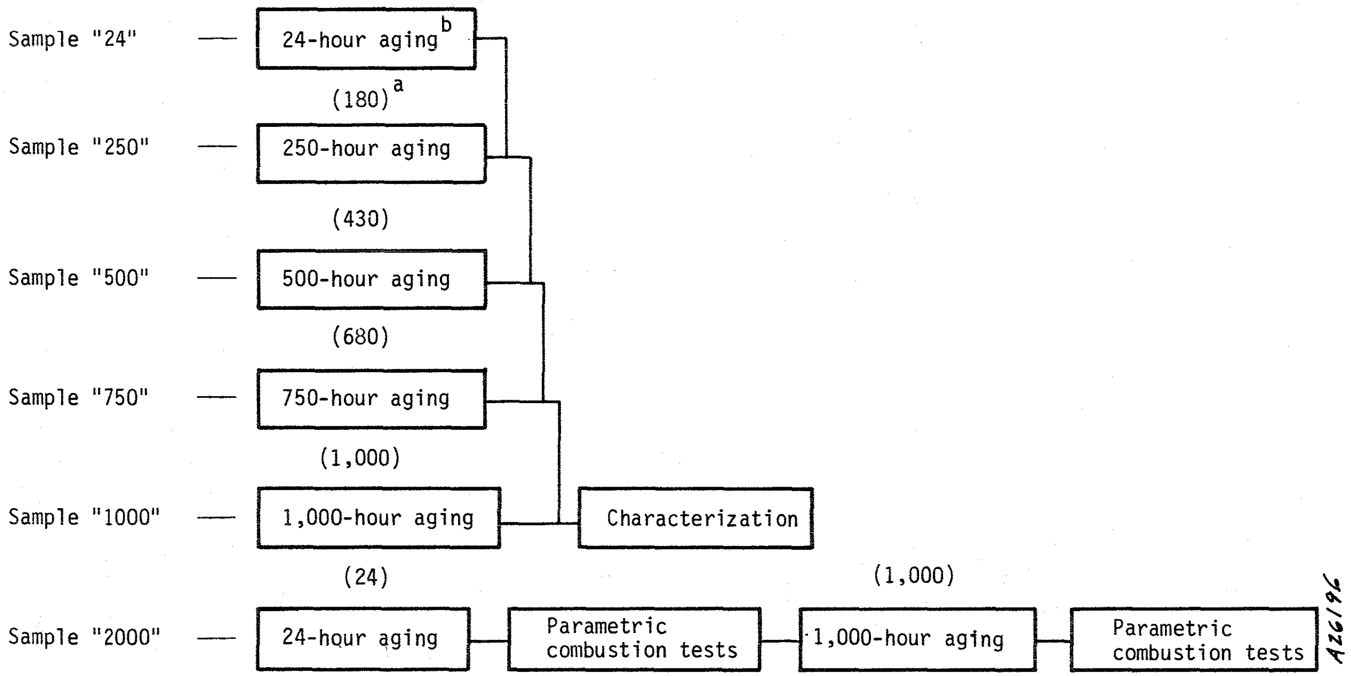

[a] Numbers in parentheses indicate actual furnace aging hours
[b] Planned cumulative aging time

Figure 5-1. Furnace Aging and Combustion Screening Test Plan also prepared. Because of delays in receiving MBI-D, it was aged only for 180, 430, and 680 hours. Also, only a limited amount of ATT-E was available in tube form; therefore, no samples were obtained for the 180-, 430-, and 680-hour aging conditions.

Except for the time-at-temperature, furnace aging conditions were identical to those used in the 24-hour evaluation. At the end of each test period the furnace was cooled and appropriate samples were removed; the furnace was then reignited for the next test period.

## 5.1 FURNACE AGING TEST RESULTS

### UOP-B

As received, the UOP-B surface was uniformly black in color and the substrate appeared to be virgin parent material. There were local regions where the coating developed a dried mud-cake appearance apparently due to an excessively thick coating. Qualitatively, the strength of the substrate, as determined by breaking off small samples, appeared to degrade as a function of aging time. After 180 hours of aging, the substrate remained light in color showing that there was little, if any, penetration of catalyst into the substrate. The surface was not as dark and developed a somewhat silvery appearance which was assumed to be due to noble metal agglomeration. Otherwise, the catalyst appeared in good condition.

After 430 and 680 hours of aging the surface color became lighter and more silvery. After 1,000 hours, the surface was light gray and mottled in appearance. Larger, shiny crystals appeared on the sides of the catalyst and could be easily flaked off. Apparently significant agglomeration and possibly vaporization of the noble metal occurred during the aging tests.

## OC-B

The OC-B coating was light yellow in color and appeared uniformly bonded to the substrate. SEM examination showed that the coating completely covered the substrate. The physical structure of the surface had the dried mud-cake appearance shown in figure 5-2. After 24 hours of aging, the structural stability and catalyst adherence remained excellent; however, the surface color became lighter. SEM examination showed the formation of spherical nodules (figure 5-3) of catalyst material. The nodules increased in size as the aging time increased as shown in figures 5-4 and 5-5. After 680 hours, the color was uneven and with the SEM, small regions of substrate could be detected. After 1,000 hours, silicon (probably as silica) was detected on the surface and probably comes from the furnace refractory material or the silicon carbide radiation shields.

## ATT-A

ATT-A was a nickel oxide (NiO) catalyst on an MCB-12 honeycomb. One of the three 1-inch thick elements also had 1.5 weight percent of platinum (Pt) and would be the lead element of the reactor. The pretest NiO elements had a uniform light green color; however, the NiO/Pt element had a black and green-black color. The black was characteristic of platinum and SEM/Kevex analysis showed that the green-black color was probably inefficiently calcined platinum hexachloride and nickel oxide. Examination of a fracture surface showed good penetration of NiO into the substrate and a moderate penetration of platinum. The most significant element would be the lead element with NiO/Pt. Although all elements were examined, the remaining observations are based on the lead element samples. Similar comments apply to the NiO elements with all references

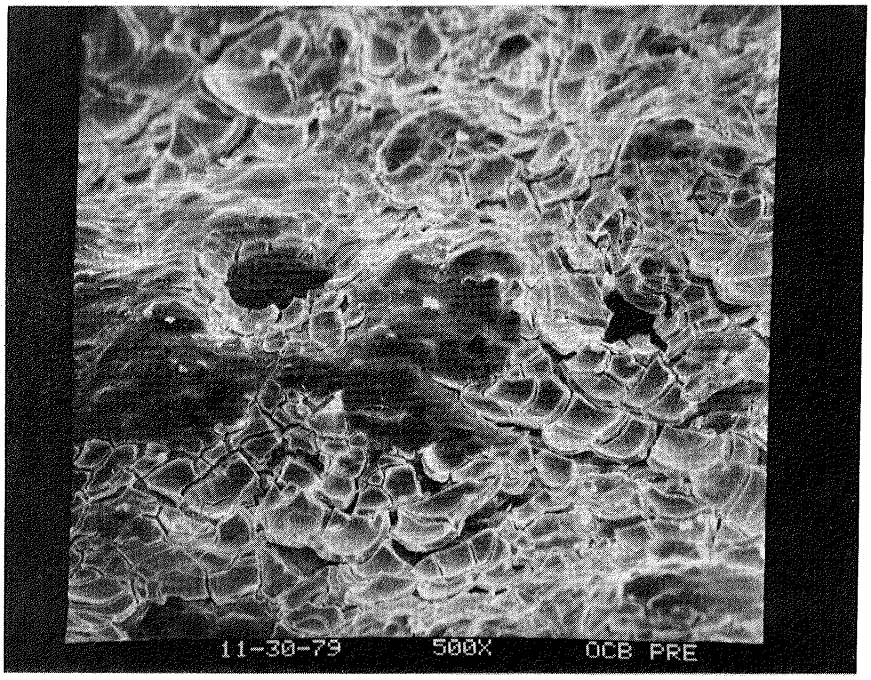

Figure 5-2. SEM Photograph, 500X Magnification, Surface of OC-B Before Aging

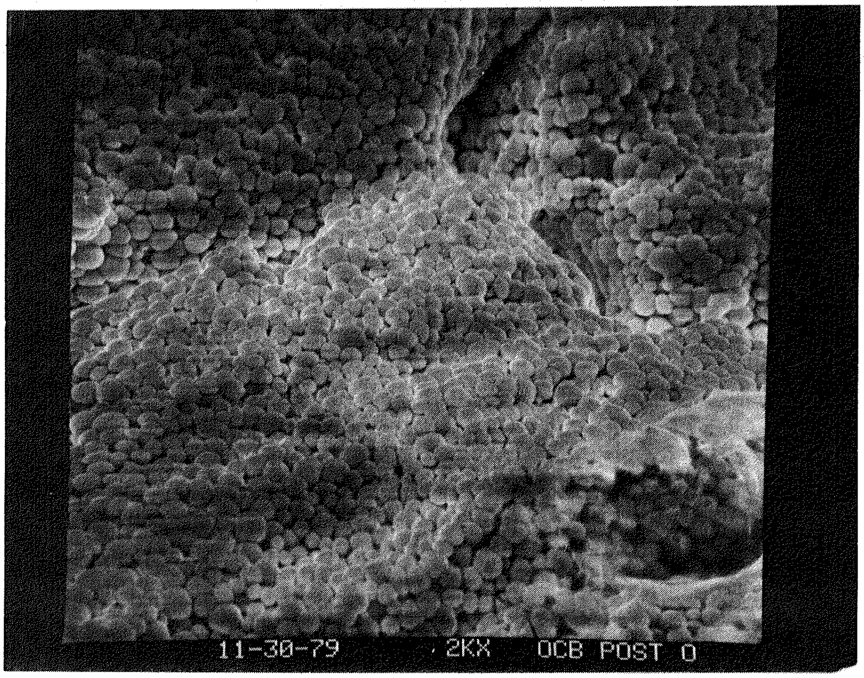

Figure 5-3. SEM Photograph, 2000X Magnification, Surface of OC-B After 24 Hours of Aging

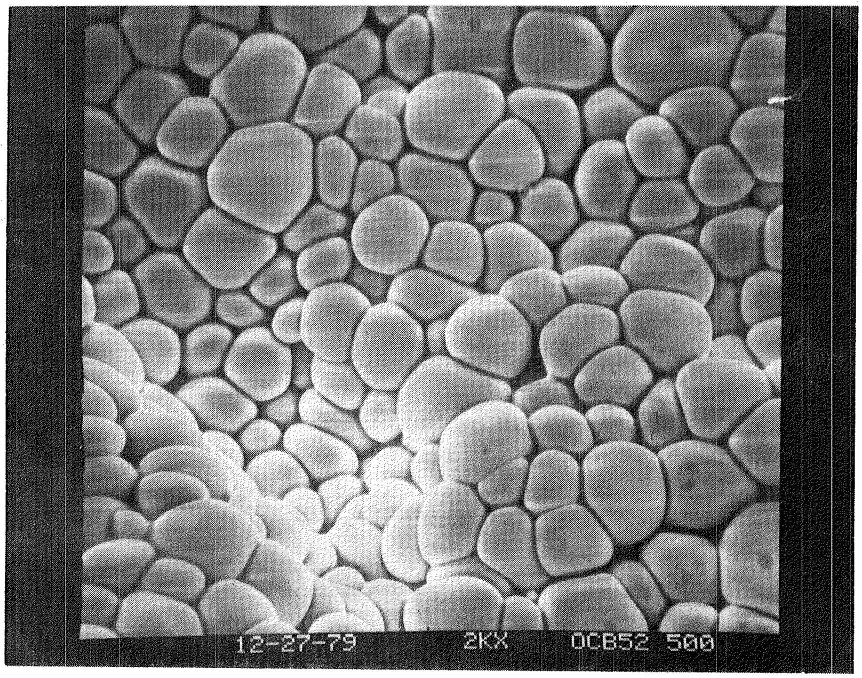

Figure 5-4. SEM Photograph, 2000X Magnification, Surface of OC-B After 430 Hours

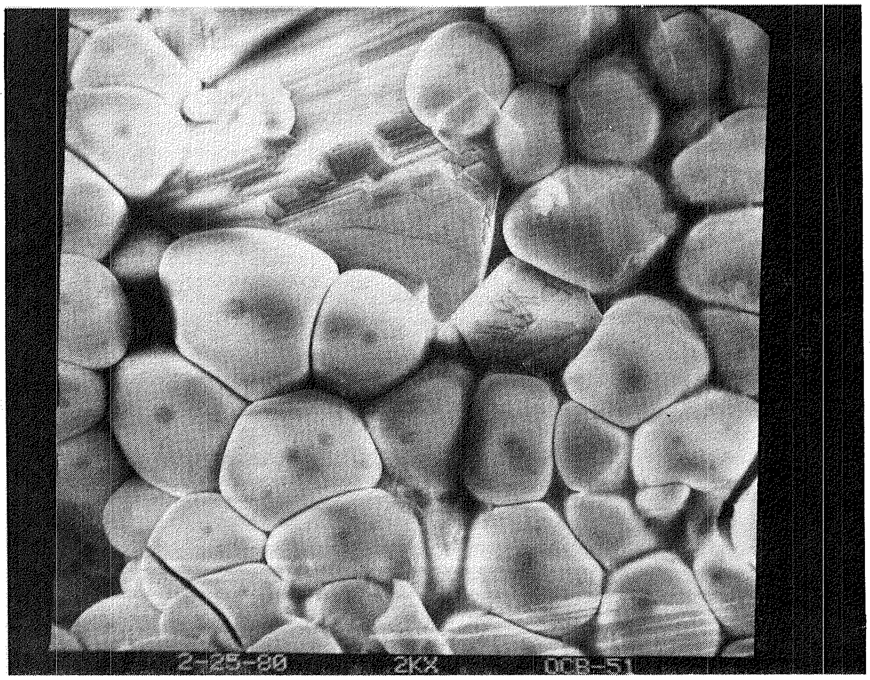

Figure 5-5. SEM Photograph, 2000X Magnification, Surface of OC-B After 1000 Hours of Aging

to Pt deleted. A pretest SEM of the lead element surface is shown in figure 5-6.

After 24 hours of furnace testing, the catalyst had a nice, even grey appearance, with good adherence of catalyst to the substrate. The fracture surface had a green-grey color characteristic of the NiO/Pt mixture. The posttest SEM, figure 5-7, and elemental analysis show a material which appears fully calcined (no chloride is present), and a NiO surface with platinum agglomerates.

After 180 hours of furnace testing, the catalyst visually appeared much as it did after 24 hours; however, the monolith was relatively easy to break. The SEM showed a surface different from that of the post-24-hour furnace test. Crystal sizes increased with aging times as can be seen by comparing figures 5-7, 5-8, and 5-9. Elemental analysis showed that this surface contained Mg, Ni, and Pt. The magnesium and nickel may have been forming a mixed-metal oxide and the extensive interaction of nickel with the substrate considerably weakened the monolith. This would explain the growth of the crystals and elemental composition. $NiAl_2O_4 \cdot MgAl_2O_4$ is the most probable mixed-metal oxide. Large areas of silvery platinum agglomeration also occurred on the outside of the monolith.

After 430 hours of furnace testing, the material was fragile and lighter green in color. Visual and SEM examination (figure 5-8) showed considerable platinum agglomeration over a surface essentially depleted in nickel. It was assumed from the even gray-green color of fracture surfaces of the monolith that considerable nickel interaction with the substrate had taken place. There was no substantive change after 680 hours, though platinum-rich and crystalline areas of nickel substrate

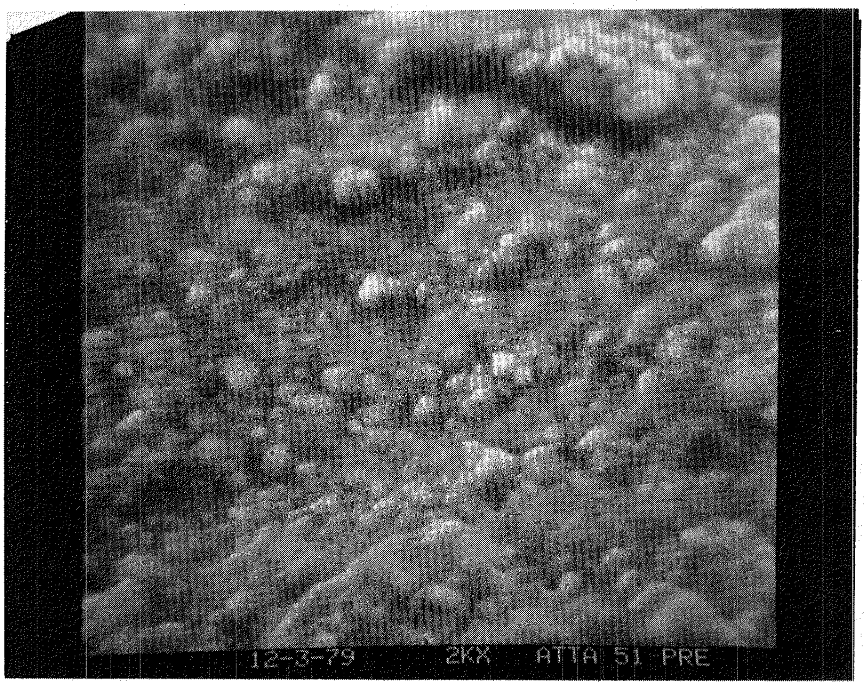

Figure 5-6. SEM Photograph, 2000X Magnification, Surface of ATT-A Before Aging

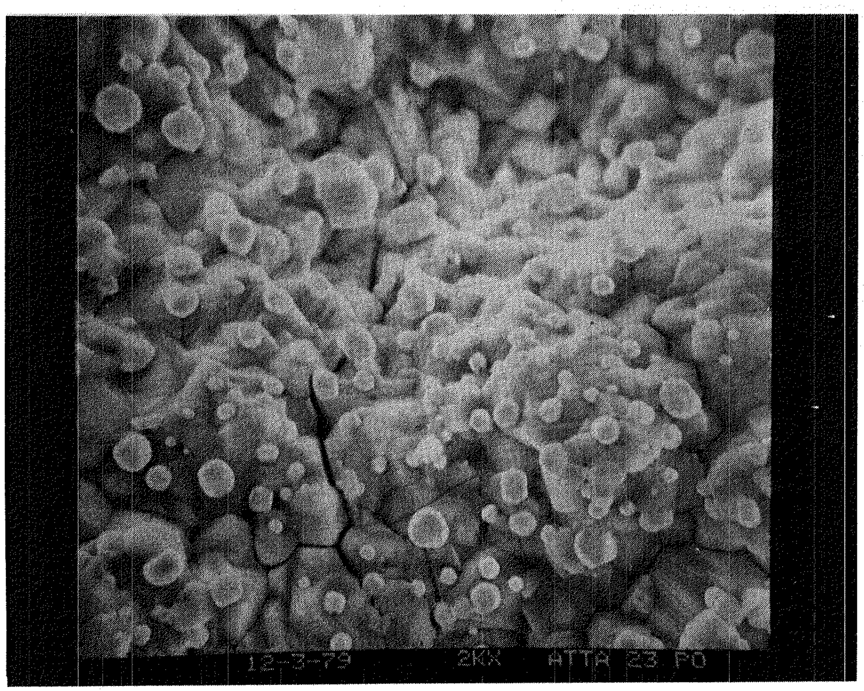

Figure 5-7. SEM Photograph, 2000X Magnification, Surface of ATT-A After 24 Hours of Aging

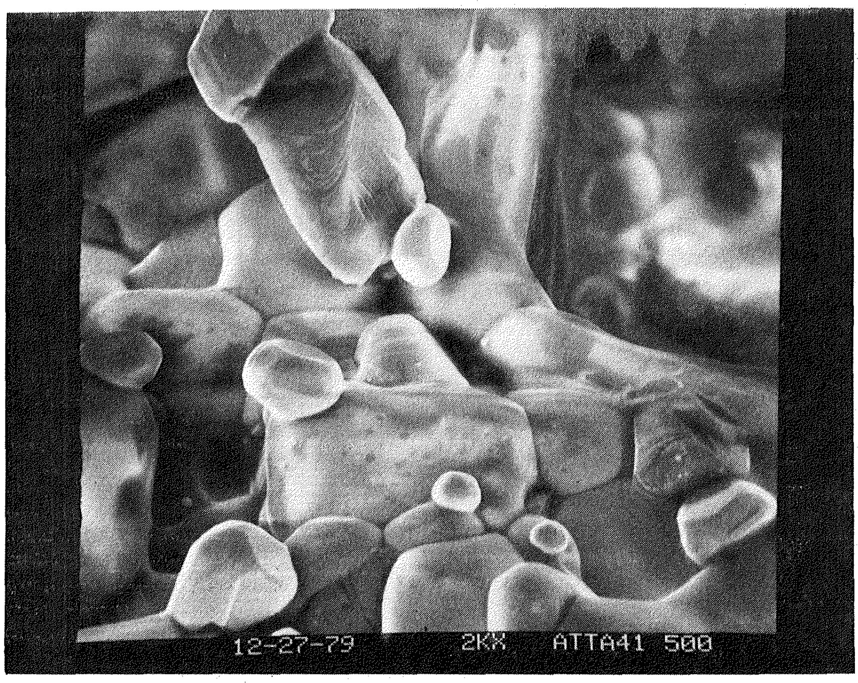

Figure 5-8. SEM Photograph, 2000X Magnification, Surface of ATT-A After 430 Hours of Aging

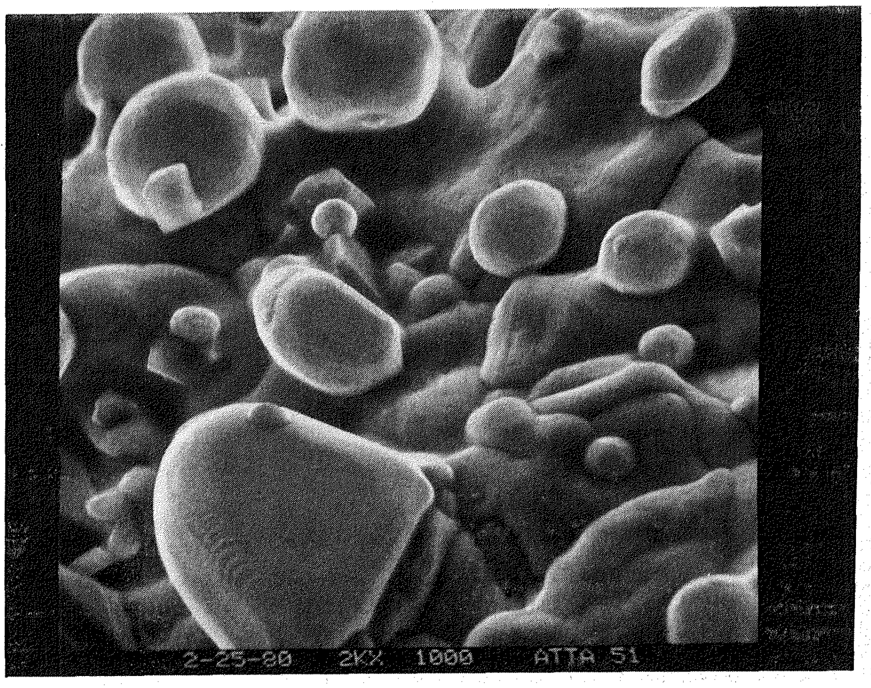

Figure 5-9. SEM Photograph, 2000X Magnification, Surface of ATT-A After 1000 Hours of Aging

solid solution were identified. After 1,000 hours, the material looked essentially the same (figure 5-9).

### ATT-C

ATT-C was not available in honeycomb form and was tested as a bundle of tubes to "simulate" a honeycomb. Unfortunately, the original batch of material was prepared with an insufficient amount of chromium and an excess of lanthanum. Lanthanum oxide is very hygroscopic, and reverted to powder upon long exposure to ambient air. Some of these samples, on the verge of crumbling, were examined with SEM/Kevex and showed considerable porosity and virtually no chromium.

New samples were prepared and verified to contain lanthanum and chromium. The SEM analyses of pretest and post-1,000-hour test samples are shown in figures 5-10 and 5-11. Kevex showed posttest regions that were high in silicon resulting in a "smooth" appearing surface. It is clear that silicon, probably as silica, is an artifact of the furnace testing procedure. Examination of some surface crystalline areas also showed a depletion of lanthanum and raises questions about the stability and homogeneity of the catalyst.

### ATT-E

Pretest visual examination of the ATT-E catalyst showed a very uneven colored coating -- the catalyst was mostly grey, but regions of pink, brown, and green surfaces were visible. The catalyst showed a considerable flaking tendency, probably due to delamination of the Torvex alumina.

SEM examination of the pretest catalyst (figure 5-12) showed crystals; X-ray analysis showed these crystals to be platinum sulfide. Elemental analysis of other areas showed a mixture of lanthanum, chromium,

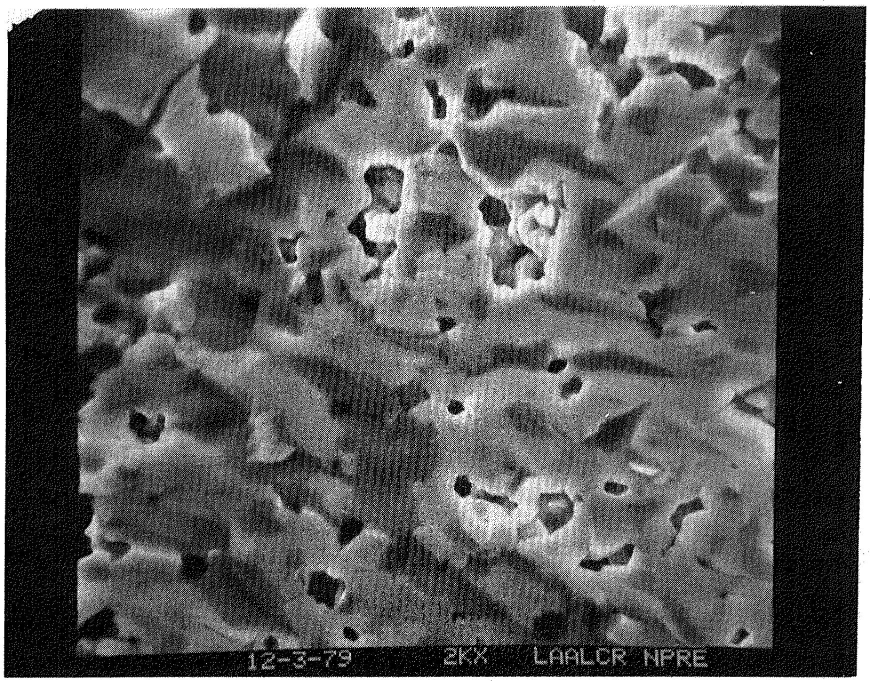

Figure 5-10. SEM Photograph, 2000X Magnification, Surface of ATT-C Before Aging

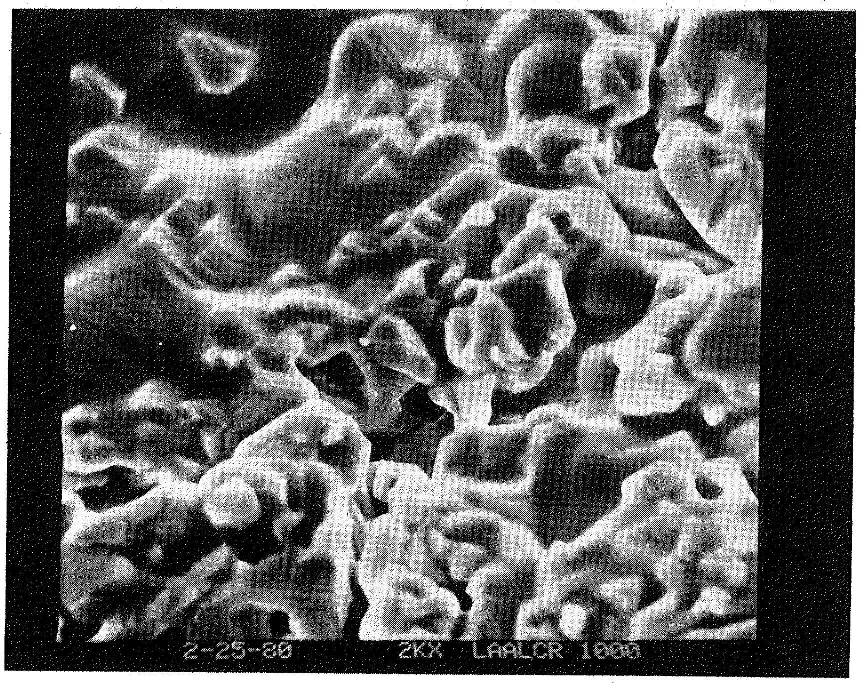

Figure 5-11. SEM Photograph, 2000X Magnification, Surface of ATT-C After 1000 Hours of Aging

Figure 5-12. SEM Photograph, 2000X Magnification, surface of ATT-E Before Aging

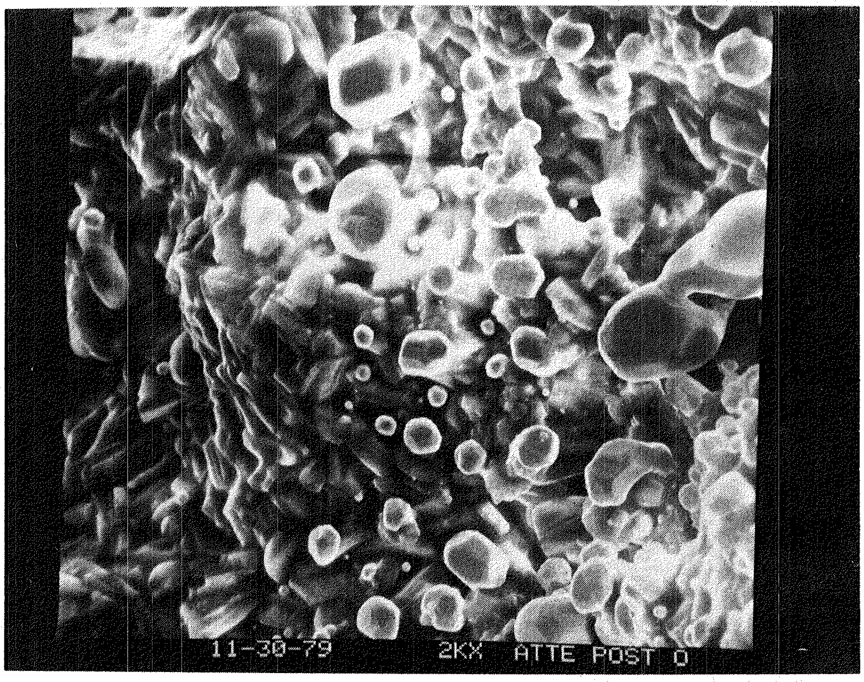

Figure 5-13. SEM Photograph, 2000X Magnification, Surface of ATT-E After 24 Hours of Aging (Grey Area)

platinum, sulfur, and chlorine. The presence of sulfur and chlorine is indicative of incomplete calcining when the catalyst was prepared.

After the 24-hour furnace test, the catalyst was greyer and more even in appearance. However, some greenish material was present but there appeared to be less of the loosely adhering material. Both grey and green areas were examined by scanning electron microscope and elemental analysis. The grey area (figure 5-13) contained lumps of a glassy (Si,Al) material. The general background showed a depletion in La, Cr, and Pt compared to the pretest sample. Complete calcining has taken place, as evidenced by a lack of sulfur and chlorine in the posttest elemental analysis.

The green portion of the material was also examined. Its appearance under SEM was substantially different from the grey portion (figure 5-14). Especially notable were the multifaceted crystals which were analyzed and found to be mostly platinum. Usually, platinum agglomerates into more rounded shapes so these faceted crystals were considered unusual. The background of the green sector was analyzed and had more chromium present than the grey portions of the catalyst. The presence of excess chromium oxide, unreacted with lanthanum, and perhaps in solid solution with alumina, would account for the green color.

After 180 hours of furnace testing, the structure of the catalyst was unchanged; problems with Torvex delamination continued, but did not increase. Some shiny areas of platinum agglomeration appeared on the outside of the catalysts. The catalyst showed a mottled appearance -- mostly grey, but with purple areas and light areas. After 430 hours of testing there was no significant difference from the 180-hour samples

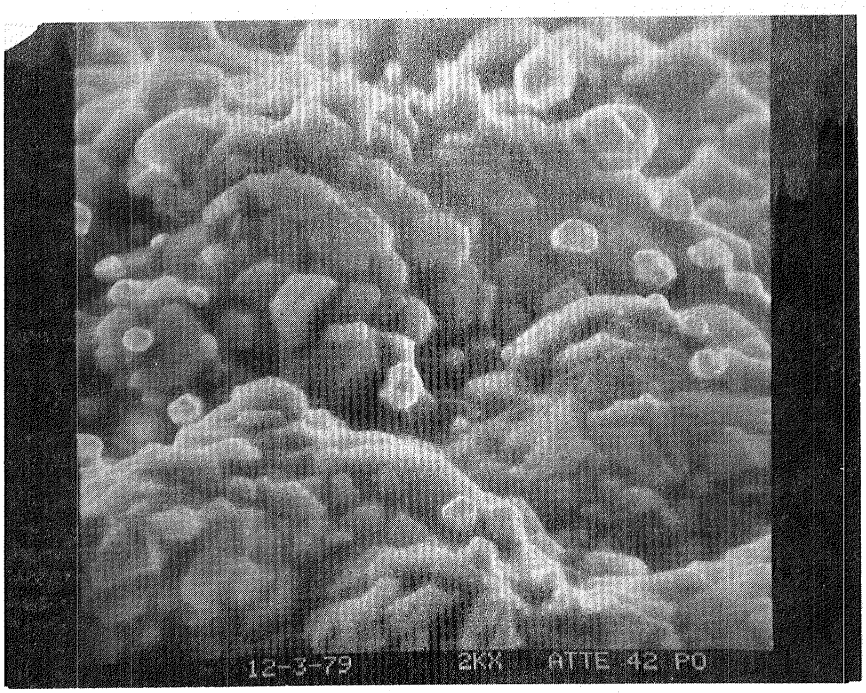

Figure 5-14. SEM Photograph, 2000X Magnification, Surface of ATT-E After 24 Hours of Aging (Green Area)

Figure 5-15. SEM Photograph, 2000X Magnification, Surface of ATT-E After 430 Hours of Aging (Purple Area)

except for some bright purple areas. These and the more general grey background were examined by SEM and Kevex elemental analysis.

The purple areas of the catalyst (figure 5-15) showed an irregular surface which, when analyzed, contained aluminum and chromium with small amounts of platinum and no lanthanum. The purple color was due to the formation of a chromia-alumina solid solution. The grey area of the catalyst (figure 5-16) showed the presence of chromium and lanthanum and considerable amounts of platinum. Shiny platinum particles covered much of the surface.

The 680-hour test samples looked the same, except that the three catalyst elements had sintered or fused together. Apparently, extended times at these elevated temperatures caused the alumina substrate to become slightly plastic; pieces that carried weight partially collapsed, and separate pieces sintered together. Otherwise, the 680-hour sample visually resembled the grey areas of the 430-hour sample.

The SEM and Kevex of the 680-hour sample showed quite a different story. The surface was depleted in platinum and chromium, and looked quite different from the surface after 430 hours. It is unwise, however, to draw too general a conclusion from this, since the 180- and 430-hour test samples showed considerable lack of homogeneity.

After 1,000 hours, the surface was variegated in color. The "background" area was examined by SEM (figure 5-17), as was the "blue" area (figure 5-18). The background was deficient in platinum and chromium compared to the original, containing considerable amounts of glassy magnesia and silica impurities, and some platinum crystals.

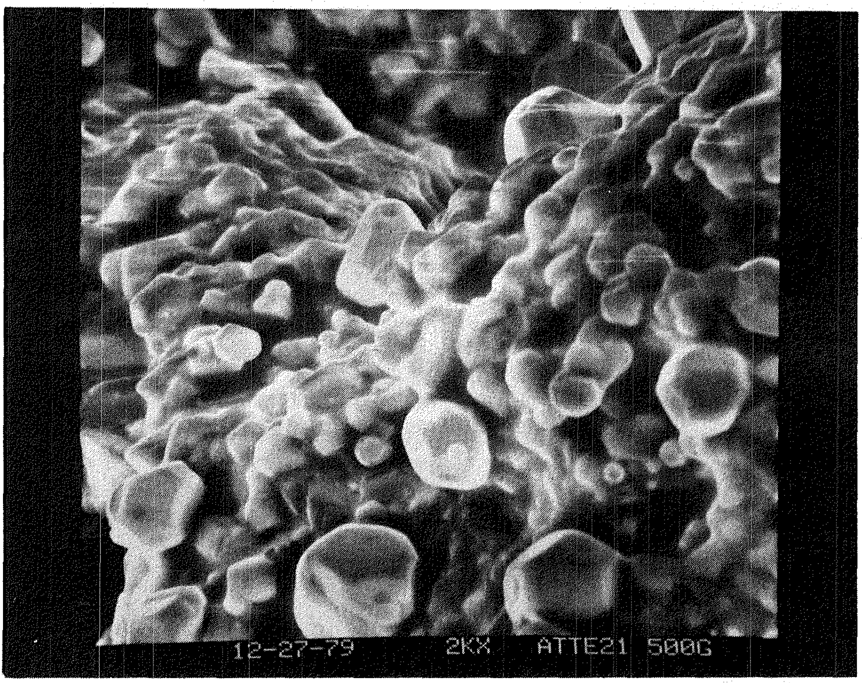

Figure 5-16. SEM Photograph, 2000X Magnification, Surface of ATT-E After 430 Hours of Aging (Green Area)

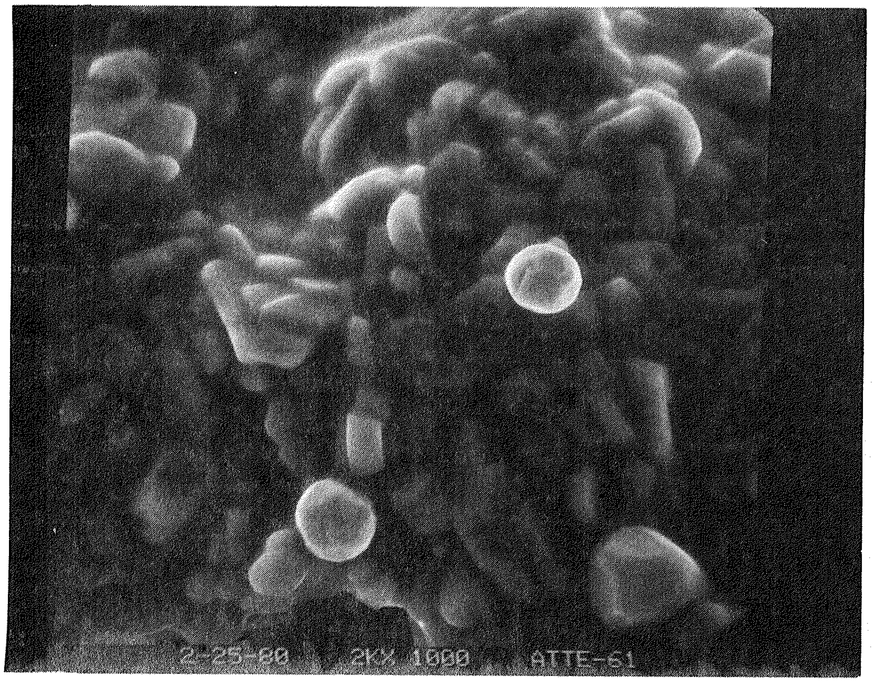

Figure 5-17. SEM PHotograph, 2000X Magnification, Surface of ATT-E After 1000 Hours of Aging

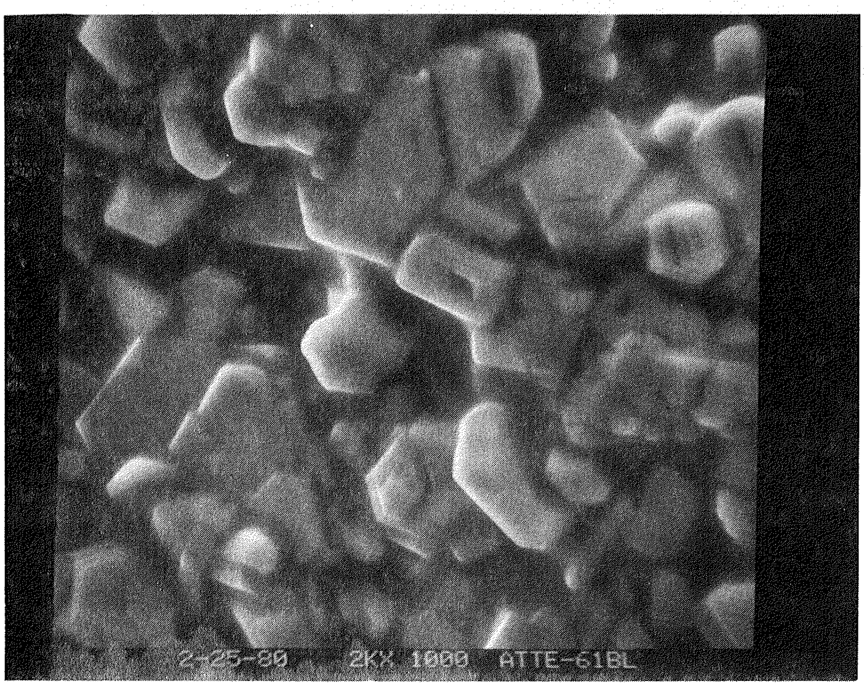

Figure 5-18. SEM Photograph, 2000X Magnification, Surface of ATT-E After 1000 Hours of Aging (Blue Area)

The blue area's surface had no platinum crystals, but contained iron, nickel, and thoria as impurities. The surface consisted of crystals of alumina and lanthanum in a glassy matrix.

The main conclusion is that these catalysts take on inconsistent coloration when formed and remain nonhomogeneous throughout the test matrix. It is difficult to tell which SEM and Kevex result can be ascribed to the test conditions and which are due to nonhomogeneity of sample taking.

### MBI-D

The original MBI-B material was a noble metal catalyst on Torvex alumina. Delamination of the Torvex was so severe that it did not seem appropriate to totally reject the catalyst on the basis of tests on so poor a substrate. It was recommended that the catalyst be reformulated on MCB-12, and submitted to an abbreviated test matrix.

MBI-D catalysts were formulated on both flex-cell and square cell MCB-12 honeycomb. As received, they were an even grey color. After 24 hours of furnace aging, they were lighter in color, but maintained good structural stability, with no flaking.

After 180 hours, this catalyst had a very uneven and mottled appearance. The structural integrity was good, but the material appeared more fragile than the untested material. The 430-hour sample was more uniform in color, and slightly darker. The 680-hour catalyst was substantially lighter in color than the 430-hour catalyst. Its color was uneven, but its physical integrity was good. After 1,000 hours of oven testing, the catalyst had some structural problems (cracking at the corners), and was uneven in appearance. Overall, it was darker than the UOP catalyst.

## 5.2 PARAMETRIC COMBUSTION TEST RESULTS

Parametric combustion tests were attempted on the six catalytic reactor systems included in table 4-2. These tests were attempted after 24 hours and 1,000 hours on the "2,000" sample as shown in figure 5-1. The general operating procedure for each test included a combustion conditioning period of about 1/2 hour at the maximum temperature. This was done at the beginning of a test following light-off in an attempt to eliminate catalyst performance changes during parametric measurements. Such changes have been noted during testing in other programs but the catalysts usually reached a steady condition within 1/2 hour.

Three segments of each monolithic type catalyst were stacked to form reactors 6.35 cm in diameter by 7.62 cm in length. The 2.54 cm thick segments all had effective cell diameters of approximately 0.32 cm. In the case of the Trans-Tech tubes, the reactor consisted of a tube bundle 5.08 cm in diameter by 7.62 cm in length. The bundle was oriented so that the tube axes were parallel to the reactant flow stream. Bed temperature measurements were taken by up to six R-type thermocouples placed within the bed as shown in figure 2-8. Emissions samples were taken with a watercooled stainless steel gas sample probe placed approximately 20 cm downstream of the catalyst bed exit. Species concentration measurements for $CO_2$, CO, $O_2$, $NO_x$, and unburned hydrocarbons were done with flow analyzers in the Acurex emissions bench.

The parametric testing was designed to evaluate aged catalyst combustion performance as well as the structural integrity of the substrate material. The measurements were conducted in the Acurex catalytic test facility at 1 atmosphere pressure with no. 2 diesel fuel. The nominal preheat temperature of the incoming combustion air was 800K.

However, two catalyst sets, the Trans-Tech tubes and the OxyCat monoliths, were tested at a lower preheat of approximately 700K due to facility limitations at that time.

The thermocouple which measured the preheat temperature was placed downstream of the liquid fuel nozzle and ahead of the catalyst reactor. As such, the measured temperature reflected the dilution and vaporization effect of the liquid fuel and ranged from 761K to 783K for the remaining catalyst tests. The target velocity of the incoming reactant mixture to the catalyst bed was 15 m/s based on the measured preheat temperature and 1 atmosphere pressure. Measurements at this velocity were attempted in all tests. Where catalyst activity was not sufficient to maintain combustion, the velocity was reduced to enhance stability.

The primary variable in the parametric testing was the air-fuel ratio of the reactant mixture. This was varied so that emissions measurements and observations could be made at catalyst bed temperatures ranging from a maximum of 1,700K down to 1,200K in increments of approximately 50K.

### 5.2.1 Parametric Combustion Tests, After 24 Hours of Furnace Aging

The following paragraphs describe the results of parametric combustion tests on sample "2000" following 24 hours of furnace aging. Operating procedures are given when they differ from the general techniques. Also discussed are the observations and measurements for each test.

#### ATT-C

This test was performed on the oven-aged catalytically active $LaAlO_3 \cdot LaCrO_3$ tubes. Each tube was 7.62 cm long and 0.635 cm in diameter. As described, the reactor was fashioned from a tube bundle with an overall diameter of 5.08 cm. The tubes were placed vertically in a cast refractory catalyst holder within the combustor housing. The mounting was designed to be nonrigid so that thermal expansion would not cause excessive damage. A 1.27 cm thick Torvex alumina honeycomb supported the bundle. Due to the smaller size of the reactor and its nonrigid configuration, only one thermocouple was used to measure the bed temperature. This thermocouple was located in the center of the reactor.

The air-fuel mixing duct upstream of the catalyst for this test was constructed of quartz tubing to allow a view of the catalyst front face. To prevent radiant heat loss, the tube was insulated with refractory fiber through which a small view window was cut. Catalyst performance was judged not only from emissions and bed temperature measurements, but also from the visual uniformity of both front and back faces of the catalyst.

Combustion lightoff was first attempted catalytically by passing preheated, premixed air and fuel over the reactor bed. This was unsuccessful so a second attempt involved the use of a propane torch to light the aft end of the catalyst bed. However, this too was not fully successful as combustion would not stabilize within the reactor.

Apparently, the low amount of catalyst activity prevented the reaction from moving completely into the bed. Instead, combustion remained downstream both in the gas phase and on some exit surfaces including the platinum thermocouple wires. Following these attempts, the test facility was set up with an opposed jet upstream of the reactor which was very successful in the EPA program (reference 2) in achieving a rapid and uniform ignition of catalyst beds. Although the catalyst was lit off fully and uniformly with the opposed jet, combustion performance quickly degraded when the jet was turned off.

The test data are shown in table 5-1. As previously described, the measured preheat temperature throughout this test was approximately 700K ($800^{o}F$). Opposed jet light-off was first done at the face velocity of 15.24 m/s (50 ft/s) and data point 1 shows readings taken almost immediately after the opposed jet was shut off. Performance degraded rapidly without support from the opposed jet and the front face darkened due to insufficient heat release on the catalyst. Within 10 minutes after the opposed jet was shut off, both faces were dark, the bed temperature was only slightly above the preheat level, and the CO and hydrocarbon emissions were very high. Similar performance was exhibited after light-off at a face velocity of 10.76 m/s (35 ft/sec) shown by data point 2. The catalyst was reignited with the opposed jet at 8.84 m/s (29 ft/s). At this lower velocity the combustion stability and uniformity were improved, particularly at bed temperatures above 1,756K ($2{,}700^{o}F$). However, within about 7 minutes at data point 4, a dark inactive area appeared on the front face. The dark area did not seem to grow appreciably and the emissions remained steady until data point 5 where the fuel flow was reduced slightly. This was intended to bring the bed temperature closer to 1,700K. However, as 1,700K was approached, the bed temperature fell rapidly and both the front and back faces again became nearly fully dark. This was accompanied by increasing CO and UHC emissions as combustion within the bed faded.

The catalyst was lit off a fourth time at 7.35 m/s (24.1 ft/s) and the combustion was stabilized at over 1,700K. Data point 6 was taken at this condition. No visual nonuniformities were apparent and temperature and emission levels remained stable for over 10 minutes. It was noted earlier that the catalyst performance did not degrade significantly when

## Table 5-1 Parametric Test Data for ATT-C After 24 Hours of Furnace Aging

| Data Point | TA (Percent) | Air Flow (scfm) | Face Velocity (ft/sec) | Diesel Flow (lbm/min) | Heater Exit Temperature ($^oF$) | Preheat Thermocouple ($^oF$) | Bed Temperature Center ($^oF$) | Exit Thermocouple ($^oF$) | UHC (ppm) | CO (ppm) | $NO_x$ (ppm) | $CO_2$ (Percent) | $O_2$ (Percent) |
|---|---|---|---|---|---|---|---|---|---|---|---|---|---|
| 1 | 212 | 27.1 | 50.0 | $7.03 \times 10^{-2}$ | 1,130 | 819 | 2,800 | 2,159 | 17.0 | 22.5 | 9.6 | 7.2 | 12.0 |
| 2 | 207 | 19.0 | 35.3 | $5.03 \times 10^{-2}$ | 1,130 | 830 | 2,740 | 1,903 | 31.0 | 27.5 | 8.8 | 7.1 | 12.2 |
| 3 | 201 | 16.1 | 29.2 | $4.39 \times 10^{-2}$ | 1,130 | 800 | 2,750 | 1,956 | 11.0 | 17.5 | 11.5 | 7.4 | 11.6 |
| 4 | 211 | 16.1 | 28.8 | $4.19 \times 10^{-2}$ | 1,130 | 782 | 2,700 | 1,946 | 10.0 | 12.5 | 9.3 | 7.2 | 12.0 |
| 5 | 215 | 16.1 | 28.3 | $4.12 \times 10^{-2}$ | 1,130 | 760 | 2,550 | -- | 12.0 | 6.0 | 5.0 | 6.2 | 13.0 |
| 6 | 221 | 13.2 | 24.1 | $3.14 \times 10^{-2}$ | 1,130 | 809 | 2,600 | 1,833 | 10.0 | 12.5 | 7.0 | 6.7 | 12.3 |
| 7 | 212 | 26.7 | 49.5 | $6.93 \times 10^{-2}$ | 1,130 | 826 | 2,850 | 2,053 | 20.0 | 6.3 | 16.0 | 7.2 | 12.0 |
| 8 | 209 | 26.7 | 48.7 | $7.03 \times 10^{-2}$ | 1,130 | 808 | 2,650 | 2,195 | 14.0 | 17.5 | 9.5 | 7.0 | 12.2 |
| 9 | 201 | 26.7 | 48.6 | $7.30 \times 10^{-2}$ | 1,130 | 803 | 1,550 | 2,272 | 12.0 | 17.5 | 15.5 | 7.8 | 11.0 |

the reactant mixture was adjusted to give a nominal bed temperature of 1,700K or higher. Based on this observation, it was decided to increase the face velocity while holding the air-fuel ratio steady. This was successful and a face velocity of 14.94 m/s (49 ft/s) was reached as recorded at data point 7. However, an increased amount of downstream combustion was visible and this is apparent in the UHC and $NO_x$ emission measurements. Again, as the air-fuel ratio was adjusted to reduce the bed temperature, the combustion rapidly faded. Data point 9 was taken while the catalyst temperature was falling. The emissions analyzers and sample system do not react as quickly as the thermocouples so the poor emissions are not indicated in table 5-1.

In summary, the Trans-Tech tubes gave poor combustion performance below a catalyst temperature of 1,700K for a face velocity range of 7.35 m/s to 14.94 m/s. Furthermore, once a visual nonuniformity appeared, indicating an area of low activity, it was not possible to restore good performance by adjusting the air/fuel ratio or face velocity within the test range. The catalyst had to be relit with the upstream opposed jet to reestablish good combustion performance.

### OC-B

This and all subsequent tests were performed with three segment monolith catalysts as described earlier. In this test, as in the ATT-C test, facility limitations prevented testing at preheat temperatures significantly greater than about 700K (800$^{o}$F).

Table 5-2 shows that five in-depth thermocouples, designated R2 through R6, were used to measure the bed temperature. Figure 2-9 represents their placement with R2 at the top, R3 and R4 in the center segment, and R5 and R6 in the bottom segment. The measurement junctions

## Table 5-2. Parametric Test Data for OC-B After 24 Hours of Furnace Aging

| Data Point | TA (Percent) | Air Flow (scfm) | Face Velocity (ft/sec) | Bed $\Delta P$ (in. $H_2O$) | Preheat Temperature ($^oF$) | Catalyst Temperature | | | | | | UHC (ppm) | CO (ppm) | $NO_x$ (ppm) | $NO_x$ (Percent) | $CO_2$ (Percent) |
|---|---|---|---|---|---|---|---|---|---|---|---|---|---|---|---|---|
| | | | | | | R1 ($^oF$) | R2 ($^oF$) | R3 ($^oF$) | R4 ($^oF$) | R5 ($^oF$) | R6 ($^oF$) | | | | | |
| 1 | 239 | 23.8 | 30.9 | NA | 948 | -- | 2,430 | 2,600 | 2,600 | 2,650 | 2,650 | 2.0 | 10.0 | 4.2 | 5.7 | 14.0 |
| 2 | 240 | 16.6 | 20.8 | NA | 898 | -- | 2,470 | 2,600 | 2,620 | 2,620 | 2,630 | 1.0 | 8.8 | 5.2 | 5.9 | 13.7 |
| 3 | 175 | 8.6 | 10.5 | NA | 867 | -- | 2,540 | 2,650 | 2,650 | 2,650 | 2,630 | 0.0 | 12.5 | 21.0 | 7.5 | 11.5 |
| 4 | 194 | 8.6 | 10.3 | NA | 835 | -- | 2,402 | 2,525 | 2,525 | 2,520 | 2,510 | 0.0 | 8.8 | 8.8 | 6.8 | 12.5 |
| 5 | 226 | 8.6 | 9.8 | NA | 775 | -- | 1,310 | 2,420 | 2,430 | 2,430 | 2,420 | 0.0 | 6.3 | 5.8 | 6.1 | 13.5 |
| 6 | 226 | 8.6 | 9.5 | NA | 737 | -- | 1,200 | 1,350 | 1,850 | 2,100 | 2,550 | 0.0 | 7.5 | 5.5 | 5.9 | 13.7 |
| 7 | 240 | 16.6 | 21.2 | NA | 924 | -- | 2,450 | 2,560 | 2,570 | 2,560 | 2,600 | 25.0 | 18.8 | 4.3 | 5.9 | 13.6 |
| 8 | 240 | 16.6 | 20.4 | NA | 873 | -- | 2,470 | 2,620 | 2,620 | 2,660 | 2,650 | 15.0 | 12.5 | 4.2 | 6.0 | 13.5 |
| 9 | 240 | 16.6 | 20.2 | NA | 856 | -- | 1,150 | 1,250 | 1,300 | 1,320 | 2,050 | 25.0 | 50.5 | 6.5 | 5.9 | 14.0 |

of R3 and R5 were vertically aligned at one radial location while those of R2, R4, and R6 were at the same radial distance but on the opposite side.

This catalyst showed low activity during combustion testing, similar to the preceding Trans-Tech catalyst. Opposed jet light-off was first attempted at 15 m/s (50 ft/s) but combustion faded in the bed within 2 minutes after the jet was shut off. Data point 1 in table 5-2 shows measurements taken at 9.14 m/s (30 ft/s) following reignition. Bed temperature measurements and emission levels show satisfactory performance but this abated within 5 minutes and the catalyst became dark and inactive. Data point 2 represents slightly better performance after light-off at 6.34 m/s (20 ft/sec), and the catalyst was stabilized at about 1,728K (2,650$^{o}$F) after opposed jet light-off. Data point 3 shows the readings taken at this condition. Note that the temperature distribution within the catalyst bed is quite uniform. However, the measured bed temperature is about 200K lower than the adiabatic flame temperature at 175 percent theoretical air ($\phi_{FA}$ = 0.57) predicted by equilibrium calculations. A very small dark region (about 10 percent of the area) appeared on the front face but it did not increase in size. All other measurements show stable operation at this condition. However, the high CO and $NO_x$ emissions may indicate low catalyst activity with gas phase reactions continuing downstream. At data point 4 the air-fuel ratio was adjusted to reduce the bed temperature to approximately 1,656K (2,520$^{o}$F). The emissions improved somewhat and catalyst stability and uniformity were maintained. The lower CO and $NO_x$ emissions measurements are attributed to the effects of a more fuel-lean mixture on the homogeneous reaction downstream of the catalyst, not to increased activity of the catalyst itself. The leaner mixture gave a lower CO concentration (although a higher yield of CO per mass of fuel is likely in the cooler flame) and the reduced flame temperature resulted in lower thermal $NO_x$ emissions.

The bed temperature was further reduced to 1,600K (2,420°F) at data point 5 by flowing a leaner mixture. This temperature appeared to be a minimum for stable performance at 3.05 m/s (10 ft/s) face velocity as the combustion died out in the bed within 5 minutes. As a check, another attempt was made to stabilize at this bed temperature by shutting down and relighting with the opposed jet. The behavior was the same and data point 6 indicates the resulting low temperature measurements. Again, the readings were taken quickly and the lag in the emissions monitoring bench masks the true performance. The adiabatic flame temperature for no. 2 diesel at the stoichiometry and preheat of data point 6 is approximately 1,658K (2,524°F) which is much higher than the measured levels.

Since data points 3 and 4 showed promising catalyst performance at the higher bed temperature, another attempt was made to operate at 6.34 m/s (20 ft/sec). Data point 7 shows the measurements taken after the opposed jet light-off at this condition. The bed temperature measurements looked uniform and interestingly they were quite close to the predicted adiabatic flame temperature, at least initially. However, the UHC and CO emission measurements gave an indication of poor performance and the bed combustion was almost completely out within 15 minutes. At this point, the bed was fully dark and gave no visual indication of activity. Data point 9 shows the bed temperature and emissions measurements.

A similar conclusion could be drawn with this catalyst as with the Trans-Tech tubes. That is, below a catalyst temperature of about 1,644K (2,500°F), combustion performance was poor and could not be improved without reignition with the opposed jet. Also, combustion within the catalyst could not be stabilized at a face velocity of 6 m/s (20 ft/s) or higher.

### ATT-E

For this test, six in-depth thermocouples were placed in the monolith. However, two thermocouples were damaged during installation so that only four were available for bed temperature measurements. The nonfunctioning thermocouples were both located in the first, or upstream segment. Thermocouples R3 and R4 were located in the center segment and the last segment contained R1 and R2. The measurement junctions of R2 and R4 were at the same radial distance as R1 and R3 but on the opposite side.

This catalyst was more active than those tested previously and gave better performance. This allowed the completion of the parametric test matrix. Table 5-3 shows that data were gathered for face velocities of 4.02 m/s, (13 ft/s), 6.83 m/s, (22 ft/s), and over 14.9 m/s (50 ft/s). Data points 1 through 11 cover about 1 hour of operation. This time was used as an aging period and for some adjustments in the facility preheaters and does not represent any appreciable turndown in the catalyst bed temperature.

Although the catalyst exhibited stable performance which did not degrade with time, the bed temperature was somewhat nonuniform and about 300K below the calculated adiabatic temperature. Throughout this aging period approximately 10 to 20 percent of the catalyst back face was dark, indicating low activity. The catalyst front face was hidden from view in this and all subsequent tests. Also, the measurements of CO and UHC indicate incomplete combustion within the bed.

# Table 5-3. Parametric Test Data for ATT-E After 24 Hours of Furnace Aging

| Data Point | TA (Percent) | Air Flow (scfm) | Face Velocity (ft/sec) | Bed $\Delta P$ (in.$H_2O$) | Preheat Temperature (°F) | Catalyst Temperature | | | | | | UHC (ppm) | CO (ppm) | $NO_x$ (ppm) | $NO_x$ (Percent) | $CO_2$ (Percent) |
|---|---|---|---|---|---|---|---|---|---|---|---|---|---|---|---|---|
| | | | | | | R1 (°F) | R2 (°F) | R3 (°F) | R4 (°F) | R5 (°F) | R6 (°F) | | | | | |
| 1 | 147 | 11.8 | 13.4 | 0.6 | 772 | 2,656 | 1,432 | 1,986 | 2,588 | -- | -- | 4.0 | 37.5 | 33.0 | 8.4 | 9.6 |
| 2 | 148 | 11.9 | 13.3 | 0.6 | 756 | 2,792 | 1,963 | 2,230 | 2,670 | -- | -- | 4.0 | 35.0 | 33.0 | 8.4 | 9.6 |
| 3 | 148 | 11.9 | 13.2 | 0.6 | 746 | 2,645 | 1,849 | 2,197 | 2,387 | -- | -- | 3.0 | 27.5 | 27.0 | 7.9 | 10.5 |
| 4 | 162 | 11.9 | 13.2 | 0.6 | 740 | 2,428 | 1,724 | 2,002 | 1,805 | -- | -- | 2.0 | 25.0 | 24.0 | 7.4 | 11.0 |
| 5 | 170 | 11.9 | 13.1 | 0.6 | 737 | 2,180 | 1,664 | 1,839 | 1,642 | -- | -- | 1.5 | 17.5 | 24.0 | 7.1 | 11.5 |
| 6 | 173 | 11.9 | 13.1 | 0.6 | 734 | 1,710 | 1,615 | 1,683 | 1,594 | -- | -- | 1.0 | 17.5 | 20.5 | 6.8 | 14.0 |
| 7 | 153 | 19.6 | 22.4 | 0.8 | 772 | 2,595 | 1,874 | 2,158 | 2,029 | -- | -- | 1.0 | 45.0 | 36.0 | 8.1 | 10.0 |
| 8 | 157 | 20.2 | 22.4 | 0.8 | 773 | 2,547 | 1,873 | 2,127 | 2,063 | -- | -- | 0.8 | 42.5 | 35.0 | 7.9 | 10.4 |
| 9 | 148 | 11.9 | 14.0 | 1.4 | 804 | 2,672 | 1,978 | 1,913 | 2,598 | -- | -- | 0.0 | 42.5 | 36.0 | 7.9 | 11.5 |
| 10 | 148 | 11.9 | 13.3 | 1.4 | 756 | 2,578 | 1,691 | 1,787 | 2,258 | -- | -- | 0.0 | 75.0 | 35.0 | 7.9 | 10.6 |
| 11 | 148 | 11.9 | 13.3 | 1.3 | 745 | 2,623 | 1,708 | 1,946 | 2,172 | -- | -- | 0.0 | 53.5 | 34.0 | 7.9 | 10.6 |
| 12 | 146 | 19.7 | 22.4 | 1.6 | 772 | 2,631 | 1,718 | 1,931 | 1,406 | -- | -- | 0.0 | 73.0 | 47.0 | 8.5 | 10.2 |
| 13 | 153 | 19.7 | 22.4 | 1.7 | 774 | 2,598 | 1,749 | 1,865 | 1,446 | -- | -- | 0.0 | 67.5 | 44.0 | 8.2 | 10.6 |
| 14 | 158 | 19.6 | 22.5 | 2.0 | 778 | 2,487 | 1,861 | 1,772 | 2,336 | -- | -- | 0.0 | 45.0 | 36.0 | 7.9 | 11.0 |
| 15 | 159 | 19.6 | 22.6 | 1.8 | 783 | 2,309 | 1,820 | 1,648 | 2,182 | -- | -- | 0.0 | 40.0 | 32.0 | 7.7 | 11.4 |
| 16 | 164 | 19.7 | 22.7 | 1.8 | 788 | 1,909 | 1,743 | 1,556 | 2,072 | -- | -- | 0.0 | 40.0 | 30.0 | 7.5 | 11.7 |
| 17 | 168 | 19.7 | 22.7 | 1.7 | 791 | 1,412 | 1,710 | 1,474 | 1,499 | -- | -- | 0.0 | 35.0 | 26.0 | 7.1 | 12.4 |
| 18 | 181 | 37.7 | 48.2 | 3.4 | 926 | 2,598 | 1,865 | 1,625 | 2,616 | -- | -- | 0.0 | 42.5 | 29.0 | 7.6 | 11.6 |
| 19 | 184 | 37.7 | 49.0 | 3.5 | 946 | 2,611 | 1,887 | 1,709 | 2,597 | -- | -- | 0.0 | 40.0 | 27.0 | 7.3 | 12.0 |
| 20 | 189 | 37.6 | 48.8 | 3.5 | 944 | 2,602 | 1,888 | 1,762 | 2,572 | -- | -- | 0.0 | 37.5 | 25.0 | 7.2 | 12.0 |
| 21 | 190 | 37.6 | 48.9 | 3.6 | 947 | 2,510 | 2,870 | 1,723 | 2,494 | -- | -- | 0.0 | 35.0 | 24.0 | 7.0 | 12.4 |
| 22 | 202 | 37.6 | 49.0 | 3.6 | 949 | 2,421 | 2,839 | 1,698 | 2,373 | -- | -- | 0.0 | 32.5 | 22.0 | 6.8 | 12.7 |
| 23 | 206 | 37.6 | 49.1 | 3.6 | 951 | 2,330 | 1,824 | 1,679 | 2,287 | -- | -- | 0.0 | 30.0 | 21.0 | 6.7 | 13.0 |
| 24 | 210 | 37.6 | 49.2 | 3.6 | 954 | 2,236 | 1,808 | 1,679 | 2,173 | -- | -- | 0.0 | 27.5 | 20.0 | 6.4 | 13.3 |
| 25 | 214 | 37.6 | 49.2 | 3.5 | 954 | 2,149 | 1,798 | 1,674 | 2,112 | -- | -- | 0.0 | 27.5 | 20.0 | 6.3 | 13.4 |
| 26 | 218 | 37.6 | 49.2 | 3.6 | 955 | 2,040 | 1,785 | 1,667 | 2,033 | -- | -- | 0.0 | 30.0 | 19.0 | 6.2 | 13.6 |
| 27 | 224 | 37.6 | 49.2 | 3.6 | 956 | 1,950 | 1,771 | 1,660 | 1,982 | -- | -- | 0.0 | 25.0 | 18.0 | 6.1 | 13.7 |
| 28 | 225 | 37.6 | 49.3 | 3.6 | 957 | 1,873 | 1,746 | 1,640 | 1,843 | -- | -- | 0.0 | 25.0 | 17.0 | 5.8 | 14.0 |
| 29 | 229 | 37.6 | 49.3 | 3.6 | 958 | 1,803 | 1,736 | 1,634 | 1,823 | -- | -- | 0.0 | 25.0 | 17.0 | 5.7 | 14.0 |
| 30 | 240 | 37.6 | 49.3 | 3.5 | 959 | 1,740 | 1,728 | 1,629 | 1,520 | -- | -- | 0.0 | 32.5 | 16.0 | 5.7 | 14.4 |

Some data were collected at a face velocity of 6.83 m/s (22 ft/s) as indicated by data points 12 through 17. Again, the combustion remained stable but the catalyst back face had darker appearing regions that covered about 40 to 50 percent of the area. The thermocouple measurements were nonuniform and somewhat below the adiabatic flame temperature levels.

Finally, the face velocity was increased to 14.9 m/s (49 ft/s) and the preheat temperature was adjusted to about 780K (950°F) as measured. Parametric measurements were taken starting at 1,700K (2,600°F) at data points 18, 19, and 20, and ending at 1,222K at point 30. The combustion performance of the catalyst remained stable except at bed temperatures below 1,367K (2,000°F). An estimated 40 to 60 percent of the catalyst back face area was dark through these measurements. The minimum bed temperature that could be maintained appeared to be 1,222K at point 30. At this condition the catalyst back face appeared to be over 70 percent dark. Below this temperature, combustion within the bed could not be sustained and the bed temperature would decrease significantly with increased emissions of CO and UHC.

### ATT-A

Four in-depth thermocouples were operational to measure the catalyst bed temperature. Thermocouples R1 and R2 were located in the back (downstream) segment, R3 was in the center segment, and R5 measured the front segment temperature. The measurement junctions of R1, R3, and R5 were vertically aligned at one radial location while R2 was on the opposite side at the same radial distance from the center.

The catalyst performed well throughout the parametric combustion test. The face velocity for all of the data (table 5-4) averaged 14.6 m/s (48 ft/s) and the preheat temperature ranged from 761K (909°F) to 776K

## Table 5-4. Parametric Test Data for ATT-A After 24 Hours of Furnace Aging

| Data Point | TA (%) | Air Flow (scfm) | Face Velocity (ft/sec) | Bed $\Delta P$ (in.$H_2O$) | Preheat Temperature (°F) | Catalyst Temperature R1 (°F) | R2 (°F) | R3 (°F) | R4 (°F) | R5 (°F) | R6 (°F) | UHC (ppm) | CO (ppm) | $NO_x$ (ppm) | $NO_x$ (%) | $CO_2$ (%) |
|---|---|---|---|---|---|---|---|---|---|---|---|---|---|---|---|---|
| 1 | 180 | 37.4 | 47.2 | 3.2 | 909 | 2,609 | 2,625 | 2,184 | -- | 1,889 | -- | 0 | 30.0 | 29.0 | 7.3 | 11.0 |
| 2 | 182 | 37.3 | 47.2 | 3.2 | 913 | 2,610 | 2,595 | 2,200 | -- | 1,901 | -- | 0 | 37.5 | 27.0 | 7.3 | 11.0 |
| 3 | 184 | 37.6 | 47.7 | 3.4 | 915 | 2,586 | 2,586 | 2,205 | -- | 1,917 | -- | 0 | 40.0 | 27.0 | 7.3 | 11.0 |
| 4 | 189 | 37.6 | 47.7 | 3.5 | 916 | 2,491 | 2,478 | 2,156 | -- | 1,894 | -- | 0 | 37.5 | 24.0 | 7.1 | 11.5 |
| 5 | 191 | 37.6 | 47.8 | 3.5 | 918 | 2,416 | 2,350 | 2,119 | -- | 1,875 | -- | 0 | 37.5 | 23.0 | 7.1 | 11.5 |
| 6 | 197 | 37.6 | 47.8 | 3.5 | 918 | 2,348 | 2,244 | 2,087 | -- | 1,855 | -- | 0 | 37.5 | 21.0 | 6.9 | 14.0 |
| 7 | 206 | 37.6 | 49.9 | 3.5 | 921 | 2,244 | 2,098 | 2,024 | -- | 1,815 | -- | 0 | 30.0 | 19.5 | 6.6 | 12.0 |
| 8 | 207 | 37.6 | 47.9 | 3.4 | 922 | 2,150 | 1,983 | 1,972 | -- | 1,782 | -- | 0 | 27.5 | 18.0 | 6.4 | 15.0 |
| 9 | 224 | 37.6 | 48.0 | 3.4 | 924 | 2,055 | 1,906 | 1,909 | -- | 1,741 | -- | 0 | 26.3 | 15.5 | 6.1 | 12.5 |
| 10 | 234 | 37.6 | 48.1 | 3.3 | 926 | 1,970 | 1,843 | 1,846 | -- | 1,702 | -- | 0 | 22.5 | 14.5 | 5.8 | 14.5 |
| 11 | 250 | 37.6 | 48.2 | 3.2 | 929 | 1,883 | 1,754 | 1,659 | -- | 1,645 | -- | 0 | 17.5 | 12.5 | 5.3 | 14.0 |
| 12 | 279 | 37.6 | 48.3 | 3.1 | 933 | 1,791 | 1,670 | 1,664 | -- | 1,579 | -- | 0 | 25.0 | 11.5 | 4.7 | 14.2 |
| 13 | 313 | 37.6 | 48.5 | 3.0 | 937 | 1,699 | 1,586 | 1,578 | -- | 1,510 | -- | 28 | 82.0 | 4.4 | 4.0 | 14.9 |
| 14 | 184 | 37.6 | 47.8 | 3.7 | 917 | 2,632 | 2,608 | 2,238 | -- | 1,937 | -- | 0 | 37.5 | 27.0 | 7.4 | 11.0 |

($937^{\circ}F$) as measured. The catalyst was aged for 1/2 hour as indicated by data points 1, 2, and 3 of table 5-4. No appreciable changes were seen in either temperature or emissions during the aging period.

Although some slightly darker areas were visible on the catalyst back face, it appeared to be much more uniform than any of the previous catalysts. The parametric test matrix was followed by adjusting the air-fuel ratio to give bed temperatures ranging from 1,700K ($2,600^{\circ}F$) to 1,200K ($1,700^{\circ}F$) in approximate 50K increments. Even at the lowest bed temperature (i.e., the most fuel-lean mixture) combustion was very stable and the catalyst back face was visually quite uniform. However, data point 13 indicates that combustion within the catalyst was incomplete as CO and UHC emissions increased considerably. Throughout the data points the measured bed temperature was approximately 200K less than the calculated adiabatic flame temperature. At the more fuel-lean conditions (i.e., data points 10, 11, and 12) this difference approached 300K.

At data point 14 the fuel-air ratio was readjusted to bring the bed temperature back to approximately 1,700K. The condition of data point 3 was matched to be sure that higher temperature performance was not adversely affected following data point 13. The temperature and emissions measurements were closely repeated without any reconditioning period.

### UOP-B

Bed temperature measurements for this catalyst were taken with five in-depth thermocouples. The front segment contained thermocouple R1 while R3 and R4 were located in the middle segment and R5 and R6 in the back segment. The measurement junction of R1 was vertically aligned with R3 and R5. Located on the opposite side were the junctions of R4 and R6.

This catalyst performed very well throughout all of the conditions of the parametric test matrix (table 5-5). The face velocity for all of the data averaged 14.8 m/s (48.5 ft/s) and the preheat temperature ranged from 764K (915°F) to 781K (945°F) as measured. Here too, the catalyst was conditioned for about 1/2 hour, shown by data points 1 through 4 of table 5-5, before parametric data were taken.

The back face of the catalyst bed remained very uniform visually with no dark areas appearing at any condition. The bed temperature measurements were also quite uniform, even at the minimum temperature condition of data points 16 and 17. Again, there was some difference between the measured bed temperature and the calculated adiabatic flame temperature. The measured levels ranged from 100K to about 280K below the predicted values with the higher discrepancy appearing in the lower bed temperature ranges. Some of this difference may be explained by fuel flow measurement error which increases as the fuel flowmeter approaches the bottom of its scale. Except for a slight increase in CO at the lowest bed temperature, the emissions measurements as shown in table 5-5 indicate good catalyst performance at all bed temperatures.

### MBI-D

This was the last catalyst to be tested under the parametric combustion task. Four in-depth thermocouples were operational to measure bed temperatures. Thermocouples R1 and R2 were located in the front segment, R3 was in the center, and R6 was in the back segment. The measurement junction of R1 was vertically aligned with R3 while those of R2 and R6 were on the opposite side. One of the segments of this catalyst set had crumbled after the oven test and had to be replaced with a new, unaged segment. This segment was located at the front of the bed followed by the two aged pieces.

Table 5-5. Parametric Test Data for UOP-B After 24 Hours of Furnace Aging

| Data Point | TA (%) | Air Flow (scfm) | Face Velocity (ft/sec) | Bed $\Delta P$ (in.$H_2O$) | Preheat Temperature (°F) | Catalyst Temperature | | | | | | UHC (ppm) | CO (ppm) | $NO_x$ (ppm) | $NO_x$ (%) | $CO_2$ (%) |
|---|---|---|---|---|---|---|---|---|---|---|---|---|---|---|---|---|
| | | | | | | R1 (°F) | R2 (°F) | R3 (°F) | R4 (°F) | R5 (°F) | R6 (°F) | | | | | |
| 1 | 180 | 37.4 | 47.4 | 4.2 | 915 | 1,907 | -- | 2,350 | 2,314 | 2,638 | 2,618 | 0 | 27.0 | 22.0 | 7.4 | 12.0 |
| 2 | 181 | 37.7 | 48.0 | 4.3 | 920 | 1,905 | -- | 2,339 | 2,305 | 2,614 | 2,594 | 0 | 27.5 | 21.0 | 7.3 | 12.2 |
| 3 | 182 | 37.8 | 48.2 | 4.3 | 922 | 1,925 | -- | 2,372 | 2,324 | 2,635 | 2,614 | 0 | 27.5 | 21.5 | 7.3 | 12.2 |
| 4 | 185 | 37.8 | 48.2 | 4.3 | 921 | 1,920 | -- | 2,354 | 2,323 | 2,617 | 2,630 | 0 | 27.5 | 21.5 | 7.3 | 12.2 |
| 5 | 185 | 37.8 | 48.2 | 4.3 | 922 | 1,921 | -- | 2,358 | 2,338 | 2,608 | 2,659 | 0 | 33.8 | 22.5 | 7.4 | 12.2 |
| 6 | 193 | 37.8 | 48.2 | 4.4 | 922 | 1,873 | -- | 2,273 | 2,276 | 2,474 | 2,500 | 0 | 28.8 | 20.5 | 7.1 | 12.4 |
| 7 | 195 | 37.8 | 48.3 | 4.4 | 925 | 1,849 | -- | 2,336 | 2,241 | 2,388 | 2,425 | 0 | 20.0 | 18.5 | 6.9 | 12.6 |
| 8 | 199 | 37.8 | 48.3 | 4.4 | 926 | 1,819 | -- | 2,196 | 2,201 | 2,298 | 2,343 | 0 | 17.5 | 17.0 | 6.6 | 13.2 |
| 9 | 208 | 37.8 | 48.4 | 4.4 | 929 | 1,785 | -- | 2,130 | 2,148 | 2,199 | 2,241 | 0 | 15.0 | 15.0 | 6.4 | 13.4 |
| 10 | 219 | 37.4 | 48.6 | 4.2 | 931 | 1,750 | -- | 2,060 | 2,103 | 2,107 | 2,151 | 0 | 15.0 | 14.0 | 6.1 | 13.6 |
| 11 | 227 | 37.8 | 48.6 | 4.2 | 934 | 1,708 | -- | 1,952 | 2,036 | 2,014 | 2,062 | 0 | 17.5 | 12.5 | 5.8 | 14.0 |
| 12 | 236 | 37.8 | 48.7 | 4.2 | 936 | 1,666 | -- | 1,867 | 1,964 | 1,934 | 1,972 | 0 | 12.5 | 12.0 | 5.5 | 14.5 |
| 13 | 252 | 37.8 | 48.7 | 4.2 | 938 | 1,624 | -- | 1,793 | 1,882 | 1,858 | 1,878 | 0 | 10.0 | 10.6 | 5.2 | 14.8 |
| 14 | 259 | 37.8 | 48.8 | 4.2 | 939 | 1,620 | -- | 1,785 | 1,870 | 1,866 | 1,882 | 0 | 10.0 | 10.5 | 5.1 | 14.8 |
| 15 | 279 | 37.8 | 48.9 | 4.2 | 941 | 1,581 | -- | 1,720 | 1,784 | 1,789 | 1,790 | 0 | 10.0 | 9.7 | 4.8 | 15.4 |
| 16 | 305 | 37.8 | 49.0 | 4.0 | 945 | 1,535 | -- | 1,658 | 1,703 | 1,698 | 1,700 | 0 | 15.0 | 8.8 | 4.3 | 16.0 |
| 17 | 305 | 37.8 | 49.0 | 4.0 | 944 | 1,533 | -- | 1,656 | 1,699 | 1,700 | 1,701 | 0 | 22.5 | 8.4 | 4.3 | 16.0 |
| 18 | 195 | 37.8 | 48.3 | 4.3 | 926 | 1,876 | -- | 2,255 | 2,313 | 2,444 | 2,581 | 0 | 22.5 | 21.0 | 7.1 | 12.5 |

Following the initial 30-minute conditioning period, parametric data were collected as indicated in table 5-6. The catalyst performed very well although it was not quite as uniform visually as the UOP-B catalyst. Two areas covering about 20 percent of the back face were slightly darker than the surrounding areas. Also, the measured bed temperatures were not quite as uniform as those from the UOP-B catalyst test. Differences in the measured temperatures and the calculated adiabatic flame temperature showed similar behavior as the previous test.

Throughout all of the test, the catalyst operation remained steady. The emissions show only a slight performance degradation at the minimum temperature of 1,200K (1,700$^{0}$F) at data point 15. At data point 17, the fuel flow was turned up to match data points 4 and 5. The repeatability was very good in both emissions and temperature measurements.

### 5.2.2 Parametric Combustion Tests After 1,000 Hours of Furnace Aging

The results of the attempts after 1,000 hours of aging can be quickly dispensed with, since none of the reactors would sustain combustion. Interpretation of this result is more difficult since clearly some catalyst material depletion occurred during the aging process. This was evident in the visual and SEM appearances as described in section 4. However, silicon, probably as silica, was found on the surface of all samples. The silica undoubtedly is an artifact of the furnace aging procedure and probably had a poisoning or shielding effect on the catalysts.

## 5.3 DISCUSSION OF SCREENING TEST RESULTS

From the furnace aging part of the screening tests, it is apparent that chemical and physical changes could be induced by long exposure to elevated temperatures. However, the inability to perform rapid

## Table 5-6. Parametric Test Data for MBI-B After 24 Hours of Furnace Aging

| Data Pt. | TA (%) | Air Flow (scfm) | Face Velocity (ft/sec) | Bed $\Delta P$ (in.$H_2O$) | Preheat Temperature (°F) | Catalyst Temperature | | | | | | UHC (ppm) | CO (ppm) | $NO_x$ (ppm) | $CO_2$ (%) | $O_2$ (%) |
|---|---|---|---|---|---|---|---|---|---|---|---|---|---|---|---|---|
| | | | | | | R1 (°F) | R2 (°F) | R3 (°F) | R4 (°F) | R5 (°F) | R6 (°F) | | | | | |
| 1 | 197 | 37.6 | 47.8 | 4.2 | 917 | 2,306 | 1,959 | 1,921 | -- | -- | 2,579 | 0 | 31.3 | 20.0 | 7.0 | 12.6 |
| 2 | 194 | 37.6 | 47.9 | 4.3 | 922 | 2,353 | 1,989 | 1,955 | -- | -- | 2,642 | 0 | 32.5 | 20.5 | 7.1 | 12.0 |
| 3 | 197 | 37.6 | 48.0 | 4.4 | 924 | 2,306 | 1,963 | 1,935 | -- | -- | 2,593 | 0 | 30.0 | 20.0 | 7.0 | 12.6 |
| 4 | 198 | 37.6 | 48.0 | 4.4 | 925 | 2,280 | 1,952 | 1,926 | -- | -- | 2,597 | 0 | 30.0 | 19.5 | 6.9 | 12.6 |
| 5 | 198 | 37.6 | 48.1 | 4.4 | 926 | 2,268 | 1,952 | 1,925 | -- | -- | 2,577 | 0 | 27.5 | 19.0 | 6.9 | 12.6 |
| 6 | 201 | 37.6 | 48.1 | 4.5 | 926 | 2,217 | 1,933 | 1,903 | -- | -- | 2,509 | 0 | 27.5 | 18.5 | 6.8 | 12.9 |
| 7 | 206 | 37.6 | 48.1 | 4.5 | 926 | 2,154 | 1,908 | 1,877 | -- | -- | 2,421 | 0 | 25.0 | 17.5 | 6.7 | 13.2 |
| 8 | 213 | 37.6 | 48.1 | 4.4 | 927 | 2,105 | 2,881 | 1,849 | -- | -- | 2,328 | 0 | 22.5 | 17.0 | 6.6 | 13.2 |
| 9 | 214 | 37.6 | 48.1 | 4.4 | 928 | 2,061 | 1,852 | 1,822 | -- | -- | 2,235 | 0 | 20.0 | 16.4 | 6.4 | 13.4 |
| 10 | 218 | 37.6 | 48.1 | 4.4 | 928 | 2,012 | 1,833 | 1,799 | -- | -- | 2,063 | 0 | 20.0 | 15.0 | 6.1 | 13.6 |
| 11 | 225 | 37.6 | 48.2 | 4.4 | 930 | 1,970 | 1,800 | 1,770 | -- | -- | 2,063 | 0 | 20.0 | 15.0 | 6.1 | 13.8 |
| 12 | 238 | 37.6 | 48.3 | 4.3 | 932 | 1,922 | 1,748 | 1,725 | -- | -- | 1,971 | 0 | 15.0 | 13.2 | 5.7 | 14.4 |
| 13 | 238 | 37.6 | 48.3 | 4.3 | 932 | 1,902 | 1,732 | 1,712 | -- | -- | 1,878 | 0 | 15.0 | 12.5 | 5.7 | 14.5 |
| 14 | 257 | 37.6 | 48.4 | 4.2 | 936 | 1,833 | 1,684 | 1,664 | -- | -- | 1,793 | 0 | 12.5 | 11.4 | 5.2 | 15.0 |
| 15 | 302 | 37.6 | 48.7 | 4.2 | 943 | 1,698 | 1,591 | 1,569 | -- | -- | 1,653 | 0 | 80.5 | 8.4 | 4.4 | 15.8 |
| 16 | 286 | 37.6 | 48.6 | 4.2 | 942 | 1,736 | 1,617 | 1,595 | -- | -- | 1,698 | 0 | 22.5 | 9.4 | 4.6 | 15.8 |
| 17 | 198 | 37.6 | 48.1 | 4.7 | 926 | 2,284 | 1,976 | 1,937 | -- | -- | 2,600 | 0 | 30.0 | 19.5 | 7.0 | 12.6 |

temperature cycling did not subject the reactors to thermal stresses which would be representative of combustion conditions. Further, from previous combustion experience (reference 2) with some of the reactor materials, the catalyst depletion rate appears to be very slow in the furnace when compared to combustion results. This is apparently due to the very low convection rates in the catalyst during furnace aging. The low furnace convection rates allow higher partial pressures of vaporized species which in turn suppress the net vaporization rates.

All substrates tested in the furnace exhibited significant degradation in mechanical strength after 1,000 hours at temperature. On some materials, similar degradation has been observed after about 10 to 20 hours of combustion testing. Therefore, the furnace is a very conservative measure of the effects of temperature on mechanical properties.

After 24 hours of aging, combustion could be achieved on all samples but not necessarily at the prescribed baseline conditions. Of the six reactors parametrically tested, the most active was UOP-B. For this reactor, combustion was stable and uniform throughout the parametric test matrix. Qualitatively the remaining reactors are ranked in the following order of decreasing combustion performance: ATT-A, MBI-D, ATT-E, OC-B, and ATT-C. For the last two reactors, it was very difficult to achieve stable combustion conditions even at very low reference velocities.

After 1,000 hours of aging none of the reactors would sustain stable combustion. All samples examined with SEM/Kevex showed silicon on the surface and this may be part of the reason for the inability to achieve stable combustion conditions for these samples.

Since the combustion ability of the reactors after 1,000 hours of aging may have been masked by silica coatings, the selection of a reactor for durability testing was based on the parametric test results following 24 hours of aging. Of the six reactors, UOP-B was clearly the most active and stable. Even though the plan was to use the "2000" sample for an additional 1,000 hours of combustion testing, the "24" sample was selected for this combustion testing because of the possible deactivation of the "2000" sample by the silica .

# SECTION 6

# COMBUSTION DURABILITY TESTING

The purpose of the combustion durability test was to demonstrate a combustion life of 1,000 hours following 1,000 hours of furnace aging. However, as noted in section 5, none of the 1,000-hour aged samples would maintain stable combustion. Therefore, the reactor concept for durability testing was based on the parametric tests conducted following 24 hours. These results showed that UOP-B had the best performance so that the UOP-B "24" sample was used for the durability tests.

The durability test plan was to combustion test at steady conditions for 24 hours, then shut down and perform characterization measurements on the sample. The sample would then be reinstalled in the catalytic test facility and combustion testing continued for 1,000 hours or until such time that the catalyst became inactive. At various intervals, a parametric test series would be run to determine any change in the lowest temperature at which high combustion efficiency could be maintained.

Since the test sample was the "24" reactor, there was no instrumentation on the reactor. No instrumentation was added due to a concern for incurring unnecessary damage to the reactor. The only instrumentation used for this test was the normal facility instrumentation and a type-R thermocouple located 2.54 cm downstream of the reactor. During this combustion durability test, approximately 200 data points were recorded. A sampling of 18 typical data points is given in table 6-1.

Initiation of the combustion test was accomplished with only minor ignition difficulties. Test conditions were easily established and maintained for 24 hours with no observed anomalies. Combustion efficiency was high as shown in table 6-1, CO and $NO_x$ emissions were low, and the bed temperature was visually uniform.

Following 24 hours of combustion testing, a catalyst dispersion of 0.12 μmoles/gm was measured. This compares well with a value of 0.13 before combustion and an identical value for the 180-hour aged sample.

The second leg (250 hours) of combustion testing was resumed and all subsequent events of significance are shown in figure 6-1. Ten hours into the second leg (hour 34), a failure in the air preheater caused a premature shutdown.

Following repair of the air preheaters, the durability test was continued. Emissions were low and combustion efficiency was high at the nominal test condition. The periodic parametric test showed that emissions were essentially unchanged until the reactor temperatures were decreased to about 1,250 to 1,310K. At this point, CO emissions increased to about 50 ppm. At about hour 80, a small dark area was observed on the back face of the reactor. This dark area was 10 to 20 percent of the cross-section and, curiously, was not stationary. The dark area moved slowly and circumferentially around the reactor.

At about hour 110, the center of the third catalyst element (the element farthest downstream) fractured and a number of small pieces dropped to the bottom of the test section. The performance of the reactor

Table 6-1. Representative Data from Durability Test of UOP-B; $V_{ref}$ = 55 ft/s, $T_{inlet}$ = 1,100$^{o}$F, p = 1 atm

| Data Point | Air Flow (SCFM) | Diesel Flow $ft^3/min$ ($x10^{-3}$) | Diesel Flow lbm/min ($x10^{-2}$) | Vref (Ft/s) | Fuel-Air Ratio From Mass Flow Meas. | %TA From Mass Flow Meas. | T Preheat ($^{o}$F) | T Meas. 1-in. Down-stream ($^{o}$F) | $NO_x$ (ppm) | CO (ppm) | UHC (ppm) | $O_2$ (Percent) | $CO_2$ (Percent) | Elapsed Time (Hr) |
|---|---|---|---|---|---|---|---|---|---|---|---|---|---|---|
| 1 | 37.3 | 1.39 | 7.38 | 54.9 | 0.0263 | 266 | 1,136 | 2,449 | 13 | 8 | 0 | 14.0 | 5.3 | 0.3 |
| 3 | 37.3 | 1.36 | 7.22 | 56.1 | 0.0258 | 271 | 1,150 | 2,476 | 11 | 8 | 0 | 14.2 | 5.3 | 2.3 |
| 9 | 39.1 | 1.42 | 7.54 | 58.7 | 0.0257 | 272 | 1,167 | 2,472 | 11 | 13 | 0 | 14.2 | 5.1 | 9.3 |
| 14 | 38.6 | 1.39 | 7.38 | 57.5 | 0.0255 | 274 | 1,156 | 2,481 | 13 | 3 | 0 | 14.0 | 5.3 | 23.8 |
| 24 | 37.5 | 1.52 | 8.07 | 52.3 | 0.0287 | 243 | 1,051 | 2,531 | 13 | 13 | 0 | 13.2 | 5.9 | 40.1 |
| 32 | 37.6 | 1.52 | 8.07 | 52.4 | 0.0286 | 244 | 1,051 | 2,527 | 15 | 15 | 0 | 13.4 | 5.9 | 41.9 |
| 43 | 37.3 | 1.46 | 7.75 | 52.6 | 0.0277 | 252 | 1,069 | 2,570 | 15 | 25 | 0 | 13.4 | 5.5 | 63.2 |
| 52 | 37.7 | 1.52 | 8.07 | 53.9 | 0.0285 | 245 | 1,090 | 2,553 | 18 | 20 | 0 | 13.4 | 5.5 | 72.6 |
| 60 | 37.4 | 1.52 | 8.07 | 53.4 | 0.0287 | 244 | 1,088 | 2,688 | 21 | 25 | 0 | 13.0 | 6.1 | 88.3 |
| 76 | 37.7 | 1.46 | 7.75 | 53.8 | 0.0274 | 255 | 1,088 | 2,540 | 17 | 23 | 0 | 13.6 | 5.6 | 104.3 |
| 92 | 37.5 | 1.49 | 7.91 | 53.3 | 0.0281 | 249 | 1,081 | 2,536 | 19 | 23 | 1 | 13.2 | 6.3 | 121.6 |
| 99 | 37.4 | 1.24 | 6.58 | 53.3 | 0.0234 | 299 | 1,086 | 2,200 | 11 | 28 | 0 | 16.0 | 4.4 | 138.0 |
| 120 | 37.5 | 1.52 | 8.07 | 52.8 | 0.0287 | 244 | 1,068 | 2,446 | 20 | 25 | 0 | 13.0 | 6.0 | 163.3 |
| 144 | 37.5 | 1.55 | 8.23 | 54.3 | 0.0292 | 240 | 1,110 | 2,433 | 13 | 30 | 9 | 13.4 | 6.2 | 200.6 |
| 165 | 37.7 | 1.49 | 7.91 | 54.5 | 0.0279 | 251 | 1,107 | 2,424 | 16 | 30 | 0 | 13.6 | 6.2 | 234.1 |
| 175 | 37.8 | 1.55 | 8.23 | 55.1 | 0.0290 | 241 | 1,120 | 2,472 | 18 | 18 | 8 | 13.4 | 6.4 | 250.4 |
| 194 | 37.4 | 1.55 | 8.23 | 54.4 | 0.0293 | 239 | 1,119 | 2,473 | 8 | 141 | 110 | 12.5 | 6.5 | 272.0 |
| 199 | 37.3 | 1.52 | 8.07 | 54.3 | 0.0288 | 243 | 1,119 | 2,460 | 3 | 1,300 | 160 | 12.7 | 6.6 | 282.3 |

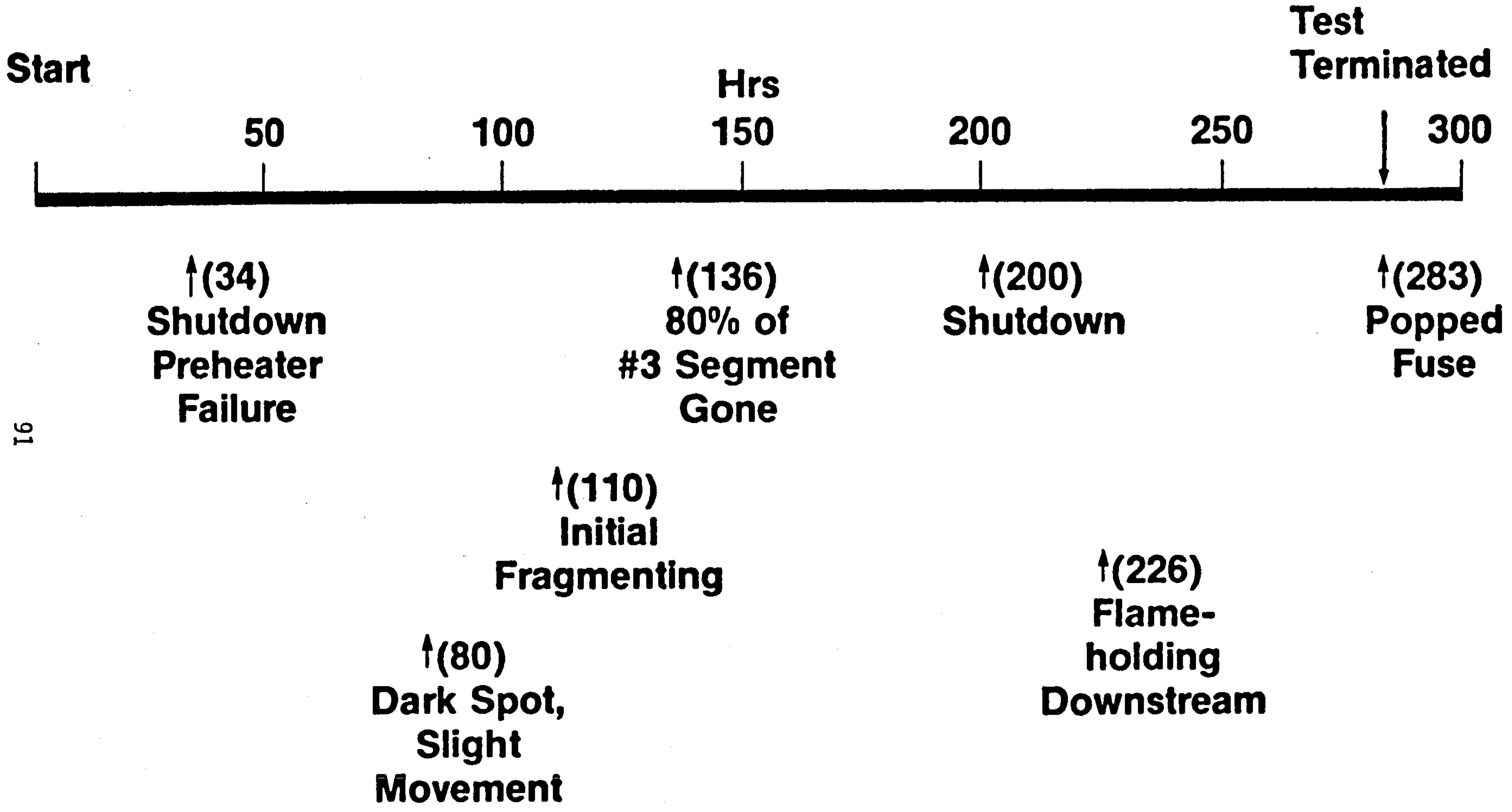

Figure 6-1. Combustion Durability Test

was, however, unchanged; that is, the emissions remained low. Small pieces of this catalyst element continued to fall out for the next 90 hours. At hour 136, about 80 percent of the third element had fallen out. By about hour 200, essentially all of the third element had fallen out and the reactor was reduced to two elements (5.0 cm). Also at about hour 200, a faulty alarm indication caused an automatic shutdown of the fuel flow to the facility. The faulty transducer was overridden, the facility restarted, and testing continued.

At about hour 226, the reactor was behaving as a flameholder, with much of the combustion occurring downstream of the reactor but going to completion before the sampling probe; therefore, measured emissions were low during this period.

At about hour 250 the catalyst became unstable with some noticeable combustion oscillations. At hour 283, a fuse for the air preheaters failed causing a facility shutdown.

The remaining catalyst segments were removed from the facility for examination. There was some minor fracturing and the substrate was much weaker than untested material, but otherwise these two segments were intact. The coloration of the segments suggests that there was very little active metal left on the reactor. A subsequent dispersion measurement indicated essentially zero dispersion.

Since prior to blowing the fuse, the combustion was unstable and the dispersion measurement indicated very little available active surface material, it was decided that there would be very little benefit to be gained by further testing of UOP-B.

The honeycomb substrate materials Corning MCB-12 and DuPont Torvex alumina were judged at the start of this program to have the highest probability of satisfying program goals. The durability test described indicated that none of the substrates or catalysts tested in phase 1 were adequate to meet the advanced automotive gas turbine combustion conditions. However, combustion results may have been misleading since furnace aging left silicon, a potential poison, on all of the catalysts.

The durability tests of a noble metal catalyst (UOP-B) on a zirconia spinel honeycomb (MCB-12) showed that the first indication of significant loss of catalyst occurred after only 80 hours at the 1,700K combustion conditions. Furthermore, initial fragmenting of the substrate occurred shortly thereafter at about 110 hours. Visual examinations suggest that there was little, if any, interaction between the catalyst/washcoat combination and the substrate; therefore, the test should represent the uncoupled effects of high-temperature combustion on degradation of a noble metal catalyst and substrate deterioration. Although the strength of the substrate was significantly reduced by exposure to the test conditions, the actual fragmentation of the honeycomb may have been a consequence of the reactor mounting method.

The catalytic reactors evaluated in this phase of the program did not meet the program objective of demonstrating that durable catalytic reactors can be designed for the advanced automotive gas turbine engine. All reactors tested were from the best available ceramic and catalyst technology and were selected mostly as a result of recommendations from catalyst suppliers. None of the available honeycomb substrates survived 100 hours of hot combustion conditions without signs of degradation. A catalyst life of a few thousand hours would probably be a minimum condition for an automotive gas turbine. Moreover, for most of the proposed gas turbine designs, many thermal cycles would be required. Even though cycling was not intentionally addressed in this program, it is clear that maximum benefits of catalytic combustion will require further development of structurally stable substrates, durable catalyst coatings, reactor designs, and mounting methods.

# SECTION 7

# PHASE II CATALYTIC REACTOR EVALUATION

The objective of the phase II effort was to evaluate additional substrate and catalyst materials, and to seek guidelines for recommending further research in catalytic reactor design. It was clear that concentration should be on materials that have low vapor pressures at elevated temperatures and good high-temperature stability. Thus, current technology noble metal catalysts would not be acceptable, at least in the catalyst sections where high temperatures are to be sustained. New developments here were directed toward metal oxides that could be applied to a honeycomb substrate by slurry coating or solution impregnation. Two new materials were selected based on a limited amount of available data that suggested good structural behavior under combustion conditions.

The new catalytic reactors were combustion tested to assess their potential performance as durable high-temperature catalytic reactors. One catalyst was then used to design a catalytic reactor for a short combustion durability demonstration using propane for fuel. Committed NASA funding was only sufficient to cover about 250 hours of durability testing. At that point, the tests were proceeding so smoothly that the EPA, under contract no. 68-02-3122, provided funding for an additional 750 hours. The work accomplished and results obtained in Phase II are described in the following paragraphs.

## 7.1 PHASE II CATALYTIC REACTOR MATERIAL DESCRIPTIONS

Three different honeycomb materials were used in phase II. Two of these, JNM and JNX, were proprietary materials from a ceramics manufacturer and the third, Corning MCB-1, was a magnesia-alumina-titanate. In contrast to the uniform cell density used in phase I (approximately 100 cells/in$^2$), the honeycombs used in this second phase were "graded" (reference 2) cells with the large cell honeycomb having about 9 cells/in$^2$ and the finest cell honeycombs having about 200 cells/in$^2$. Graded cell honeycomb sets were selected for two reasons. First, it was expected that the lower catalytic activity of metal oxides would benefit from the low transfer coefficients on thick web, large cell honeycombs. Second, because of variations in grain size used for different cell densities, the preparation and testing of a catalyst coating would yield information on catalyst adhesion and catalyst/substrate interactions. All substrate elements were 5 cm diameter by 2.5 cm long.

Catalyst coating selections were based on a combination of previous experience, estimated or known vapor pressures, anticipated high temperature stability, potential catalytic activity at high temperatures and intuition. Catalyst materials included lanthanum/chromium oxides, yttria/chromium oxide and magnesium aluminate iron ferrite (MAFF) which were slipcoated on the substrates and terbium/cerium/thorium (TCT) oxides which were coated by solution impregnation and calcination. The slip coating method puts a distinct surface layer of the oxide catalyst onto the substrate. The solution impregnation method allows the formation of catalyst throughout the depth of the substrate webs. Slipcoated reactors were sintered at 1,700K and solution impregnated reactors were calcined at about 1,200K. Table 7-1 provides a summary description of each phase II reactor.

The slipcoated catalysts on MCB-1 were all very uniform and appeared to have very good catalyst-to-substrate bonds. Each reactor element "picked up" about 2 grams* of oxide coating (approximately 5 percent by weight). LaCr/MCB and YCr/MCB surfaces had small red color regions believed to be an oxide of chrome that was different from the parent oxide of the slip.

The oxide pick-up on the JNM substrates was greater, about 6 grams (approximately 12 percent by weight) even though the slip and procedure for applying the slip were identical to that used with the MCB-1 substrates. As a consequence, the coatings were thicker, and for YCr/JNM and MAFF/JNM, some cracking of the coating was observed. The coatings, however, appeared to have chemically reacted with and diffused partly into the substrate. As with the MCB-1 substrates, there were red-colored regions on the surface of LaCr/JNM and YCr/JNM.

The oxide pick-up on the solution impregnated reactors was not measured; however, the oxide mixture appeared to be uniformly dispersed throughout the substrate for both TCT/JNM and TCT/JNX.

Of the catalysts prepared for this second testing phase, the most uniform were the solution-dipped (TCT) catalysts. These showed uniform penetration on both the JNM and JNX substrates. The MAFF material, prepared by slip coating, was very uniform on the MCB-1 substrate and less so on the JNM substrate (probably due to the thicker coatings); however, both looked good. The remaining two materials, LaCr and YCr, showed

---

*Coating pick-up was determined by weight gain after drying at 1,300K.

## Table 7-1. Phase II Reactor Descriptions

| Designation | Substrate | Catalyst | Cell Densities (Cells/$in^2$) | Application Method |
|---|---|---|---|---|
| LaCr/MCB | Corning MCB-1 | Lanthanum/chromium oxides 5 percent weight | 9, 16, 100 | Slip coating |
| YCr/MCB | Corning MCB-1 | Yttria/chromium oxide 5 percent weight | 9, 16, 100 | Slip coating |
| MAFF/MCB | Corning MCB-1 | Magnesium aluminate-iron ferrite; 5 percent weight | 9, 16, 100 | Slip coating |
| LaCr/JNM | Proprietary | Lanthanum/chromium oxides 12 percent weight | 9, 16, 100, 200 | Slip coating |
| YCr/JNM | Proprietary | Yttria/chromium oxide 12 percent weight | 9, 16, 100, 200 | Slip coating |
| MAFF/JNM | Proprietary | Magnesium aluminate-iron ferrite; 12 percent weight | 9, 16, 100, 200 | Slip coating |
| TCT/JNM | Proprietary | Terbium/cerium/thorium oxides | 9, 16, 100, 200 | Solution impregnation |
| TCT/JNX | Proprietary | Terbium/Cerium/Thorium oxides | 9, 16, 100, 200 | Solution impregnation |

various levels of Cr reactions and in some cases, loss of material due to vaporization. This effect was mild for the YCr and severe for the LaCr; therefore, the best candidates for testing were judged to be the TCT and MAFF materials, YCr being second, and the LaCr being last.

## 7.2 PHASE II COMBUSTION SCREENING TESTS

Graded cell catalytic reactors were assembled from 5.0 cm diameter by 2.5 cm long elements. Four elements were used for the JNM and JNX materials while the MCB-1 materials consisted of three elements. The reactors were instrumented with R-type thermocouples in each element and mounted within the refractory-insulated test section as described in section 2 and combustion testing was attempted at the design test conditions given in section 1.

Five of the eight candidate catalysts were not active at the combustion conditions tested. These were the MAFF and LaCr formulations on both MCB-1 and JNM substrates and the YCr catalyst on the JNM substrate. In addition to step-by-step increases in the reactor surface temperature, the upstream face velocity was reduced to 4.5 m/s in each case in an attempt to enhance catalytic combustion. Even with these measures, the reactor surface temperatures fell nearly to the preheat level within 60 seconds following opposed jet shutoff. As a check on possible adverse effects of incomplete liquid fuel atomization or vaporization, propane was tested on the MAFF/MCB and LaCr/JNM reactors. However, as with diesel fuel, these catalysts were inactive on propane. Partial melting of the substrate occurred in each of these five catalysts as temperatures were pushed to increasingly higher levels in attempts to get self-sustaining catalytic activity.

Three reactors, however, did demonstrate limited catalytic activity and allowed the collection of combustion data. In order of increasing apparent performance, these were the YCr/MCB, TCT/JNX, and TCT/JNM reactors. Reduced test data for these reactors are shown in tables 7-2, 7-3, and 7-4, respectively. Each reactor required very high surface temperatures before activity was sustained. Measured temperatures approached 1,810K in some cases. Much higher local temperatures (greater than 1,900K) were apparently encountered due to nonuniformities which caused some substrate melting and damage. These temperature nonuniformities were probably due to the low levels of catalyst activity and their unstable operation during light-off. During a period of lower catalyst temperature, a small surface buildup of hydrocarbons may occur so that the hydrocarbon concentration on the surface is higher than the controlled free stream levels. That is, during fuel-lean operation, a mixture closer to stoichiometric may form on the catalyst surface. As the catalyst temperature swings to a higher value during an instability, these hydrocarbons burn off and drive the surface temperature much higher than that dictated by the set point fuel-air ratio. In each case, the measured quasi-steady-state catalyst temperature was somewhat below the adiabatic flame temperature based on measured $CO_2$ in the exhaust (see appendix). Since the calculated adiabatic flame temperature was based on the emissions of $CO_2$, further reactions may have been occurring elsewhere outside of the reactor, as in downstream flameholding.

For the YCr/MCB reactor, the measured concentrations of carbon monoxide and unburned hydrocarbons in the exhaust were reasonably low; however, the measured reactor temperature was significantly below the predicted adiabatic flame temperature. This fact, coupled with the

## Table 7-2. Combustion Test Data for YCr/MCB (Diesel/Air)

| Data Point | Air Flow (SCFM) | Vref (ft/s) | Percent T/A from Emissions | T Preheat ($^oF$) | T Adiabatic From Emissions ($^oF$) | T Measured 1 in. Downstream ($^oF$) | Combustion Efficiency | | $NO_x$ (ppm) | CO (ppm) | UHC (ppm) | $O_2$ (%) | $CO_2$ (%) | $NO_x$ Corrected to 15% $O_2$ (ppm) | Elapsed Time (Hr) |
|---|---|---|---|---|---|---|---|---|---|---|---|---|---|---|---|
| | | | | | | | From Emissions (%) | Based on T (%) | | | | | | | |
| 1 | 17 | 31 | 183 | 818 | 3,013 | 2,363 | 97.7 | 70.39 | 23 | 160 | 100 | 9.6 | 8.2 | 12 | 0.05 |
| 2 | 17 | 31 | 179 | 818 | 3,039 | 2,474 | 98.6 | 74.56 | 30 | 57 | 70 | 9.5 | 8.4 | 16 | 0.25 |
| 3 | 17 | 31 | 179 | 814 | 3,035 | 2,500 | 98.8 | 75.91 | 35 | 56 | 60 | 9.2 | 8.4 | 18 | 0.50 |
| 4 | 27 | 52 | 181 | 886 | 3,050 | 2,518 | 99.0 | 75.42 | 40 | 77 | 44 | 9.0 | 8.3 | 19 | 0.75 |
| 5 | 27 | 52 | 186 | 885 | 3,000 | 2,527 | 99.4 | 77.64 | 42 | 58 | 22 | 9.5 | 8.1 | 20 | 1.50 |
| 6 | 27 | 52 | 183 | 885 | 3,038 | 2,516 | 99.5 | 75.75 | 45 | 63 | 14 | 9.7 | 8.2 | 21 | 1.92 |
| 7 | 27 | 53 | 186 | 891 | 3,013 | 2,536 | 99.5 | 77.52 | 43 | 58 | 17 | 9.6 | 8.1 | 20 | 2.14 |
| 8 | 27 | 53 | 193 | 896 | 2,963 | 2,441 | 99.6 | 74.75 | 34 | 53 | 13 | 10.2 | 7.8 | 16 | 2.34 |
| 9 | 27 | 53 | 191 | 893 | 2,975 | 2,470 | 99.6 | 75.74 | 38 | 50 | 14 | 10.0 | 7.9 | 17 | 2.45 |
| 10 | 27 | 53 | 191 | 893 | 2,975 | 2,434 | 99.6 | 74.02 | 37 | 50 | 15 | 10.0 | 7.9 | 18 | 2.54 |
| 11 | 27 | 53 | 200 | 900 | 2,900 | 2,306 | 99.5 | 70.03 | 30 | 44 | 17 | 10.5 | 7.5 | 13 | 2.72 |
| 12 | 27 | 53 | 196 | 899 | 2,925 | 2,263 | 99.8 | 67.32 | 28 | 45 | 2 | 10.5 | 7.7 | 13 | 2.95 |
| 13 | 27 | 53 | 215 | 901 | 2,788 | 2,023 | 99.7 | 59.46 | 21 | 36 | 7 | 11.2 | 7.0 | 9 | 3.24 |
| 14 | 27 | 53 | 212 | 901 | 2,813 | 2,006 | 99.7 | 57.79 | 21 | 38 | 9 | 11.2 | 7.1 | 9 | 3.35 |
| 15 | 27 | 53 | 221 | 903 | 2,750 | 1,903 | 99.7 | 54.14 | 19 | 34 | 7 | 11.5 | 6.8 | 8 | 3.65 |
| 16 | 27 | 53 | 221 | 906 | 2,760 | 1,800 | 99.7 | 48.22 | 21 | 38 | 9 | 11.5 | 6.8 | 7 | 3.80 |
| 17 | 27 | 53 | 221 | 906 | 2,760 | 1,622 | 99.6 | 38.54 | 22 | 40 | 10 | 11.6 | 6.8 | 7 | 3.94 |
| 18 | 27 | 53 | 228 | 909 | 2,713 | 1,368 | 99.6 | 25.44 | 20 | 39 | 11 | 11.8 | 6.6 | 8 | 4.05 |
| 19 | 27 | 53 | 235 | 909 | 2,663 | 1,329 | 99.6 | 23.95 | 18 | 38 | 11 | 13.0 | 6.4 | 7 | 4.15 |
| 20 | 27 | 54 | 272 | 921 | 2,500 | 1,234 | 99.7 | 19.82 | 12 | 27 | 6 | 13.0 | 5.5 | 5 | 4.47 |
| 21 | 27 | 54 | 267 | 923 | 2,525 | 1,220 | 99.7 | 18.54 | 12 | 28 | 8 | 13.7 | 5.6 | 5 | 4.50 |
| 22 | 27 | 54 | 295 | 928 | -- | 1,180 | 99.6 | -- | 10 | 31 | 9 | 14.0 | 5.1 | 4 | 4.79 |
| 23 | 27 | 54 | 320 | 931 | -- | 1,156 | 98.3 | -- | 7 | 168 | 22 | 14.0 | 4.7 | 3 | 4.90 |
| 24 | 27 | 53 | 191 | 894 | 2,963 | 2,615 | 99.5 | 83.18 | 40 | 63 | 18 | 10.0 | 7.9 | 18 | 5.70 |
| 25 | 27 | 53 | 189 | 894 | 2,988 | 2,637 | 99.4 | 83.24 | 40 | 54 | 22 | 10.0 | 8.0 | 18 | 5.84 |
| 26 | 27 | 52 | 165 | 887 | 3,200 | 2,721 | 99.4 | 70.29 | 70 | 78 | 23 | 8.5 | 9.1 | 35 | 5.95 |
| 27 | 27 | 52 | 167 | 884 | 3,188 | 2,980 | 99.2 | 90.97 | 97 | 135 | 23 | 8.5 | 9.0 | 49 | 5.99 |

## Table 7-3. Combustion Test Data for TCT/JNX (Diesel/Air)

| Data Point | Air Flow (SCFM) | Vref (ft/s) | Percent T/A from Emissions | T Preheat ($^{o}$F) | T Adiabatic From Emissions ($^{o}$F) | T Measured 1 in. Downstream ($^{o}$F) | Combustion Efficiency From Emissions (%) | Combustion Efficiency Based on T (%) | $NO_x$ (ppm) | CO (ppm) | UHC (ppm) | $O_2$ (%) | $CO_2$ (%) | $NO_x$ Corrected to 15% $O_2$ (ppm) | Elapsed Time (Hr) |
|---|---|---|---|---|---|---|---|---|---|---|---|---|---|---|---|
| 1 | 18 | 32 | 163 | 786 | 3,163 | 2,695 | 99.5 | 80.3 | 67 | 85 | 14 | 8.5 | 9.2 | 32 | .25 |
| 2 | 29 | 56 | 171 | 868 | 3,138 | 2,637 | 99.4 | 77.9 | 67 | 127 | 13 | 8.7 | 8.8 | 33 | .30 |
| 3 | 29 | 56 | 171 | 867 | 3,138 | 2,640 | 99.4 | 78.1 | 75 | 124 | 14 | 8.9 | 8.8 | 37 | .40 |
| 4 | 29 | 56 | 171 | 867 | 3,138 | 2,634 | 99.4 | 77.8 | 72 | 124 | 14 | 8.9 | 8.8 | 36 | .48 |
| 5 | 29 | 56 | 173 | 868 | 3,125 | 2,641 | 99.3 | 78.6 | 70 | 120 | 17 | 9.0 | 8.7 | 34 | .63 |
| 6 | 29 | 56 | 173 | 868 | 3,125 | 2,640 | 99.3 | 78.5 | 66 | 118 | 18 | 9.0 | 8.7 | 32 | .73 |
| 7 | 29 | 56 | 173 | 870 | 3,125 | 2,641 | 99.3 | 78.5 | 67 | 118 | 17 | 9.0 | 8.7 | 33 | .81 |
| 8 | 28 | 54 | 184 | 874 | 3,025 | 2,535 | 99.4 | 77.2 | 47 | 93 | 18 | 9.7 | 8.2 | 22 | .88 |
| 9 | 28 | 54 | 184 | 874 | 3,025 | 2,538 | 99.4 | 77.4 | 47 | 93 | 18 | 9.7 | 8.2 | 22 | .98 |
| 10 | 28 | 54 | 191 | 868 | 2,950 | 2,445 | 99.4 | 75.7 | 36 | 75 | 18 | 10.2 | 7.9 | 16 | 1.13 |
| 11 | 28 | 53 | 191 | 864 | 2,950 | 2,428 | 99.4 | 75.0 | 35 | 77 | 17 | 10.2 | 7.9 | 16 | 1.21 |
| 12 | 28 | 53 | 199 | 864 | 2,888 | 2,359 | 99.5 | 73.9 | 29 | 63 | 17 | 10.6 | 7.6 | 13 | 1.28 |
| 13 | 28 | 53 | 199 | 861 | 2,888 | 2,354 | 99.5 | 73.7 | 28 | 62 | 16 | 10.6 | 7.6 | 13 | 1.35 |

# Table 7-4. Combustion Test Data for TCT/JNM (Diesel/Air)

| Data Point | Air Flow (SCFM) | Vref (ft/s) | Percent T/A from Emissions | T Preheat ($^oF$) | T Adiabatic From Emissions ($^oF$) | T Measured 1 in. Downstream ($^oF$) | Combustion Efficiency | | $NO_x$ (ppm) | CO (ppm) | UHC (ppm) | $O_2$ (%) | $CO_2$ (%) | $NO_x$ Corrected to 15% $O_2$ (ppm) | Elapsed Time (Hr) |
|---|---|---|---|---|---|---|---|---|---|---|---|---|---|---|---|
| | | | | | | | From Emissions (%) | Based on T (%) | | | | | | | |
| 1 | 27 | 53 | 212 | 913 | 2,825 | -- | 99.5 | -- | 23 | 34 | 18 | 11.4 | 7.1 | 14 | 0.25 |
| 2 | 27 | 53 | 215 | 895 | 2,775 | 2,607 | 99.6 | 91.06 | 21 | 35 | 13 | 11.4 | 7.0 | 13 | 0.48 |
| 3 | 27 | 53 | 212 | 894 | 2,800 | 2,620 | 99.6 | 90.56 | 22 | 34 | 15 | 11.4 | 7.1 | 14 | 0.56 |
| 4 | 27 | 53 | 215 | 890 | 2,775 | 2,634 | 99.6 | 92.52 | 21 | 33 | 13 | 11.4 | 7.0 | 13 | 0.83 |
| 5 | 27 | 53 | 215 | 896 | 2,781 | 2,640 | 99.6 | 92.52 | 22 | 33 | 14 | 11.4 | 7.0 | 14 | 0.93 |
| 6 | 27 | 53 | 218 | 900 | 2,763 | 2,620 | 99.7 | 92.32 | 20 | 30 | 10 | 11.5 | 6.9 | 13 | 1.60 |
| 7 | 27 | 53 | 218 | 900 | 2,763 | 2,600 | 99.7 | 91.25 | 21 | 30 | 11 | 11.5 | 6.9 | 13 | 1.92 |
| 8 | 27 | 53 | 215 | 901 | 2,788 | 2,588 | 99.6 | 89.40 | 22 | 31 | 13 | 11.5 | 7.0 | 14 | 2.00 |
| 9 | 27 | 53 | 215 | 902 | 2,788 | 2,560 | 99.6 | 87.91 | 22 | 30 | 15 | 11.4 | 7.0 | 14 | 2.13 |
| 10 | 27 | 53 | 218 | 903 | 2,763 | 2,470 | 99.6 | 84.25 | 20 | 31 | 12 | 11.4 | 6.9 | 13 | 2.20 |
| 11 | 27 | 53 | 218 | 903 | 2,763 | 2,440 | 99.6 | 82.63 | 21 | 30 | 13 | 11.4 | 6.9 | 13 | 2.35 |
| 12 | 27 | 53 | 221 | 904 | 2,750 | 2,200 | 99.6 | 70.21 | 19 | 29 | 12 | 11.5 | 6.8 | 12 | 2.48 |
| 13 | 27 | 53 | 221 | 905 | 2,750 | 2,200 | 99.6 | 70.21 | 20 | 29 | 13 | 11.5 | 6.8 | 13 | 2.55 |
| 14 | 27 | 53 | 221 | 905 | 2,750 | 1,930 | 99.6 | 55.56 | 19 | 29 | 12 | 11.6 | 6.8 | 12 | 2.75 |
| 15 | 27 | 53 | 221 | 905 | 2,750 | 1,940 | 99.6 | 56.10 | 20 | 29 | 13 | 11.6 | 6.8 | 13 | 2.90 |
| 16 | 27 | 53 | 228 | 907 | 2,697 | 1,791 | 99.6 | 49.39 | 17 | 26 | 12 | 11.8 | 6.6 | 11 | 2.93 |
| 17 | 27 | 53 | 231 | 908 | 2,675 | 1,770 | 99.6 | 48.78 | 17 | 25 | 12 | 12.0 | 6.5 | 11 | 2.98 |
| 18 | 27 | 53 | 234 | 910 | 2,663 | 1,722 | 99.6 | 46.32 | 16 | 24 | 13 | 12.2 | 6.4 | 11 | 3.08 |
| 19 | 27 | 53 | 242 | 912 | 2,625 | 1,636 | 99.6 | 42.27 | 15 | 23 | 14 | 12.5 | 6.2 | 11 | 3.15 |
| 20 | 27 | 53 | 272 | 918 | 2,463 | 1,520 | 99.5 | 38.96 | 11 | 21 | 14 | 13.4 | 5.5 | 9 | 3.28 |
| 21 | 27 | 53 | 295 | 924 | -- | 1,460 | 99.4 | -- | 10 | 35 | 16 | 13.8 | 5.1 | 8 | 3.33 |
| 22 | 27 | 53 | 212 | 900 | 2,813 | 2,630 | 99.0 | 90.43 | 22 | 43 | 41 | 11.3 | 7.1 | 14 | 3.57 |
| 23 | 27 | 53 | 215 | 900 | 2,788 | 2,620 | 99.1 | 91.10 | 22 | 36 | 37 | 11.3 | 7.0 | 14 | 3.70 |

physical appearance of the catalyst exit face, which was very dark, indicated that the catalyst was operating primarily as a flameholder. Indeed, thermal flames were visible downstream of the catalyst throughout the testing.

The four-segment TCT/JNX catalyst was also very difficult to light off. Combustion was initiated at a velocity of 9.8 m/s and a measured reactor temperature of 1,810K. At this condition, localized substrate fracturing occurred on about 50 percent of the downstream segment. Finally, combustion was stabilized at about 17 m/s and a measured temperature of about 1,700K. The remaining portions of the reactor monolith were brighter and slightly more uniform in appearance than the YCr/MCB reactor. Here too, however, the catalyst was operating primarily as a flameholder as flames were visible and the highest measured monolith temperature was about 22 percent below the adiabatic flame temperature.

The TCT/JNM reactor, which was also a four-segment reactor, gave slightly improved performance over the two just described. However, the catalyst was equally difficult to light off. Similar to the TCT/JNX reactor, it was necessary to reduce the face velocity to 9.8 m/s before combustion could be sustained at about 1,810K. Again, at this condition, instabilities caused some substrate fracturing which removed about 50 percent of the back segment. The highest measured catalyst temperature ranged from 10 to 20 percent below the adiabatic flame temperature. The measured emissions of carbon monoxide and unburned hydrocarbons were, overall, the lowest of the three reactors which, when normalized by stoichiometry, results in a slightly higher combustion efficiency. Despite these improved performance indicators, however, the reactor appeared to be operating primarily in a flameholder mode with low surface activity. Nonuniformities were distinctly visible on the reactor back face, and downstream thermal combustion was readily apparent. Additionally, during the parametric characterization, the gap between measured temperature and adiabatic flame temperature based on emissions measurements increased substantially as the fuel-air ratio was reduced.

At the conclusion of the screening tests it was obvious that none of the eight reactors performed with a high degree of catalytic activity. Of the three reactors able to sustain combustion, the TCT/JNM formulation gave the best performance. This judgment was based on reactor temperature and emissions measurements as well as physical appearance. The structural performance of the substrate was at least as good as that of any of the eight reactors tested. The substrate damage was probably due to overheating during light-off instabilities rather than a steady-state loss of strength.

## 7.3 PHASE II DURABILITY REACTOR DESIGN

Based on the phase I experience and the phase II screening tests, it appeared that, individually, neither the noble metal nor the metal oxide catalyst approach would be appropriate for meeting the automotive gas turbine goals. Noble metals do not have the required durability at high temperatures and metal oxides do not have sufficient catalytic activity to achieve stable combustion conditions over anything other than a very small temperature range.

From reference 2, it was shown for a uniform cell density honeycomb that the leading edge temperature was close to the preheat temperature. As the flow progressed through the honeycomb, there would be a slow temperature rise followed by a rapid temperature gradient. The reasons for this temperature distribution were described in reference 2 and led to the formulation of the graded cell concept.

In the graded cell concept, the web thickness and cell densities could be tailored to achieve a more uniform temperature distribution within the catalyst. With this approach the blow-out mass throughput could be significantly increased since, a fraction of an inch from the leading edge of the catalyst, the surface temperature could be within a few hundred degrees of the adiabatic flame temperature.

The reactor design for the phase II durability tests is a first attempt at applying the graded cell concept to incorporate the strength and weaknesses of current noble metal and metal oxide catalyst technology. The basic premises are:

- With consideration for kinetic rates and heat and mass balances, the graded cell approach can be used to attain specific reactor temperature distributions
- Noble metal catalysts have excellent activity, especially at low temperatures, but cannot be used for sustained high-temperature application
- Metal oxide catalysts are believed to have good high-temperature durability but do not have sufficient activity for low-temperature operation except possibly with high inlet gas preheat

Although an analytical procedure is available for preliminary reactor design (reference 13) the quality of the available kinetics data and program resources did not permit a detailed analysis, therefore, a reactor was designed with the experience gained from the results of phase I and the phase II screening evaluations. This reactor used a medium-cell density, noble metal catalyst as the leading element and three graded cell metal oxide catalysts for the downstream elements. A description of the phase II durability reactor is shown in figure 7-1.

The noble metal leading edge element was selected to operate at a temperature of 1,400 to 1,500K at which good durability has been shown in previous programs (references 2 and 6). This element would essentially be a preheater for the metal oxide elements. The metal oxide elements were selected to achieve complete combustion at the advanced automotive gas turbine condition (1,700K exit temperature).

The test reactor was instrumented with four type-R thermocouples, one located at the geometric center of each reactor element as shown in figure 7-1.

## 7.4 PHASE II DURABILITY TESTS

Because of some perceived difficulties encountered in achieving a uniform, premixed, prevaporized diesel fuel mixture, the phase II durability tests were conducted using propane fuel at the following nominal conditions:

| | |
|---|---|
| • Preheat | 730K |
| • Pressure | $10^5$ Pa |
| • Face velocity | 13.5 m/s |
| • Stoichiometry | 230 percent TA |
| • Adiabatic flame temperature | 1,700K |

Representative reduced data are shown in table 7-5. At these conditions, there were no measurable unburned hydrocarbons, carbon monoxide levels on a dry basis were consistently below 20 ppm, $NO_x$ levels were below 5 ppm, and calculated combustion efficiencies were above

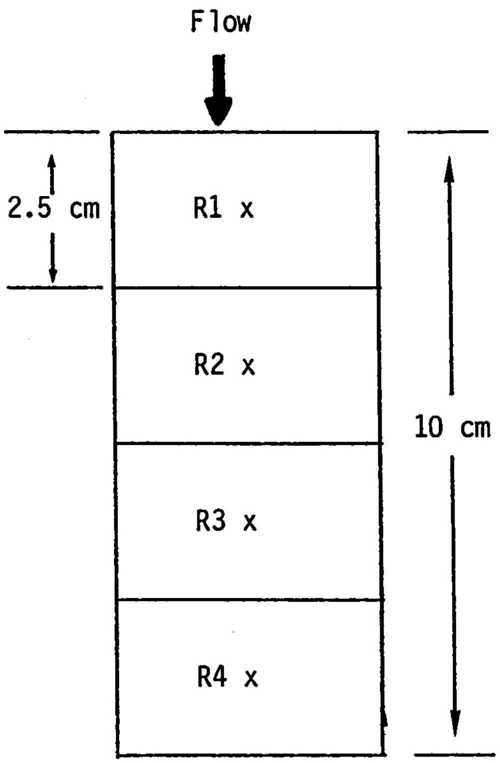

| Element No. | Substrate | Catalyst |
|---|---|---|
| 1 | Corning MCB-12<br>16 Cells/in$^2$, square | UOP-B |
| 2 | JNM<br>9 Cells/in$^2$, square | Terbium/Cerium/<br>Thorium oxides<br>12 percent weight |
| 3 | JNM<br>16 Cells/in$^2$, square | Terbium/Cerium/<br>Thorium oxides<br>12 percent weight |
| 4 | JNM<br>64 Cells/in$^2$, square | Terbium/Cerium/<br>Thorium oxides<br>12 percent weight |

Figure 7-1. Phase II Durability Reactor Description

## Table 7-5. Representative Combustion Durability Test Data for TCT/JNM (Propane/Air)

| Data Point | Air Flow (SCFM) | $C_3H_8$ SCFM | Vref (ft/s) | % T/A from Flow Measurement | % T/A From Emissions | T Preheat (°F) | T Adiabatic From Emissions (°F) | T In Depth Element 3 (°F) | Combustion Efficiency | | $NO_x$ (ppm) | CO (ppm) | UHC (ppm) | $O_2$ (%) | $CO_2$ (%) | $NO_x$ Corrected to 15% $O_2$ (ppm) | Elapsed Time (Hr) |
|---|---|---|---|---|---|---|---|---|---|---|---|---|---|---|---|---|---|
| | | | | | | | | | From Emissions (%) | Based on T (%) | | | | | | | |
| 1 | 23.5 | 0.437 | 45 | 226 | 228 | 837 | 2,650 | 2,611 | 99.85 | 97.9 | 2 | 21 | 2 | 11.4 | 5.8 | 1 | .4 |
| 2 | 23.5 | 0.433 | 45 | 228 | 228 | 839 | 2,650 | 2,565 | 99.90 | 95.3 | 3 | 20 | 0 | 11.2 | 5.8 | 2 | 1.0 |
| 6 | 23.5 | 0.421 | 45 | 235 | 236 | 846 | 2,600 | 2,534 | 99.90 | 96.2 | 3 | 15 | 1 | 11.9 | 5.6 | 2 | 4.6 |
| 12 | 23.5 | 0.422 | 45 | 234 | 236 | 848 | 2,600 | 2,548 | 99.87 | 97.0 | 2 | 15 | 2 | 12.0 | 5.6 | 1 | 10.7 |
| 22 | 23.5 | 0.416 | 45 | 237 | 236 | 828 | 2,600 | 2,537 | 99.9 | 96.4 | 2 | 14 | 1 | 11.8 | 5.6 | 1 | 20.7 |
| 38 | 23.5 | 0.420 | 45 | 235 | 232 | 829 | 2,630 | 2,551 | 99.9 | 95.6 | 1 | 13 | 0 | 11.7 | 5.7 | 1 | 30.8 |
| 47 | 23.5 | 0.420 | 45 | 235 | 232 | 832 | 2,630 | 2,561 | 99.9 | 96.2 | 1 | 13 | 2 | 11.6 | 5.7 | 1 | 40.8 |
| 65 | 23.5 | 0.418 | 45 | 236 | 224 | 824 | 2,680 | 2,531 | 99.9 | 92.0 | - | 14 | 0 | 12.0 | 5.9 | - | 50.8 |
| 75 | 23.5 | 0.420 | 44 | 235 | 228 | 833 | 2,650 | 2,556 | 99.9 | 94.8 | - | 13 | 0 | 11.6 | 5.8 | - | 60.1 |
| 85 | 23.5 | 0.420 | 44 | 235 | 228 | 830 | 2,650 | 2,596 | 99.9 | 97.0 | - | 14 | 2 | 11.5 | 5.8 | - | 70.8 |
| 96 | 23.5 | 0.421 | 44 | 235 | 228 | 835 | 2,650 | 2,587 | 99.91 | 96.5 | - | 14 | 1 | 11.5 | 5.8 | - | 77.5 |
| 116 | 23.3 | 0.423 | 44 | 233 | 224 | 836 | 2,690 | 2,581 | 99.88 | 94.1 | - | 15 | 2 | 12.4 | 5.9 | - | 102.0 |
| 185 | 23.1 | 0.418 | 45 | 232 | 224 | 899 | 2,720 | 2,609 | 99.81 | 93.9 | - | 14.8 | 5 | 12.6 | 5.9 | - | 212.0 |
| 256 | 23.1 | 0.420 | 45 | 231 | 228 | 882 | 2,690 | 2,601 | 99.93 | 95.1 | - | 14.5 | 0 | 12.5 | 5.8 | - | 320.0 |
| 378 | 23.1 | 0.432 | 45 | 225 | 216 | 884 | 2,780 | - | 99.92 | - | - | 17.3 | 0 | 12.0 | 6.1 | - | 495.6 |
| 492 | 23.1 | 0.438 | 45 | 222 | 216 | 873 | 2,760 | - | 99.90 | - | - | 18 | 1 | 11.8 | 6.1 | - | 711.6 |
| 564 | 23.0 | 0.440 | 45 | 220 | 228 | 878 | 2,680 | - | 99.91 | - | - | 18.8 | 0 | 12.0 | 5.8 | - | 855.6 |
| 647 | 23.1 | 0.450 | 45 | 216 | 224 | 881 | 2,730 | - | 99.92 | - | - | 17 | 0 | - | 5.9 | - | 1,001.6 |

99.9 percent. A chronology of events for this durability test is shown in figure 7-2. During the testing period seven parametric tests were conducted and the catalyst was shut down and restarted six times. After 1,002 hours the testing was continued with five on/off cycles, a parametric test, a short period of operation on diesel fuel, and a final test with propane.

The emissions performance of the reactor during the durability test is given in figures 7-3 and 7-4. The plots show only a fraction of the total amount of data, as measurements were recorded approximately every 2 hours. Figure 7-3 shows that the $O_2$ and $CO_2$ levels remained fairly constant throughout the test, indicating the steady-state operation. The parametric tests appear as points of reduced $CO_2$ and increased $O_2$ as the fuel/air ratio was decreased. The drift in oxygen level was probably due to a malfunctioning $O_2$ analyzer which ultimately failed at about 890 hours. A comparison of $CO_2$, CO, and UHC levels with input fuel flow results in a carbon balance fuel-air ratio which was 5 to 8 percent higher than the metered fuel-air ratio over most of the data. The average carbon monoxide concentration in the exhaust sample apparently increased slightly throughout the test, as indicated in figure 7-4, and is probably due to slow catalyst deactivation. UHC concentrations remained essentially zero during steady-state operation. The measurements shown in figure 7-4 appear to be primarily instrument noise. Parametric testing data are omitted from figure 7-4.

In spite of the slight carbon monoxide increase, figure 7-5 shows that the calculated combustion efficiency remained high throughout the durability tests. The only major influence on combustion efficiency was the parametric tests.

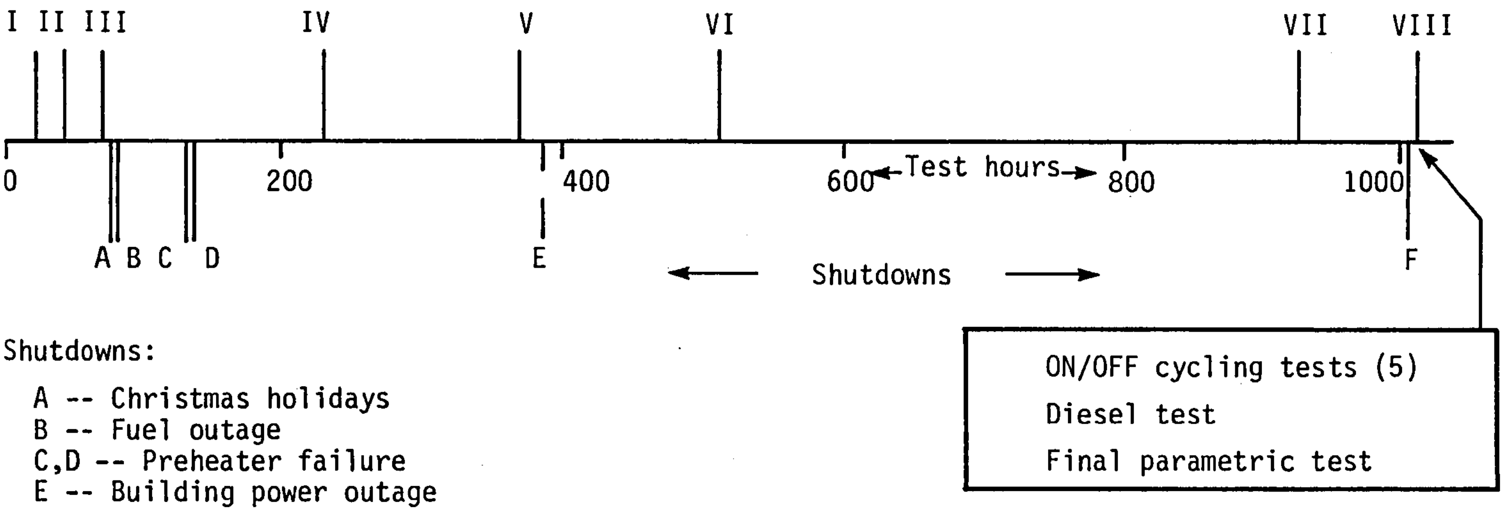

Shutdowns:

A -- Christmas holidays
B -- Fuel outage
C,D -- Preheater failure
E -- Building power outage
F -- End of life test, 1001.6 hours

Roman numerals indicate times at which parametric tests were performed.

A26195

Figure 7-2. Phase II 1000-Hour Durability Event Chart

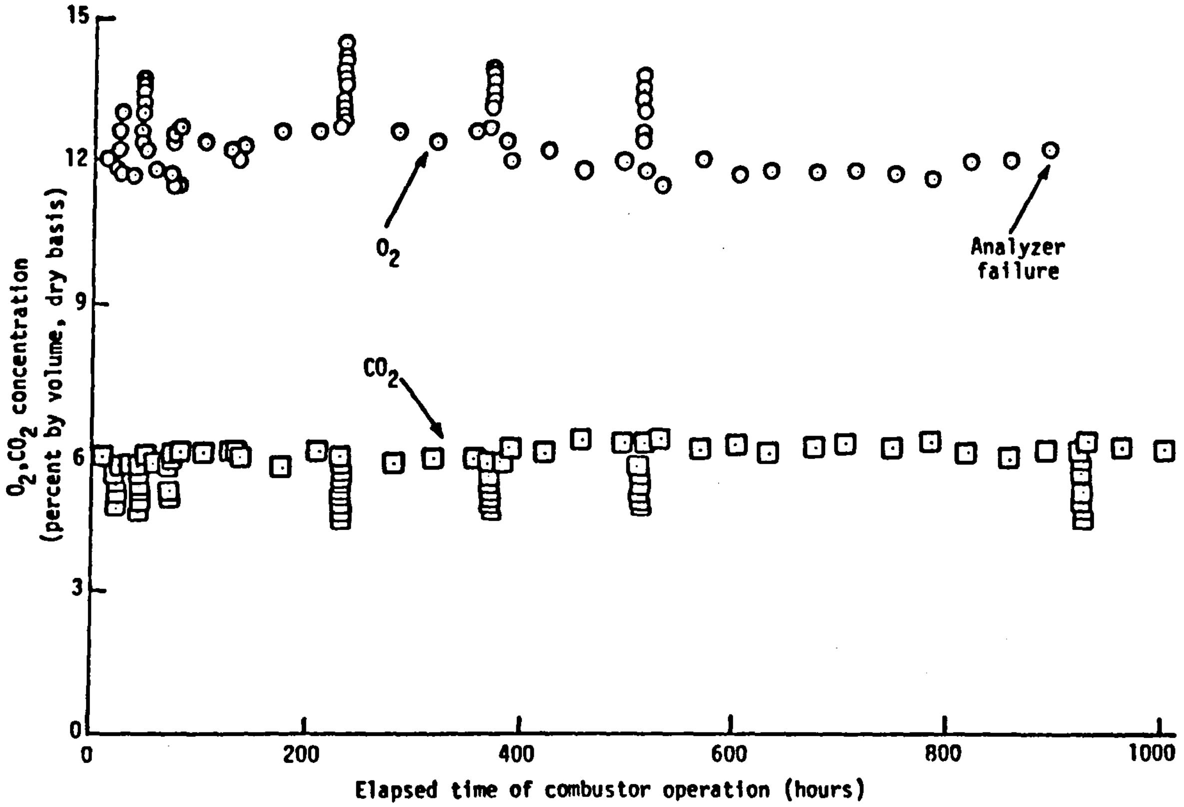

Figure 7-3. Phase II Durability Test $O_2$ and $CO_2$ Emission Levels

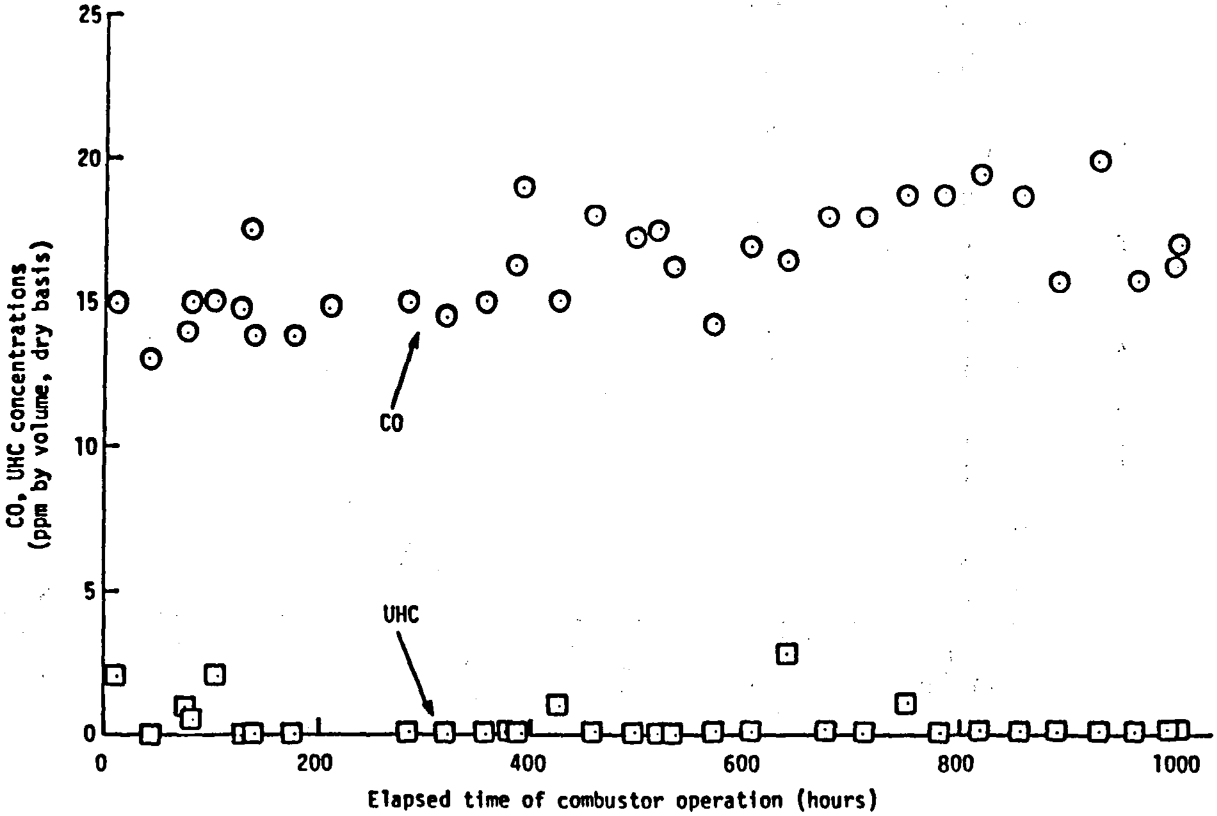

Figure 7-4. Phase II Durability Test CO and UHC Emission Levels

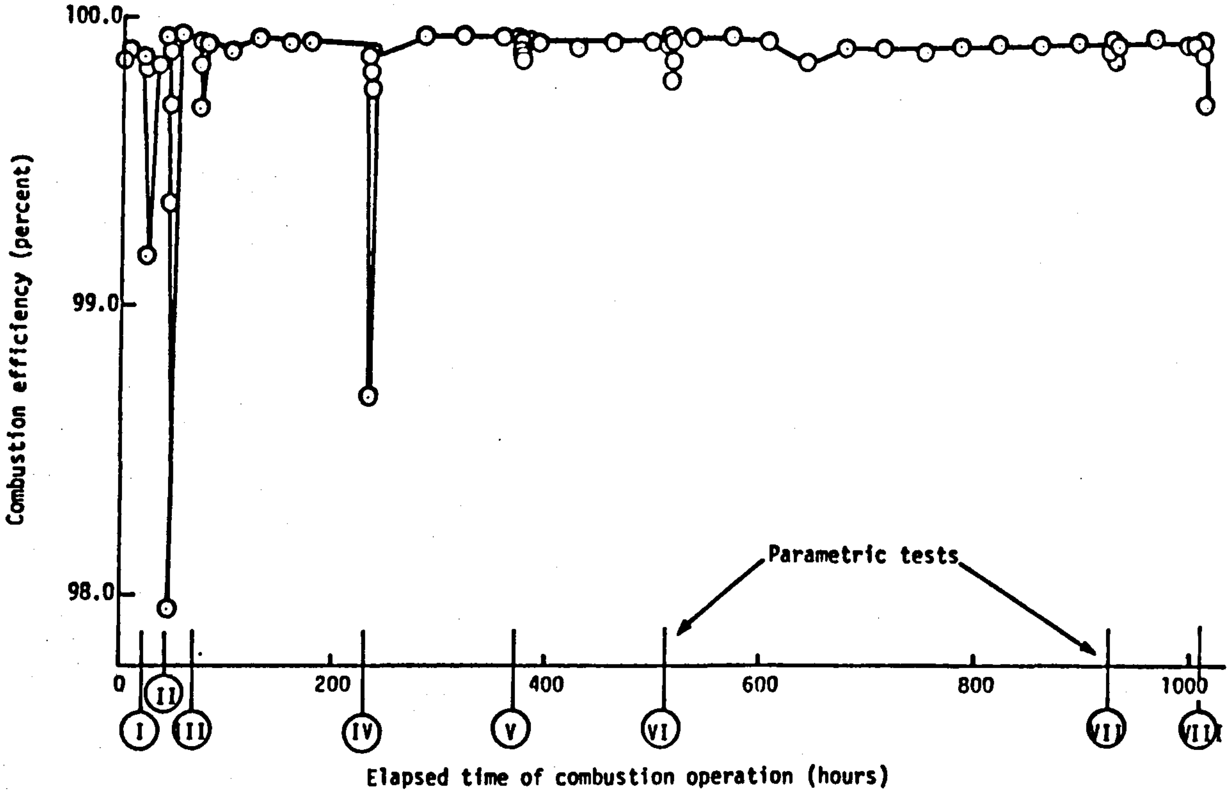

Figure 7-5. Phase II Durability Test Combustion Efficiency Performance

$NO_x$ emission levels are not shown since a malfunctioning chemiluminescent analyzer did not allow successive measurements. The instrument was functional at the beginning of the test and concentrations of from 1 to 3 ppm were recorded. A temporary repair at 740 hours gave a measurement of 4 ppm. The analyzer was fully operational prior to the on/off cycling tests and measured levels ranged from 2 to 5 ppm.

A total of eight parametric tests were conducted in which the fuel-air ratio was progressively decreased until an increase in carbon monoxide or unburned hydrocarbons was detected. The results of these tests are shown in figure 7-6 (a and b) where combustion efficiency is plotted as a function of the percent theoretical air (based on emissions of $CO_2$). An apparent change in the combustion efficiency at high theoretical air conditions as a function of combustion time was observed.

The difference between the adiabatic flame temperature and the temperature measured just downstream of the reactor increased rapidly as the mixture was leaned out in the parametric test sequence. The implication of this result is that for these fuel lean conditions the fuel was not fully combusted in the reactor and some combustion reactions were occurring between the reactor and the sampling probe.

Following the combustion durability test, the reactor was removed for inspection. The surface appeared much lighter in color, indicating a probable loss of catalyst coating. Structurally, the monolith had distorted slightly and fused to the refractory holder, but major cracks, loss of substrate, or other damage had not occurred. Photographs of the noble metal lead element and the metal oxide exit segment in the refractory holder are shown in figures 7-7 and 7-8 respectively.

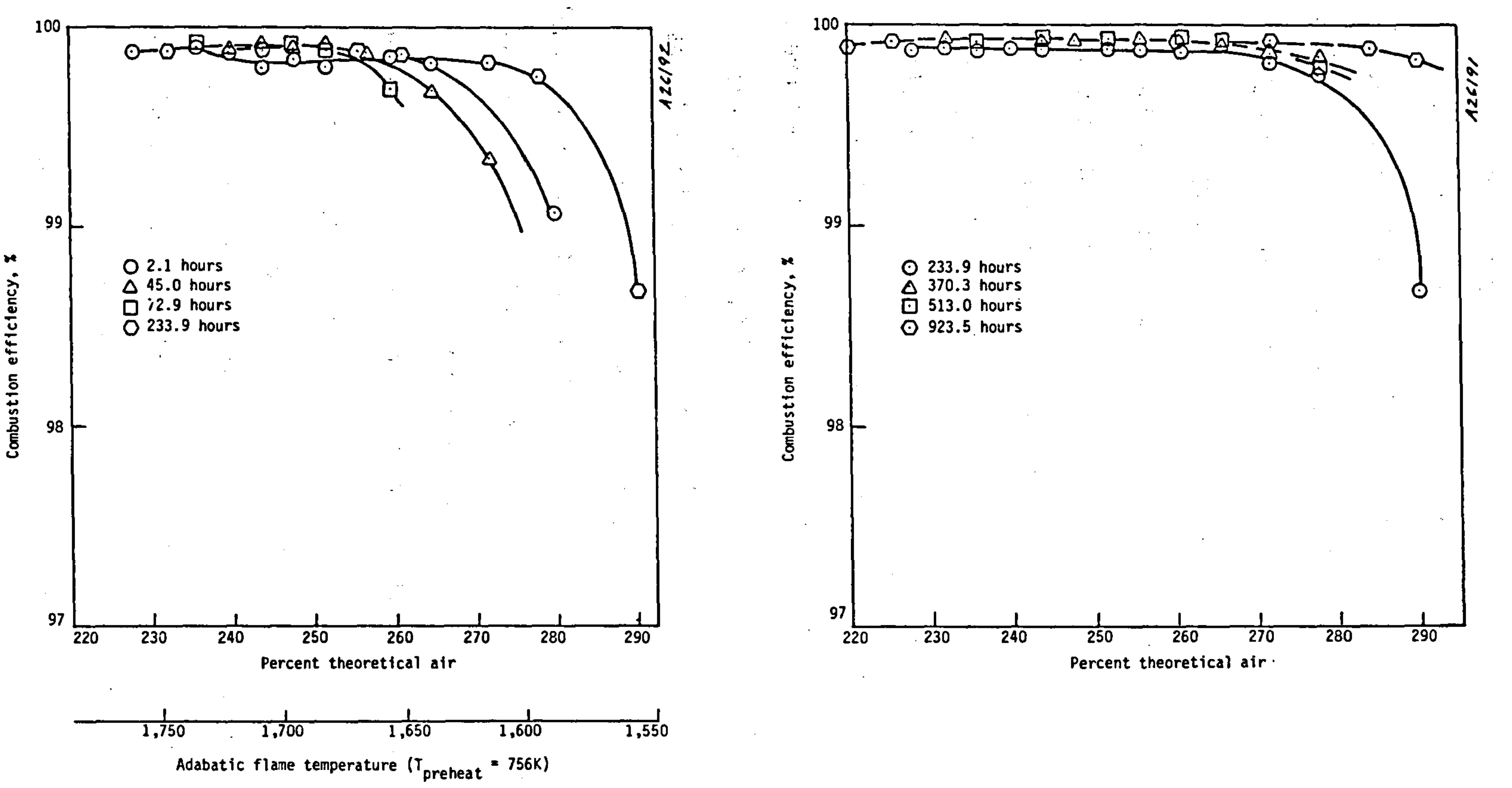

(a)

(b)

Figure 7-6. Parametric Test -- Effect of Turndown on Combustion Efficiency

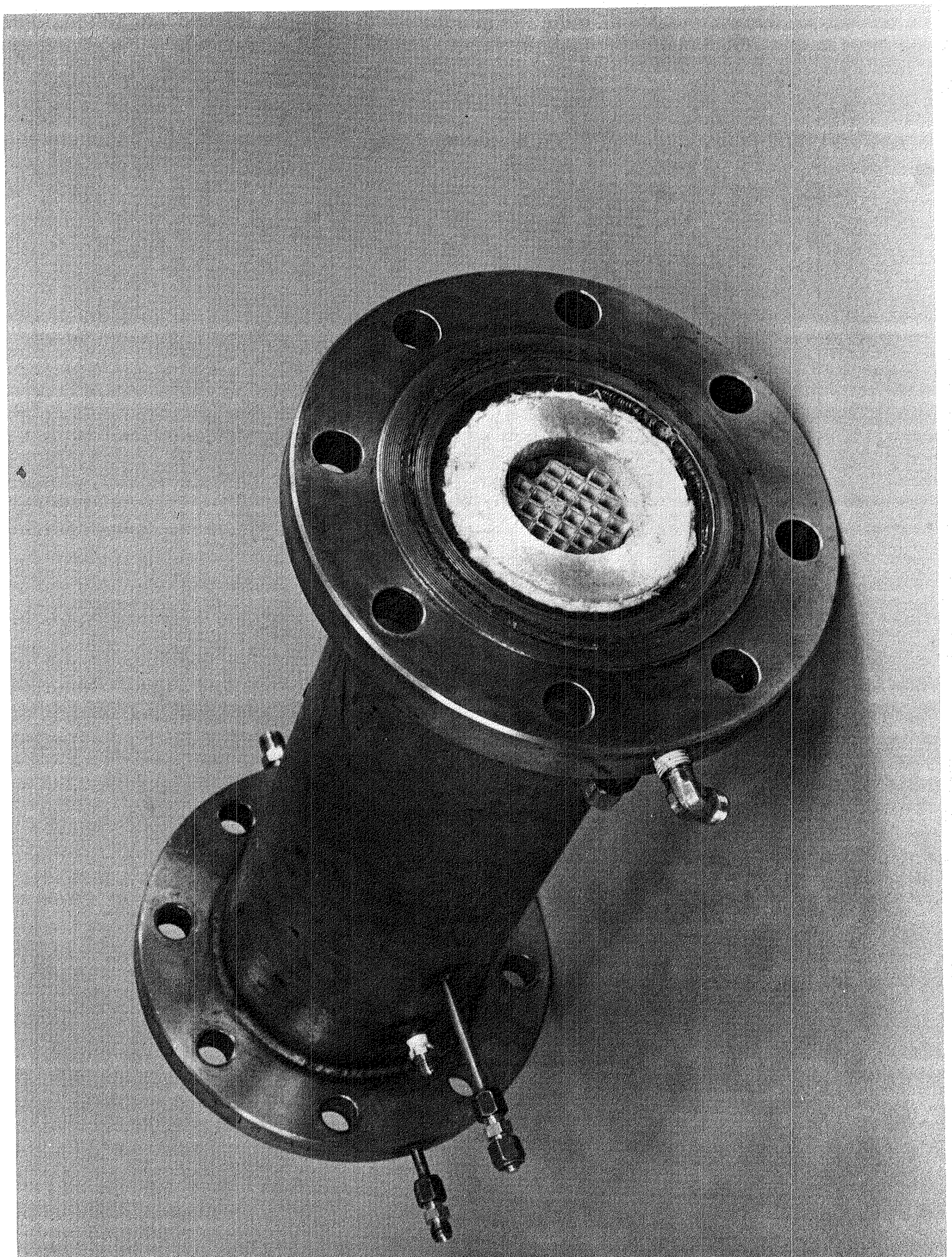

Figure 7-7. Noble Metal Element of Durability Reactor (Posttest)

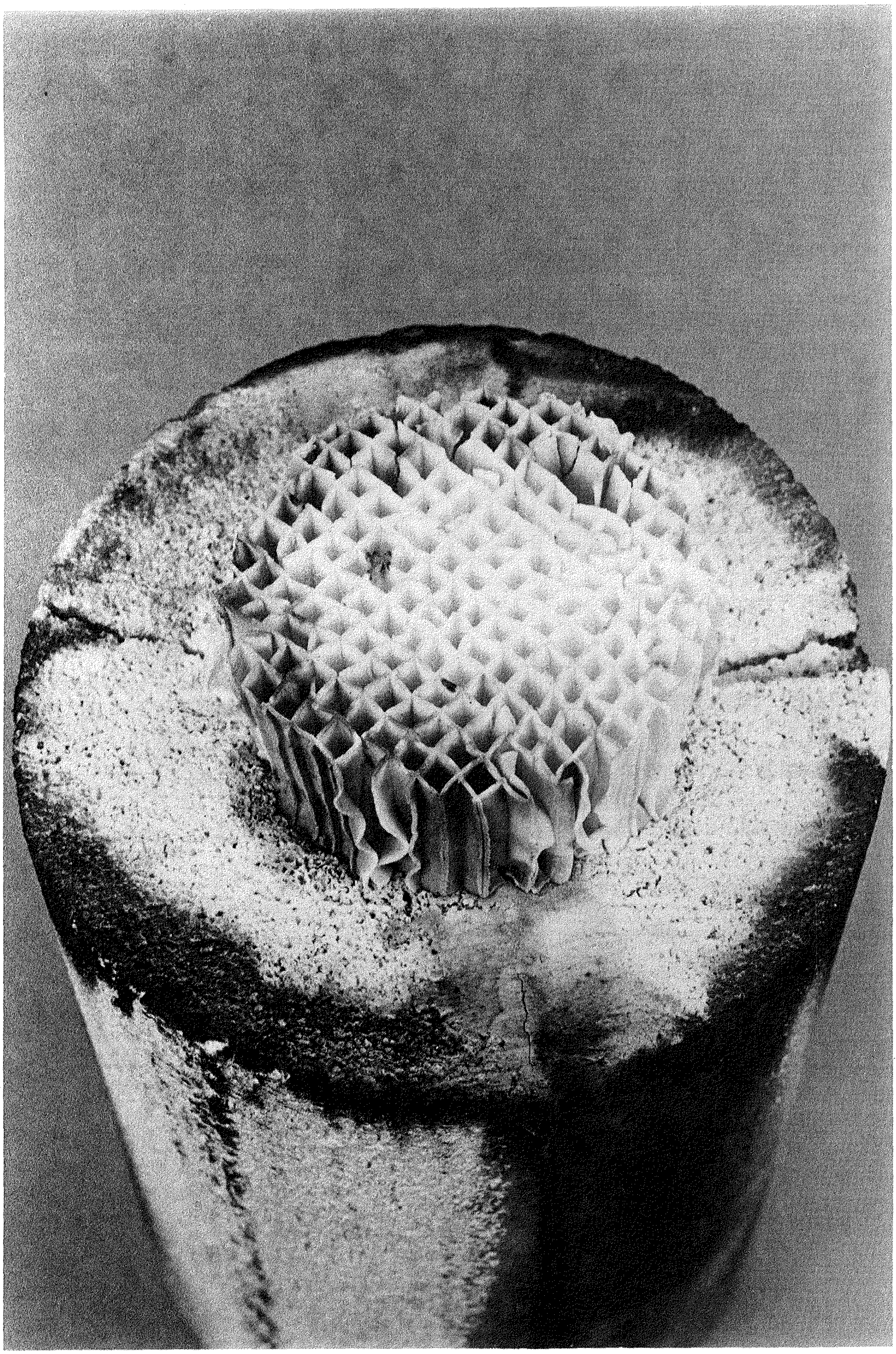

Figure 7-8. Metal Oxide Element of Durability Reactor (Posttest)

The catalyst was reinstalled for the on/off cyclic tests which resulted in the performance plot of figure 7-9. Prior to each light-off of the catalyst, the bed temperature was brought to about 900°F by passing preheated air over the reactor for about 1 hour. The first light-off was performed with the opposed jet igniter while the subsequent four light-offs were catalytic. Following each light-off, temperature and emission data were collected over a 1- to 2-hour period before shutdown. The reactor was allowed to cool for several hours following shutdown before the next light-off. During the last cycle, a final parametric test with propane was conducted to note any further changes in activity.

Following this parametric test an attempt was made to transition from propane to diesel fuel. The attempt was successful, however the catalyst became inactive within about 8 minutes of diesel combustion. The reason for this behavior is currently unclear, but fuel preparation problems as well as low initial catalyst activity were likely. Following the diesel test, the catalyst was relit on propane at the nominal test condition with no difficulty. Performance on propane fuel was therefore not adversely affected by the short exposure to diesel fuel.

In similar combustion tests conducted at the NASA Lewis Research Center (reference 14), stable combustion conditions were more difficult to achieve with propane than with diesel fuel. The difficulties encountered in the current test program therefore suggest that the vaporization of the diesel fuel was probably incomplete. An alternate, though less significant problem, may be the uniformity of the fuel-air mixture at the front face of the reactor. A final inspection of the disassembled reactor revealed no further damage or change due to the cycling tests.

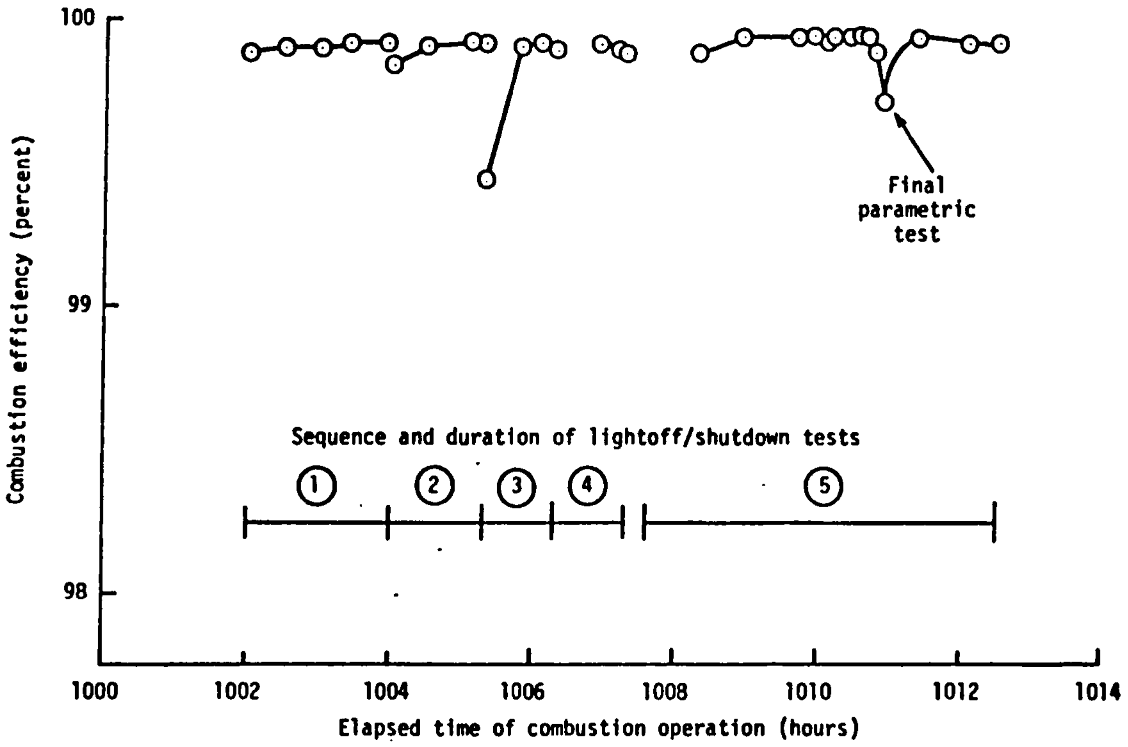

Figure 7-9. Thermal Cycling Performance

Although the phase II durability test was conducted with propane rather than diesel fuel, it demonstrated that a catalytic reactor could be designed to operate at 1,700K for extended periods. After more than 1,000 hours of sustained combustion, the reactor was still active and structurally complete. However, some loss of catalyst and distortion of the substrate was apparent (figure 7-8). Loss of the metal oxide catalyst was surprising since the oxides of terbium, cerium and thorium have very high vaporization temperatures. Apparently, even with very low vapor pressures, significant amounts of oxide are removed by the high mass transfer and combustion conditions in the reactor. The distortion of the JNM substrate is believed to be a result of continued sintering of the honeycomb material. Surprisingly, the uneven sintering did not cause any structural failures.

# SECTION 8

# CONCLUSIONS AND RECOMMENDATIONS

The objectives of the current research program were to:

- Evaluate furnace aging as a cost-effective catalytic reactor screening test
- Measure reactor degradation as a function of furnace aging and combustion time
- Demonstrate 1,000 hours of combustion durability with diesel fuel at 1,700K
- Define a catalytic reactor system with a high probability of successful integration into an automotive gas turbine engine

This program demonstrated that hour-for-hour, furnace aging was not representative of combustion on honeycomb catalytic reactors. Depletion of catalytic components was significantly more rapid for combustion than for furnace aging at the same temperature. Silicon from the furnace refractory was also found deposited on the aged reactors and may contribute to the poor combustion characteristics for furnace-aged reactors.

Reactor characteristics such as BET and noble metal dispersion were found to degrade to small and insignificant values following only 24 hours of furnace aging. No conclusions were reached on whether a minimum BET surface area or catalyst dispersion is required to achieve stable combustion at the nominal test conditions.

The combustion results of this program, added to those from other studies, demonstrate that low emissions and stable combustion operations can be achieved at advanced automotive gas turbine conditions; however, component durability and system integration issues are not fully resolved. Although these issues are clearly related, further development should proceed on parallel, but coordinated, paths.

The program described in this report focused on the question of catalytic reactor durability. It was shown that reactors can be fabricated for at least 1,000 hours of service at 1,700K combustion conditions and simultaneously yield low emissions and high combustion efficiency. At the conclusion of 1,000 hours, the reactor was still active so that its ultimate life was not determined.

During the course of the durability testing, catalyst material was lost and the substrate was somewhat distorted by the sustained high temperatures. Thus some degradation of the reactor was occurring and further catalytic reactor development should be directed at:

- The development of metal oxide catalysts with lower depletion rates
- The evaluation of long-term, high-temperature effects on JNM and comparable substrate materials
- A better understanding of the interactions between catalyst coatings and substrates, especially for metal oxide catalysts
- The development of metal oxide application methods
- The development of metal oxides into active honeycombs

- The design of graded-cell, graded-catalyst reactors to obtain optimum operating temperatures for the front noble metal element of the reactor and subsequent metal oxide elements
- An evaluation of the durability of a graded-cell, graded-catalyst reactor concept with diesel fuel at gas turbine operating pressures and temperatures
- An evaluation of the effect of cyclic testing on reactor durability
- An evaluation of the systems requirements for integrating a catalytic combustion subsystem into an automotive gas turbine

A durable graded-cell, graded-catalyst reactor for high-temperature combustors would be designed as shown in figure 8-1. The lead element would be a large cell, thick web honeycomb with a very active noble metal catalyst. The cell size, web thickness, and element length would be selected such that the energy balance would result in a mean element temperature between 1,250K and 1,450K. At these temperatures a noble metal catalyst would have a reasonably long life. The high catalytic activity of the noble metal and the lower transfer coefficients on the thick web honeycomb would promote stable combustion conditions. The downstream honeycomb elements would be a fine cell structure with a high geometric surface area to encourage rapid heating of the gas phase. This will result in significant gas phase reactions which, in turn, result in high combustion efficiency and low CO emissions. Since these elements operate at high temperatures (near adiabatic conditions) even moderate to low activity catalysts would be sufficient to maintain diffusion limited surface reaction rates. In this zone of the catalytic reactor, catalyst durability is more important than high catalytic activity. Therefore, the

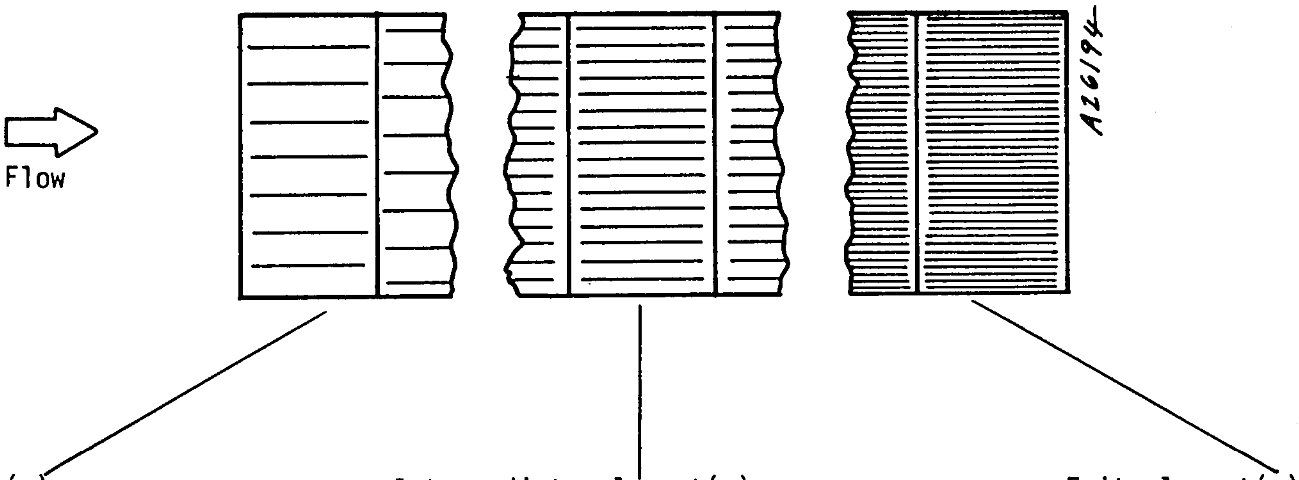

Lead element(s)

- Large cell sizes
- Thick webs
- High activity noble metal catalyst
- Low operating temperature < 1,450K

Intermediate element(s)

- Medium cell sizes
- Moderate activity noble metal/metal oxide catalyst
- Moderate operating temperature 1,450 < T < 1,600K

Exit element(s)

- High geometric surface area honeycomb
- High temperature -- low vapor pressure catalyst
- High operating temperature > 1,600K

Figure 8-1. Proposed Durable High Temperature Catalytic Reactor Concept catalyst here should be a high-temperature, low-vapor-pressure metal oxide. Between the high-temperature exit element and the low-temperature lead element the catalyst material may be a medium activity metal oxide or noble metal/metal oxide mixture. The selection of materials for each catalyst element could in this manner yield a reactor tailored to achieve a beneficial temperature distribution that optimizes catalytic activity and catalyst material durability.

# APPENDIX

## ADIABATIC FLAME TEMPERATURE BASED ON $CO_2$ MEASUREMENTS

Exhaust emissions for the combustion of no. 2 diesel fuel and propane with air were calculated for fuel lean conditions with the Acurex ACE equilibrium chemistry code (reference 15). Adiabatic flame temperatures for air preheat temperatures between 589K (600°F) and 811K (1,000°F) were also calculated. The $CO_2$ and $O_2$ levels on a dry basis and the adiabatic flame temperatures for diesel are shown in figures A-1 and A-2 and those for propane are shown in figures A-3 and A-4.

In the measurement of exhaust gas concentrations in the Acurex Catalytic Combustion Test Facility, the $CO_2$ measurement is more accurate than the $O_2$ measurement. The stoichiometry and adiabatic flame temperatures based on emissions as shown in tables 7-2 through 7-5 were therefore determined with the $CO_2$ concentration. The $O_2$ concentrations were used only as qualitative checks.

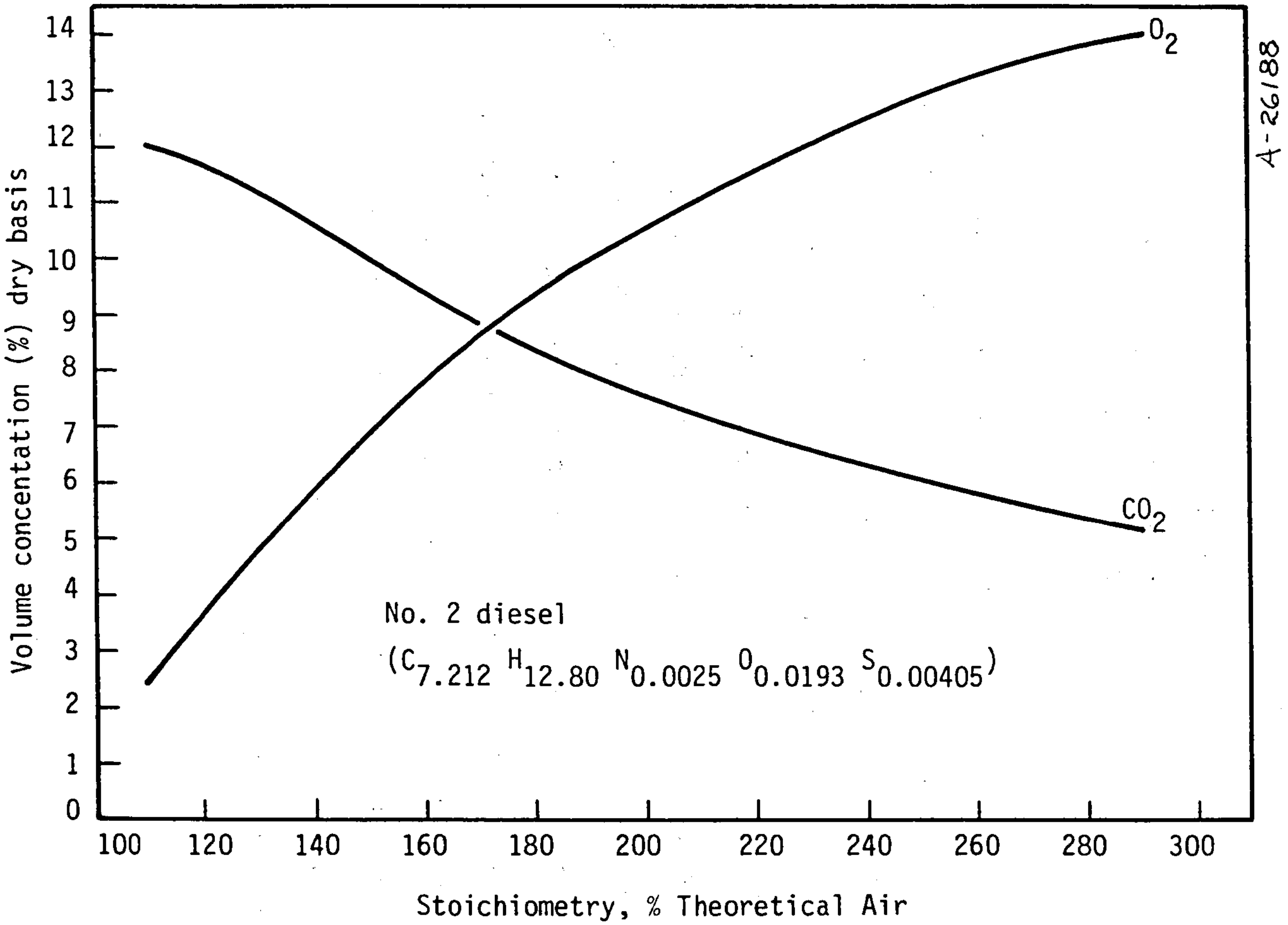

Figure A-1. $CO_2$ and $O_2$ Emissions for Diesel/Air Combustion at 1 atm pressure and 900°F Air Preheat

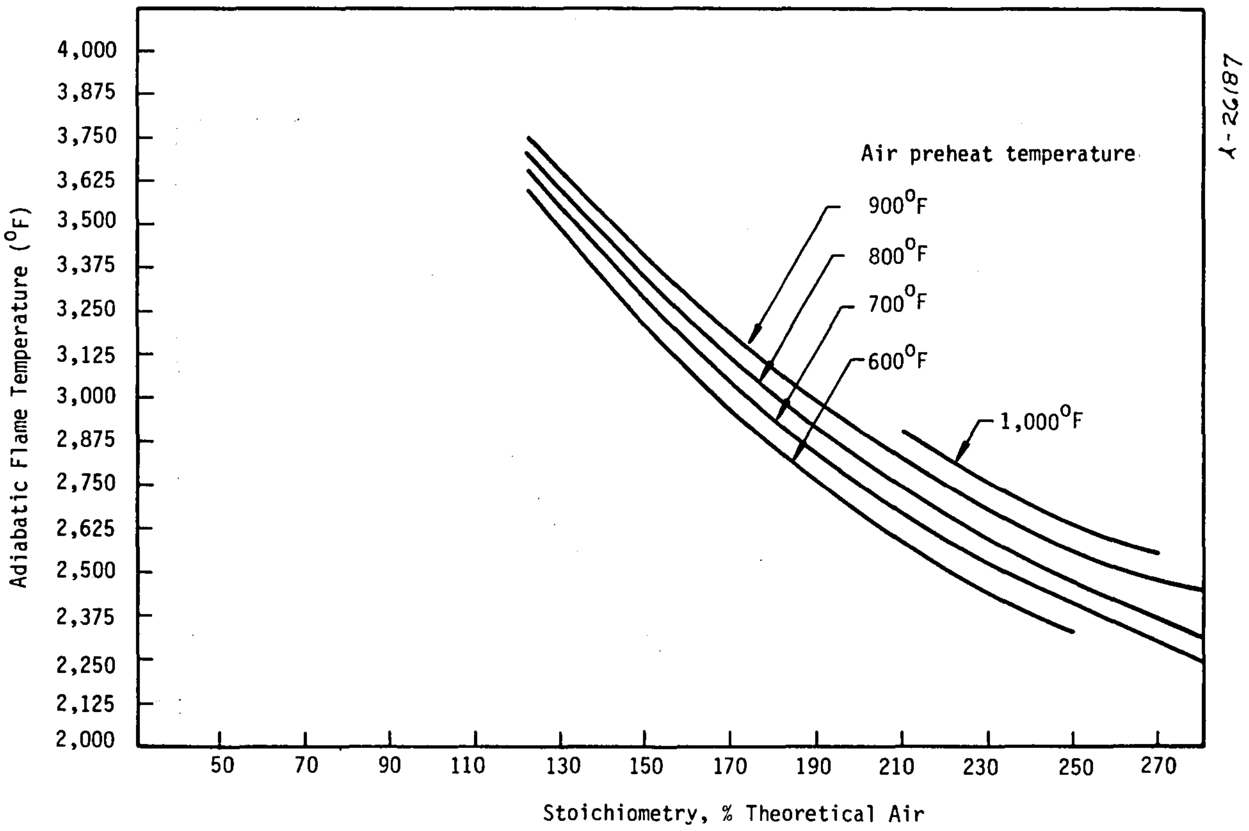

Figure A-2. Adiabatic Flame Temperature for Diesel/Air Combustion at 1 atm Pressure

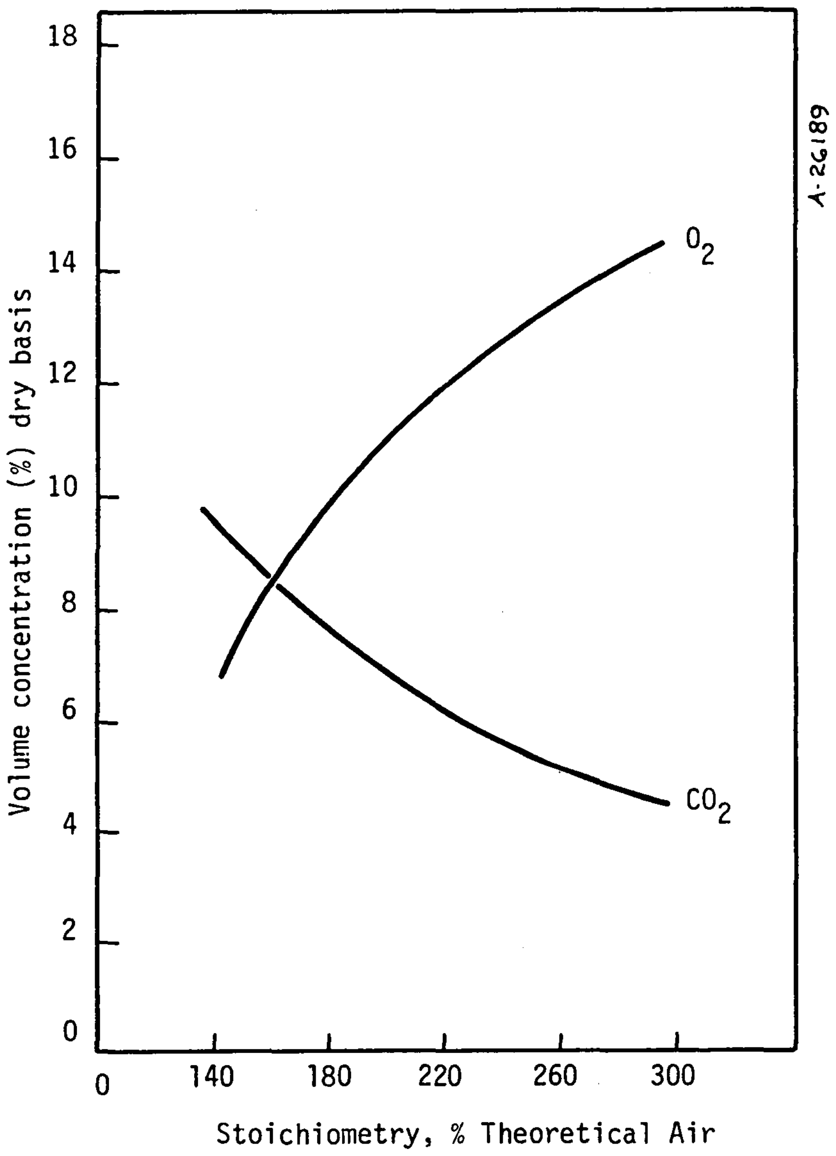

Figure A-3. $CO_2$ and $O_2$ Emissions for Propane/Air Combustion at 1 atm Pressure and 700°F Air Preheat

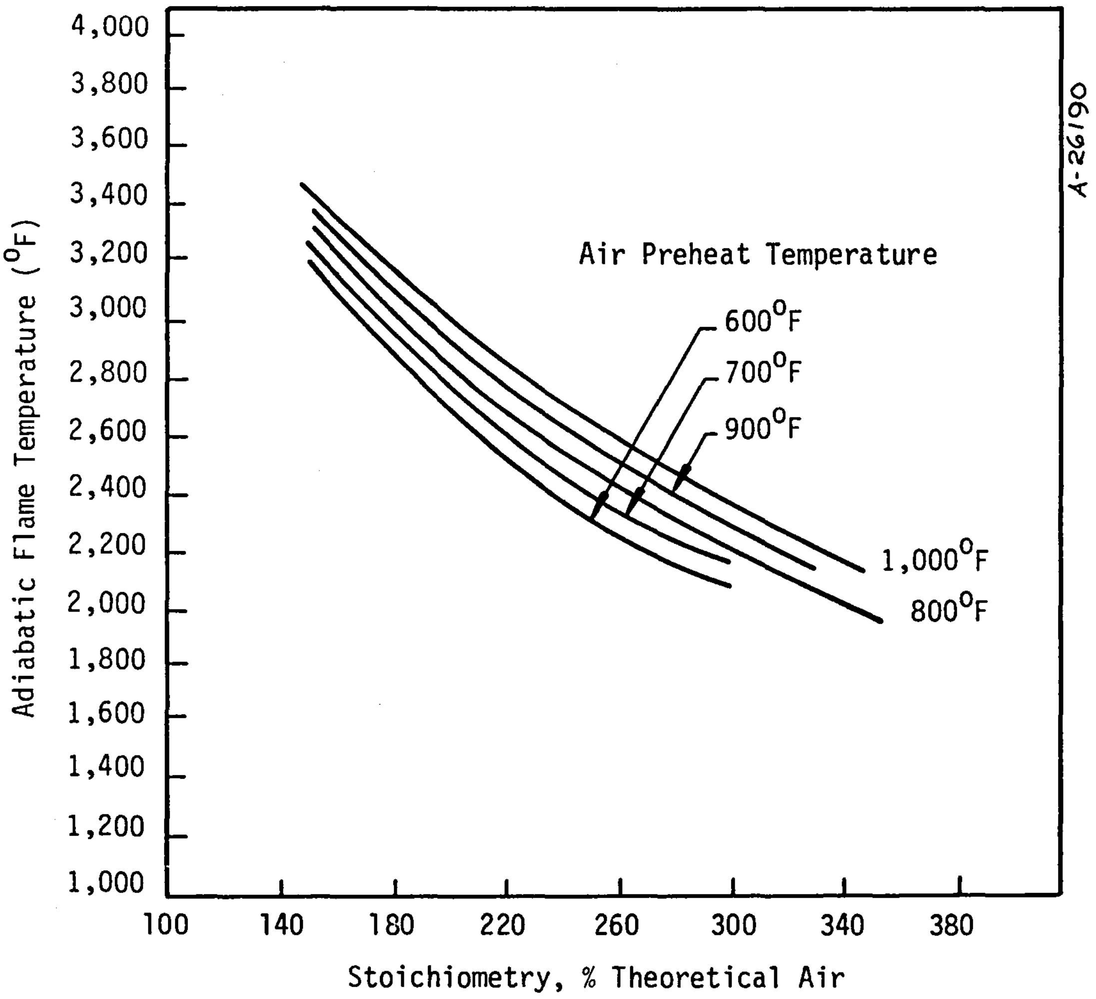

Figure A-4. Adiabatic Flame Temperature for Propane/Air Combustion at 1 atm Pressure

# REFERENCES

1. Mumford, S. E., W. S. Y. Hung, and P. P. Singh, "A Potential Low-$NO_x$ Emission Combustor for Gas Turbines Using the Concept of Hybrid Combustion," Journal of Engineering for Power, October 1977, p. 361.

2. Kesselring, J. P., et al., "Catalytic Combustion Component and System Prototype Development," Second Annual Report, EPA Contract No. 68-02-3122, Acurex Corporation, Mountain View, California, November 1980.

3. Heck, R. M. et al., "Durability Testing at One Atmosphere of Advanced Catalysts and Catalyst Supports for Automotive Gas Turbine Engine Combustors, Part 1," Final Report, NASA CR-135132, Engelhard Minerals and Chemicals Corporation, June 1977.

4. Olson, B. A., et al., "Durability Testing at 5 Atmospheres of Advanced Catalysts and Catalyst Supports for Gas Turbine Engine Combustors," Final Report, DOE/NASA/9416-802, NASA CR-159839, Engelhard Minerals and Chemicals Corporation, April 1980.

5. DeCorso, S. M., et al., "Catalysts for Gas Turbine Combustors -- Experimental Test Results," Journal of Engineering for Power, April 1977, p. 159.

6. Chu, E. K., G. C. Snow, and H. Tong, "Catalytic Combustion of Coal-Derived Liquid Fuels," Final Report EPRI AP-1666, Research Project 989-3 for EPRI, Acurex Corporation, Mountain View, California, January 1981.

7. Krill, W. V., J. P. Kesselring, E. K. Chu, and R. M. Kendall, "Catalytic Combustion for System Applications," ASME publication 79-HT-54, Joint ASME/AIChE 18th National Heat Transfer Conference, San Diego, California, August 8, 1979.

8. Bulzan, D. L. and R. R. Tacina, "Catalytic Combustion of Coal-Derived Liquids," DOE/NASA/10350-21, NASA TM-81594, Twenty-Sixth Annual Gas Turbine Conference, Houston, Texas, March 8-12, 1981.

9. Kaye, S. E., et al., "Development of a System to Utilize Flue Gas from Enhanced Recovery Underground Combustion Projects," SPE-8360, 54th Annual Fall Technical Conference and Exhibition of the Society of Petroleum Engineers of AIME, Las Vegas, Nevada, September 23-26, 1979.

10. "Development of a Catalytic Combustor for Aircraft Gas Turbine Engines," Technical Report AFAPL-TR-76-80, Government Research Laboratories, Exxon Research and Engineering Company, Linden, New Jersey, September 1976.

11. Brunauer, S., Emmett, P. H., Teller, E., "Adsorption of Gases in Multimolecular Layers," Journal of the American Chemical Society, Vol. 60, p. 309, 1938.

12. Szaniszlo, A. J., "The Advanced Low-Emissions Catalytic-Combustor Program: Phase I - Description and Status," ASME publication 79-GT-192, Gas Turbine Conference & Exhibit & Solar Energy Conference, San Diego, California, March 12-15, 1979.

13. Kendall, R. M. and Kelly, J. T., "Premixed One-Dimensional Flame (PROF) Code User's Manual," Acurex Final Report 78-277, June 1978.

14. Anderson, D. N., NASA Lewis Research Center, private communication.

15. Powars, C. A. and Kendall, R. M., "User's Manual, Aerotherm Chemical Equilibrium (ACE) Computer Program," Aerotherm (Acurex) Report UM 69-7, May 1969.

16. Kesselring, J. P., <u>et al.</u>, "Catalytic Combustion Component and System Prototype Development," First Annual Report, EPA Contract No. 68-02-3122, Acurex Corporation, Mountain View, California, October 1979.

| | | |
|---|---|---|
| 1. Report No.<br>NASA CR-165396 | 2. Government Accession No. | 3. Recipient's Catalog No. |

4. Title and Subtitle

DEVELOPMENT OF HIGH TEMPERATURE DURABLE CATALYST FOR USE IN CATALYTIC COMBUSTORS FOR ADVANCED AUTOMOTIVE GAS TURBINE ENGINES

5. Report Date
September 1981

6. Performing Organization Code

7. Author(s)
H. Tong, G. C. Snow, E. K. Chu, R. L. S. Chang,
M. J. Angwin, and S. Pressagno

8. Performing Organization Report No.

10. Work Unit No.

9. Performing Organization Name and Address
Acurex Corporation
Energy and Environmental Division
485 Clyde Avenue
Mountain View, CA 94042

11. Contract or Grant No.
DEN 3-83

13. Type of Report and Period Covered
Contractor Report

12. Sponsoring Agency Name and Address
U.S. Department of Energy
Office of Vehicle and Engine R&D
Washington, D.C. 20545

14. Sponsoring Agency ~~Code~~ Report No.
DOE/NASA/0083-1

15. Supplementary Notes

Final Report. Prepared under Interagency Agreement DE-AI01-77CS51040. Project Manager, D. N. Anderson, Aerothermodynamics and Fuels Division, NASA Lewis Research Center, Cleveland, Ohio 44135.

16. Abstract

An experimental program was performed to develop durable catalytic reactors for advanced gas turbine engines. This program was performed as part of DOE's Gas Turbine Highway Vehicle Systems Project. Objectives of this program were to evaluate furnace aging as a cost-effective catalytic reactor screening test, measure reactor degradation as a function of furnace aging, demonstrate 1,000 hours of combustion durability, and define a catalytic reactor system with a high probability of successful integration into an automotive gas tuebine engine. In the first phase of this program, 14 different catalytic reactor comcepts were evaluated, leading to the selection of one for a durability combustion test with diesel fuel at 1,700 K combustion conditions. The durability reactor, a proprietary UOP noble metal catalyst, failed structurally after about 136 hours and the catalyst was essentially inactive after about 226 hours. In Phase II, eight additional catalytic reactors were evaluated and one of these was successfully combustion-tested for 1,000 hours at 1,700 K on propane fuel. This durability reactor used graded-cell honeycombs and a combination of noble metal and metal oxide catalysts. The reactor was catalytically active and structurally sound at the end of the durability test.

17. Key Words (Suggested by Author(s))
Automotive gas turbine
Combustion
Catalytic
Catalyst
Honeycomb

18. Distribution Statement
Unclassified - unlimited
STAR Category 44
DOE Category UC-96

| | | | |
|---|---|---|---|
| 19. Security Classif. (of this report)<br>Unclassified | 20. Security Classif. (of this page)<br>Unclassified | 21. No. of Pages | 22. Price* |

* For sale by the National Technical Information Service, Springfield, Virginia 22161

☆USGPO: 1982 — 559-091/3228

**End of Document**